THP1 model of Classical monocytes for the study of Non-alcoholic fatty liver disease

MSc Graduation Assignment

Abigail Groenenboom

University of Enschede, 2023

UNIVERSITY OF TWENTE.

Abstract

Monocyte-like cell lines are invaluable as models for monocytes in research regarding natural biological states as well as in the context of pathology, treatment target discovery and drug testing. However, reports regarding findings relating monocyte-like cells are regularly contradictory due to the plasticity of monocytes and their sensitivity to culture conditions. In addition, two prominently used models, THP1 and U937, are naturally at the preceding stage of promonocytes. Hence, differentiation of the cell lines to a mature profile is required for use in research. However, maturation and differentiation of monocytes is still poorly understood, and as a result no replicable protocol for THP1 and/or U937 cell lines has yet been established. This research investigates the effect of a number of maturation protocols, and potentially influential culture specifics that are prone to vary between labs, on the maturity profile of promonocytes through flow cytometry of expression levels of CD14, CD16, CD13 and HLA-DR.

Acknowledgements

Contents

1 Introduction

1.1. Non-alcoholic fatty liver disease: an increasing global burden

NHS defines non-alcoholic fatty liver disease (NAFLD) as *a range of conditions caused by build-up of fat in the liver*[1]. Risk factors for NAFLD include obesity, unhealthy diet, sedentary lifestyle, high blood pressure and cholesterol, advanced age, genetic predisposition, and metabolic diseases[1–5].

NAFLD comprises four stages, starting with (hepatic) steatosis, a build-up of fat in the liver cells that remains difficult to diagnose[6]. Estimations based on magnetic resonance spectroscopy suggest approximately 30% of the general population to be afflicted by steatosis, defined as >5% of hepatocytes being steatotic[7].

Prolonged and/or severe steatosis can result in chronic inflammation of the liver. This second stage, non-alcoholic steatohepatitis (NASH), is associated with 10-fold increased risk of liver-related death and doubled cardiovascular risk[8]. Both steatosis and steatohepatitis are associated with progressive fibrosis, with double the progression rate in NASH[9].

Denoting the third stage of NAFLD, (reversible) fibrosis is the overgrowth, hardening and/or scarring of tissue as a result of an abnormal wound-healing response[10]. Fibrosis disrupts the liver architecture, resulting in hepatocyte loss and deregulation of liver functioning, ultimately leading to liver failure[11]. The degree of fibrosis is considered the strongest predictive factor for life-threatening complications relating to progression of NAFLD[12].

Substantial, permanent fibrosis in the liver is considered the end-stage of NAFLD and is referred to as cirrhosis[13]. The liver's reduced capacity for local immune surveillance and dysregulation of the inflammatory cytokine production may in turn give rise to simultaneous systemic inflammation and immunodeficiency, a phenomenon termed cirrhosis-associated immune dysfunction (CAID)[14]. In addition, NAFLD is associated with 10-fold increased risk of hepatocellular cancer in early stages and 500-fold increased risk in case of cirrhosis[15].

Current numbers relating to NAFLD prevalence are presented in Figure 1 below. Primarily due to liver failure, cirrhosis and HCC claim the lives of over 2 million people each year[16]. In addition, NAFLD patients have higher health-care costs, increased years of disability and lower quality of life[17–19]. NAFLD prevalence is forecasted to increase with 40% between 2020 and 2040, and NASH is expected to become the leading indicator for liver transplantation[20]. The rapidly increasing incidence and prevalence of NAFLD and its complications, as well as the associated healthcare burden, urgently warrant preventive measures in the form of global and national policy. The irreversible nature of advanced liver disease also warrants the development of curative therapies, however.
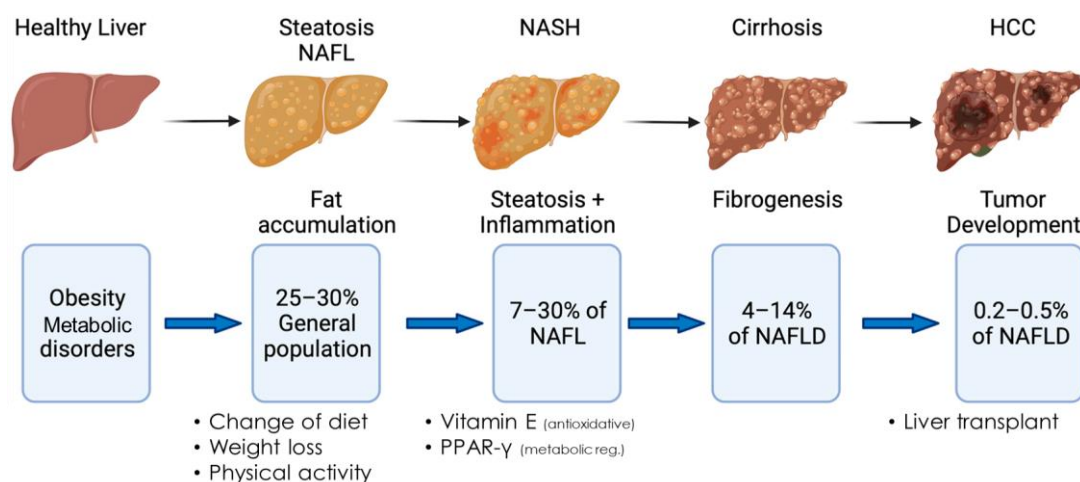

Figure 1 NAFLD progression and current treatment options[21]. Adapted from Engelmann and Tacke (2022)[22].
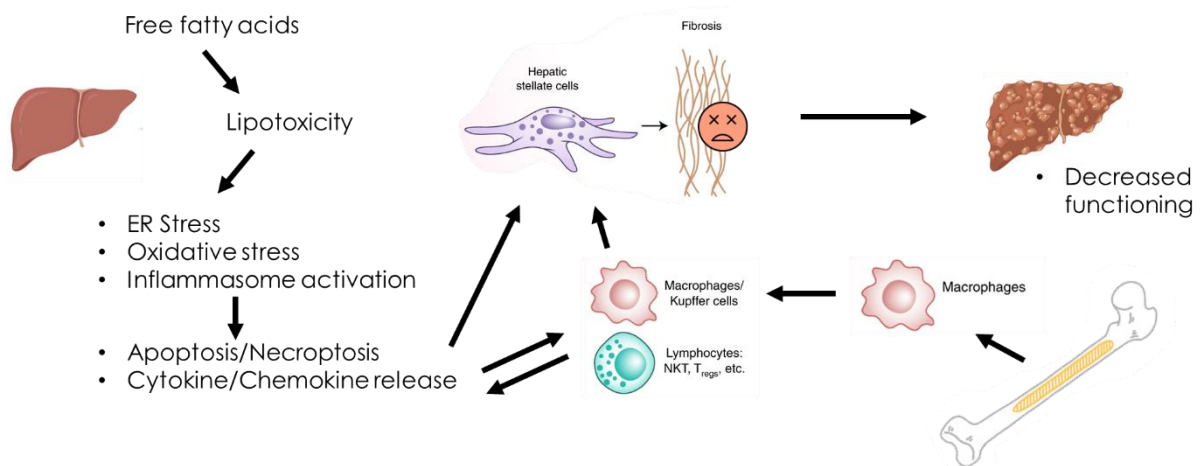
Figure 2 A simplified overview of NAFLD pathology illustrating the role of monocytes/macrophages.

1.2. Cure for advanced NAFLD remains elusive

Although steatosis can be remedied through a change of lifestyle including diet, physical activity and weight loss, no therapies currently exist for reversing fibrosis[23]. Two pharmacological treatments are recommended for selected NASH patients: Vitamin E (not recommended in diabetes) and Pioglitazone (not recommended in type 1 diabetes), although no definitive improvement in fibrosis score has been established[21]. A number of therapeutic targets for reversing fibrosis is under investigation, but no pharmacological therapies have been incorporated in (inter)national treatment guidelines yet[24]. After progression to the stage of cirrhosis and/or HCC, only liver transplantation remains as a means of saving a patient's life.

1.3. Monocytes: a promising target in the treatment of NAFLD

Chronic inflammation of the liver and subsequent fibrosis are mostly orchestrated by immune cells. When the liver's capacity to process the primary metabolic energy substrates, carbohydrates and fatty acids, is overwhelmed, the result is an accumulation of toxic lipid species. These lipotoxic metabolites, generally saturated free fatty acids, induce hepatocellular injury and death through endoplasmic reticulum stress and oxidative stress[25] as well as (NLRP3) inflammasome activation[26].

NLRP3 inflammasomes mediate caspase 1-dependent release of the pro-inflammatory cytokines IL-1β, IL-18 and TNF-α, and may additionally initiate gasdermin D-mediated pyroptotic cell death[27,28]. Pyroptosis results in the release of the NLRP3 inflammasome into the extracellular space, where internalization by hepatocytes and resident macrophages, Kupffer cells (KCs), leads to a self-perpetuating pro-inflammatory response[29,30]. In addition, surviving lipotoxicity-undergoing hepatocytes release microvesicles that further promote activation of NLRP3 when internalized by other hepatocytes and macrophages[31]. NLRP3 directly stimulates hepatic stellate cells (HSC) to induce fibrosis[32].

However, despite the pro-inflammatory response of resident cells to lipotoxicity, it's newly recruited circulating monocytes (CMs) that have been shown to be the major cause of fibrosis in in the liver[33,34]. Monocytes derive from the bone marrow and circulate in the blood stream to perform phagocytosis, antigen presentation and cytokine production[35]. In NAFLD, CMs infiltrate the liver following their recruitment by resident cells, where they differentiate into macrophages. Unfortunately, their pro-inflammatory nature combined with their communicative nature then leads them to be the primary orchestrator of fibrosis[36].

Resident cells involved in CM recruitment are Kupffer cells, liver sinusoid endothelial cells (LSECs), hepatic stellate cells (HSCs) and hepatocytes[37–39]. Owing to their macrophage heritage, Kupffer cells play an important role in cellular communication and regulation, and thus in liver homeostasis. Due to the self-perpetuating nature of lipotoxicity-based inflammation explained above, KC's also tend to play a large part in further worsening NAFLD. In patients with NAFLD enlarged and aggregated (more pro-inflammatory) KC populations are seen in the liver, correlating with the severity of the disease[40]. However, it is again circulating monocytes that largely lay at the root of this problem: CMs have been shown to supplant native Kupffer cells; CMs' pro-inflammatory nature then exacerbates local inflammation and further increases recruitment of CMs, adding an extra layer to the self-perpetuation of liver inflammation[41].

The involvement of CMs both directly through fibrosis and indirectly through supplantation and worsening inflammation makes them an attractive target in the search for NAFLD treatments. Additionally worth noting is that CMs of NAFLD patients have been proven to differ from healthy volunteers even before entering the liver. Exemplified by the paradox of a paradigm that is CAID, circulating monocytes still warrant a lot of study.

1.4. Monocyte subpopulations

It must be noted that monocytes comprise a number of subtypes that differ in their response to inflammation [42]; CMs can be both pro-inflammatory and anti-inflammatory, and contrasting findings have been published regarding the nature of the subtypes. Distinguished based on the markers CD14 and CD16, the three primary types of monocytes are CD14++CD16- Classical monocytes (cMo), CD14+CD16+ Intermediate monocytes (iMo), and CD14loCD16++ Nonclassical monocytes (ncMo). Classical monocytes typically comprise 90% of the monocytes in a human body. Nonclassical monocytes are derived from cMo through differentiation via the intermediate type if cMo are so stimulated by their environment[43].

Under normal circumstances, cMos infiltrate tissue if an inflammatory response is called for, while ncMos patrol along the walls of the blood circulation for pathogens and other threats[44,45]. In NAFLD, however, ncMos are more than twice as infiltrative as cMos, and cMos in the chronically-inflamed liver are stimulated to undergo differentiation to the ncMos type[46].

1.5. Markers for maturation and the challenge of monocyte plasticity

Perhaps not wholly unsurprisingly, being so intricately linked to functioning and response type to inflammation, the primary markers for monocyte maturity are CD14 and CD16 expression. Additionally, CD13 expression is associated with maturity whereas HLA-DR expression is associated with immaturity[47].

CMs have high plasticity, which allows them to easily adapt to different environments. An important feature for cells that are just as likely to end up in a lung as they are in a broken finger bone. However, although of great benefit inside the body, monocyte plasticity is a challenging variable inside a wells plate or culture flask. Monocyte maturation as well as polarization remain poorly understood and difficult to steer as desired for therapeutical approaches[48].

In Vivo, monocytes are modelled for study in the lab through Monocyte-like cell lines such as THP-1, HL-60, U-937 and CRL-9855™ cells[49–51]. Both Riddy et al. *2018*[49] and Duweb et al. *2022*[50] concluded THP-1 to be the closest, simplified model for macrophage differentiation purposes.

Although often used as surrogates for monocyte research, THP-1 and U937 cells are originally promonocytes and require differentiation to a mature profile for representative use in biological study. The level of maturity of unstimulated promonocytes varies significantly between reports,

however, ranging from no to up to 90% CD14 expression in controls[52]. Additionally, contradicting findings have been reported regarding the sensitivity of e.g. THP1 cells to stimulation. As a result, no definitive protocol has yet been established for the maturation of THP1 to a cMo mature profile.

As monocyte functioning and responsiveness is closely related to the CD14/CD16 maturity profiles, monocytes in the context of behavioural and genetic differences between monocyte subtypes cannot be studied with the use of promonocytes. Neither can monocytes in the context of pathologies and therapeutic targets be modelled by promonocytes. Additionally, without maturation to a classical profile, cells cannot differentiate to intermediate or
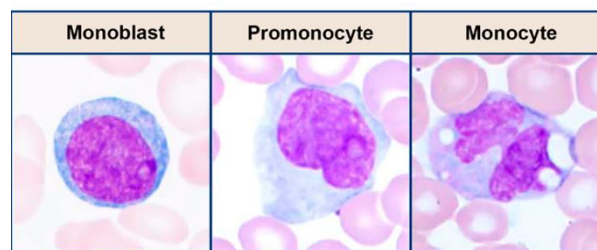It is therefore of great value for the field that a reliable protocol for promonocyte maturation is established.

Figure 3 Monoblast, Promonocyte and Mature monocyte morphology. Adapted from Osman et al. 2021[53]

1.6. THP1 and U937 maturation protocols yield inconsistent results

Below, a number of tested protocols is discussed to illustrate the variability in responses of THP1 and U937 to stimulation.

Riddy et al 2018[49] used 16 ng/mL PMA for 48 hours to differentiate THP-1 and U937 into a macrophage-like phenotype with comparable CD14 expression, but a pro-inflammatory CD marker profile, compared to natural CD14+ PBMCs. Their findings implied that U937 and to a lesser extent THP1 contain a mixed pro-inflammatory phenotype.
It is worth noting that in Riddy's study, U937 failed to respond to chemoattractants, which was ascribed to under-expression of corresponding receptors. This indicates U937 to be unsuitable for migration studies. U937 mRNA levels did not reflect this difference and were comparable to CD14+ PBMCs, implying other factors being involved in protein expression.

Takashiba et al 1999[54] cultured THP-1 with 200 nM (~300 ng/mL) PMA for 4 days. Cells adhered after 20 hours. They claim flow cytometry (FC; addressed in depth in section 3.4, p.21) revealed high expression levels of CD14, although the results supporting this conclusion were not published. 20 nM (~30 ng/mL) PMA induced adherence after 3-4 days, while 2 nM (~3 ng/mL) PMA was insufficient to induce adherence.
The cells were maintained in RPMI 1640 media supplemented with 2 mM l-glutamine–100 U of penicillin per ml–100 µg of streptomycin per ml–25 mM HEPES (C-RPMI) and 5% fetal bovine serum (all from Gibco BRL, Gaithersburg, Md.). For the induction of cell differentiation, cells (5 × 10⁵ to 10⁶ per ml) were seeded in macrophage serum-free medium (macrophage-SFM; Gibco BRL) with 2 to 200 nM PMA for 24 h (29). After incubation, non-attached cells were removed by aspiration, and the adherent cells were washed with C-RPMI three times. THP-1 cells in macrophage SFM with no PMA were used as control (undifferentiated) cells.

García et al. 1999[55] cultured U937 with 20 ng/mL PMA for up to 5 days. At 72hr, PMA induced a significant increase in CD14 expression.
The cells were washed in serum-free Opti-MEM medium (Gibco) prewarmed to 37°C. The cells were then resuspended in Opti-MEM containing 10 µg/mL DOTMA/DOPE solution (Lipofectin) (Gibco) and

sterilized oligonucleotide at a concentration of 10 µM. The cells were incubated for 4 hours at 37°C, and the medium was removed and replaced with normal growth medium containing 20 ng/mL PMA and a fresh dose of oligonucleotide; Normal growth medium: RPMI 1640 (Gibco, Paisley, UK) supplemented with 5% FCS, 2 mM glutamine, and 50 µg/mL gentamicin at 37°C in a humidified atmosphere with 5% CO_2.

Liu et al. 2005[56] cultured U937 with 0.1 mM VitD3 for 24 hours to investigate their response to LPS. The cells were found to stably express CD14 mRNA and protein. CD14 expression in turn enhanced sensitivity to LPS. LNF-α production in CD14^{+} cells was quadrupled compared to the control. The cells were cultured in an agarose-coated bottle.

Baek et al. 2009[57] cultured U937 for 48 hours with 10 nM PMA to induce a macrophage-like phenotype and 100 nM vitamin D3 to induce a mature monocyte phenotype.

Finally, Aldo et al. 2013[52] investigated the effect of 10 ng/mL PMA and M-CSF/CSF1 on THP1 cells. This protocol is discussed further in section 3.3.2 (p.16)

2 Aim of my research

The aim of this research can be defined as successful and replicable maturation of a promonocyte line to a mature, classical monocyte phenotype for use in subsequent biological research.

2.1. Research objectives

1. Determination of the maturity profile of monocyte-model cell line species in the lab
2. Determination of the most representative cell line in context of this research between the cell lines available to me
3. Determination of the effect of a number of common variables in biological research on the maturation profile of promonocytes during stimulated maturation,
   including adherence, seeding density, passaging and revival origin, and subjection to flow cytometry
4. Development of a replicable differentiation protocol for maturation of promonocytes to a classical mature profile

3 Method

3.1. Materials

Materials relevant to this research and their manufacturer details are listed in Tables 1-4 below.

Table 1 Manufacturer details for notable lab equipment

Description	Manufacturer	Type
Cell culture		
Centrifuge	Hettich	Universal 32 type 1605
Automated Cell Counter	Logos	Luna L10001
Automated Cell Counter	Logos	Luna L40001
Counting chamber	VWR	631-1159
Upright brightfield microscope	FisherScientific	Unknown
CO2 Incubator	ESCO	CCL170B-8
Waterbath	Memmert	WNB14
Laminar Flow Hood (LFH)	CleanAir	Unknown
Antibody staining		
Centrifuge	Eppendorf	Centrifuge 5804
Roller mixer	Stuart	SRT6D
Magnetic Stirrer	FisherBrand	FS RT Basic Stirrer 120 11676264
Vortex	IKA	Yellow Line TTS2
Vacuum gas pump	VWR	PMS20405-96
Cooled Centrifuge	ThermoScientific	Hereaus Fresco 21 Centrifuge 75002425
Balance	Mettler Toledo	MS104S/01
Liquid Nitrogen Tank	Worthington	LS750B-R 35 liter
Liquid Nitrogen Tank	Air Liquide	ARPEGE 40
Fume hood	Unknown	Unknown
Fluorescence microscopy		
Automated Inverted Fluorescence Microscope	Nikon	Ti-E
Digital Camera	Hamamatsu	ORCA-Flash4.0LT
PE filter cube	NIKON	TRITC-B
Flow cytometry		
Flow cytometer	BD	Facs Aria II

Table 2 Manufacturer details for reagents excluding antibodies and fluorophores

Reagent	Manufacturer	Cat.no.
RPMI-1640 with L-glutamine	Capricorn	Ca RPMI-A
Penicillin/Streptomycin (pen/strep)	Capricorn	CA PS-B
Fetal bovine serum	Merck	F7524
CSF-1	Peprotech	
Phorbol 12-myristate 13-acetate (PMA)	Selleckchem	S7791
Cholecalciferol (VD3)	Sigma aldrich	C9756
0,05% trypsin-EDTA, phenol red	FisherScientic	25200-072
Trypan blue solution 0,4%	Sigma Aldrich	T8154-100ml
Formaldehyde, 36.5-38% in H2O	Merck	F8775-500ml
Phosphate-buffered saline (PBS) (tablets)	Merck	524650-1EA

Table 3 Manufacturer details for antibodies and fluorophores

Antibody	Fluorophore	FACS channel / FM filter		Manufacturer	Cat.no.
		Excitation (nm)	Emission/BW (nm)		
Mouse-anti human CD14	AF647	488	530/30	BD Pharmingen	562690
Mouse-anti human CD16	PerCP-Cy5.5	488	585/42		560717
Mouse-anti human CD13	PE	488	695/40		YY030507
Mouse-anti human HLA-DR	AF488	633	660/20		567642
Mouse anti-human TNF-α (Capture)	x	x		R&D Systems	dy210
Biotinylated Goat Anti-Human TNF-α (Detection)	x	x			
x	Streptavidin-PerCP	PE filter cube (ex.543/22;dm.562;em.593/40)		BioLegend	405213

Table 4 Manufacturer details for consumables

Consumable	Surface	Manufacturer	Cat.no.
6-wells plate	TC-treated	VWR	734-2323
12-wells plate			734-2324
T-75 flask			734-2313
T-25 flask		Greiner Bio One	690175
Cell counting slides		Westburg	LB L12002
Flow cytometry tubes (4.5 mL)		Greiner Bio one	120101
Flow cytometry tubes (4.5 mL, sterile)			120161

3.2. Cell culture specifics and technical procedures

3.2.1. THP1 and U937 revival and culture

THP1 and U937 cell lines were revived according to standard (monocyte) revival protocol and kept in culture in T-75 flasks. Flasks were kept in vertical position to prevent adherence and preserve the monocyte identity as far as possible. Medium used was RPMI with L-glutamine, 10% FBS and 1% pen/strep. Cells were cultured at 37 °C, 5% CO_2.

Following revival, both lines were let to rest for 10 days to allow THP1 to activate before splitting and use in experimentation. During the resting period, medium was enriched with 10% extra FBS to a total of 20% FBS. In addition, medium was refreshed by adding extra medium to flasks and resuspending cells to separate clumps, rather than spinning and removing old medium, to better preserve the cells.

Cells were counted through automated cell counting with Trypan Blue before splitting and (experimental) seeding. After counting, cells were centrifuged for 5 minutes at 1000 RPM and resuspended in medium at $1 * 10^6$ cells/mL unless stated otherwise.

3.2.2. Washing steps

Washing steps comprised washing cells twice by centrifugation with excess PBS (5 minutes at 0.5 x1000 G, followed by careful aspiration of the supernatant) and resuspension in medium at $1 * 10^6$ cells/mL, unless stated otherwise.

3.2.3. Cell collection after stimulation

Following stimulation (detailed in section -1300699856.652.28549, p.15), suspended cells were collected in a centrifuge tube. Adhered cells were subjected to Trypsine for 10 seconds before neutralizing with PBS. The bottom of the container was then scraped, and loosened cells were added to the suspended fraction unless stated otherwise. Cells were again counted through automated cell counting with Trypan Blue, centrifuged for 5 minutes at 1000 RPM and resuspended in medium at $1 * 10^6$ cells/mL unless stated otherwise.

3.2.4. Antibody staining

Throughout this research, cells were stained (1:100) with CD14, CD16, HLA-DR and/or (1:200) CD13 antibody (AB) for a cell density of $1 * 10^6$ cells/mL. Generally, 200 uL cell suspension was added to Eppendorfs and, with the fluorescent light turned off in the LFH, mixed with AB staining solution as dictated by the required conditions. Samples were then incubated for an hour in the dark at 4 °C and washed (see 3.2.2 above). In the case of sorting conditions, between 1.5 and 2.6 mL of cell suspension ($1 * 10^6$ cells/mL) was stained to ensure worthwhile cell numbers for cell sorting.

In addition to fully stained samples and negative controls, conditions are stained with combinations of two and/or three antibodies to create experimental controls for fluorescence-overlap compensation. Compensation is discussed in depth in section 0 (p.23).

3.2.5. Cell fixation

Due to time constraints, in certain cases, stained cells were fixated and stored before continuing with analysis. Following the washing after the staining incubation, cells were resuspended in 4% formaldehyde in PBS and fixated for 15 minutes at room temperature. Cells were washed again and resuspended in PBS at $1 * 10^6$ cells/mL. Samples were stored (overnight) in the dark at 4 °C until analysis.

3.2.6. Preparation for flow cytometry

Following stimulation (addressed in section -1300699856.652.30560, p.15), and fixation as necessitated, cells were analysed with flow cytometry, the underlying principles and procedures of which are discussed in section 3.4 (p.21). Prior to analysis, however, cells require to be transferred to a particular type of vial that fits inside the loading port of the flow cytometer: flow cytometry tubes[58]. In addition, appropriate vessels must be provided for cell capture in case of (fluorescence-activated) cell sorting.

Coating flow cytometry tubes for cell sorting

During cell sorting, selected cells are deflected from the waste stream towards a designated container. However, fluctuations in cell trajectory may cause cells to hit the receptacle wall rather than land in the intended suspension fluid. Tubes for flow cytometry are generally comprised of polystyrene, a material that promotes cell adhesion[59]. As a result, cells that hit the dry surface are likely to get stuck and no longer be recoverable for continued experimentation, even with centrifugation[60]. In addition, cells adhered above the fluid level may dehydrate and die.

Thus, sterile flow cytometry tubes were prepared for collecting sorted cells by adding $1{\sim}1.5$ mL medium and washing on a roller for 5 minutes to fully cover the inner tube surface.

Cell suspensions for flow cytometry

Due to the large body of fluid surrounding the cells, cell suspensions to be analyzed by the flow cytometer may be pipetted directly into untreated FC tubes. Still, suspensions are generally diluted with (filtered) PBS in case of markedly high cell densities and/or small samples: While the BD FACSAria II can handle high cellular throughput and acquire up to 70 000 events per second[58], tuning flow cytometer settings requires an active flow. Appropriate dilution ensures that cells are not unnecessarily lost during the initialization process and enough cells remain for experimental measurement and/or sorting. As the flow cytometer measures the cellular throughput in real time, samples can be diluted as needed.

Flow cytometry and the matter of sterility

Like most (biological) lab equipment, flow cytometers are susceptible to contamination by factors that can affect experimental outcomes, ranging from biological species (e.g. bacteria, mold) to their derivatives (e.g. endotoxins) and traces of reagents (e.g. RNAses)[61]. Although many flow cytometers, including the FACSAria II[62], have integrated features that facilitate cleaning and decontamination, the procedures require regular application as contaminants return to pre-cleaning levels in a matter of days. It is therefore vital for continued culturing of sorted cells to work as sterile as possible and to take measures such as collecting cells in medium containing pen/strep.

3.3. Experimental protocols

3.3.1. Maturity profile exploration of stock THP1 and U937

THP1 and U937 were newly revived to determine the degree of maturation in the species used in this lab. Following the resting phase, both THP1 and U937 were stained with CD14 and CD16 AB as detailed in 3.2.4 (p.14) to create four conditions [Negative control, CD14-only control, CD16-only control, and Stained sample] for each cell line. After washing, cells were immediately taken for analysis with flow cytometry as detailed in section 3.4 (p.21). In addition, voltages for FSC, SSC, CD14 fluorophore and CD16 fluorophore channels were established; values are denoted in Table 5 (p.21).

3.3.2. Protocol 1: Maturation of THP1 and U937 with PMA and CSF1

The negligible degree of maturation for both cell lines in this lab was strongly suggestive that these cells required a rigorous maturation protocol to achieve a classical mature phenotype. As PMA is a well-established reagent for inducing a maturation response towards a macrophagic phenotype, this seemed like a good place to start. In addition, findings by Aldo et al. (2013)[52] pointed to high cell density being an important factor in monocyte maturation.

However, THP1s kept at high cell densities for a prolonged period of time were shown to become highly heterogeneous. It was hypothesized that the presence of M-CSF, a potent growth factor that stimulates proliferation and differentiation of monocytes[63], might make the immature monocyte-like cells more responsive to PMA as well as more amenable to differentiation, thereby allowing maturation at cell densities that are less likely to induce heterogeneity.

In addition, the experiences of my senior researchers were taken into consideration, in the sense that the standard practice for differentiation of THP1 and U937 in this lab dictated the use of at minimum 50 ng/mL PMA; to compare, Aldo and colleagues successfully matured THP1s after 24hr stimulation with a mere 10 ng/mL PMA.

For their research, M-CSF was kept at an equal concentration of 10 ng/mL; stimulation with M-CSF allowed THP1 cells to maintain a healthy phenotype at lower cell density, but maturation wise they did not respond to this concentration as desired. Combining these aspects resulted in the decision to test a low and high concentration of both PMA and M-CSF.

THP1 and U937 were seeded in separate 12-wells plates at the confluency density of $5 * 10^5$ cells/mL[64] with PMA [25;50 ng/mL] and/or CSF1 [10;30 ng/mL] concentrations as illustrated below.
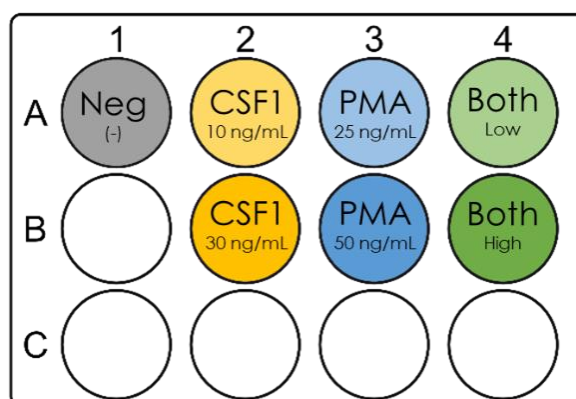
Figure 4 Plate layout for 24hr maturation of THP1/U937 with PMA and CSF1

The stimulated cells were stained same as before (3.2.4, p.14) with CD14 and CD16 AB to create the four conditions [Negative control, CD14-only control, CD16-only control, and Stained sample] for each cell line. The samples were fixated and stored (overnight) at 4 °C until flow cytometry (3.4, p.21).

3.3.3. Protocol 2: Maturation of THP1 with PMA and VD3

Following the disappointing results of protocol 1, it was decided to continue with only THP1 cells. The reasoning behind the choice of THP1 over U937 is detailed in the discussion (5.1.1, p.45). With THP1, a protocol was attempted that was inspired by the reportings of Baek2009 and Liu2005 as well as Garcia1999, all introduced in section 1.6 (p.10): Stimulation with both PMA and VD3 would be combined with an increased stimulation duration of 72 hours. In addition, suspended and adhered cell fractions following stimulation were henceforth not pooled, but analysed as separate conditions.

THP1 cells were seeded in a 12-wells plate at the confluency density of $5 * 10^5$ cells/mL[64] with PMA (16.2 ng/mL) and/or Vitamin D3 (260 µg/mL) as illustrated below and incubated for 72 hours.
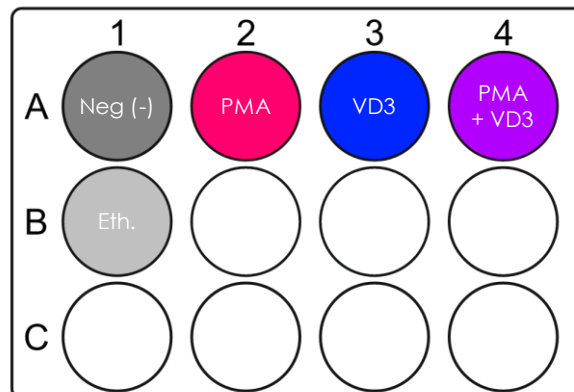
Figure 5 Plate layout for 72hr maturation of THP1 and U937 with PMA and VD3

Suspended and adhered cells were collected as in the previous protocols, but afterwards kept apart as distinct conditions. Cells were counted with Trypan Blue and Luna-I™ cell counter (n1) / Neubauer counting chamber (n2) / Luna-II™ cell counter (n3). [Negative control, CD14-only control, CD16-only control and Stained sample] were prepared for all stimulation and suspended/adhered fraction combinations. Flow cytometry settings were kept consistent with previous protocols, with one exception: between n2 and n3, the CD13 staining solution was tested and the appropriate corresponding channel voltage was determined. The result is denoted in Table 5 (p.21). However, although the CD13 staining was left out in n3 for consistency with n1 and n2, the CD13 channel voltage was not reversed due to an oversight. This is addressed in the discussion (5.1.4, p.45).

3.3.4. TNF-α secretion on PVDF membrane

In order to investigate the effect of adherence on cell maturation more substantially, the secretion of TNF-α following the second maturation protocol was compared between adhered and suspended cells with the use of anti-TNF-α AB coated membranes and fluorescence microscopy.

Membrane preparation

PVDF membranes were cut to fit into a 24-wells plate. Membranes were incubated in 100% methanol for about 1 minute and washed once with PBS for 5 minutes. Membranes were transferred to sterile 24-wells plate and incubated in 200 µL TNF-α antibody solution. Plate was incubated overnight at 4 °C. After washing with PBS once, membranes were incubated with 450 µL 3% BSA in PBS for 2 hours to block nonspecific binding. After washing with PBS once, membranes were covered with O-rings and kept overnight at 4 °C.

Cell stimulation & Supernatant incubation

Cells were seeded in a 6-wells plate at the confluency density of $5 * 10^5$ cells/mL[64] with PMA (16.2 ng/mL) or medium only. Following 72hr incubation, the suspended and adhered cell fractions were

collected and kept separate. Cells were accidentally centrifuged before counting. Supernatant from suspension cells was collected as Pre-Split secretion and stored overnight at 4 °C. Cells were resuspended in 500 μL medium. Cells were then counted with Trypan Blue and Luna-II™ cell counter. Suspended and adhered cell fractions were seeded separately in a 12-wells plate at $8.85 * 10^4$ cells /mL.

After 24hr incubation, cells were counted again with Trypan Blue and Luna-II™ cell counter. 300 μL of all conditions' supernatant, including Pre-Split, was added to a respective TNF-α AB-coated PVDF membrane in the 24-wells plate. Membranes were incubated with supernatant for 72hrs at 37 °C.

Membranes were washed with 0.05% Tween20 in PBS on shaker for 20 minutes at 300 RPM. Membranes were washed thrice with a BSA wash: 1% BSA in sterile filtered PBS on shaker for 5 minutes. Membranes were incubated with TNF-α biotinylated antibody on shaker for 2 hours. Membranes were BSA washed 4 times followed by incubation with streptavidin-PerCP for 1 hour in the dark. O-rings were removed and membranes were BSA washed thrice in the dark and washed once with MilliQ on shaker for 5 minutes in the dark. Membranes were left to dry overnight before imaging.

Fluorescence Microscopy and Image Analysis with ImageJ

Membranes were imaged with NIKON Ti-E inverted microscope (PE filter cube) (10X * 10X) (50 ms exposure time). Membranes were analysed with ImageJ: Threshold was applied according to settings presented in Figure 6 to select fluorescent area. Original values were measured to calculate average grey value for each membrane. A multi-point selection was used to measure average background value for each membrane. Fluorescence was corrected for background by subtraction: $F^{\char94} = F_{Average} - F_{Background}$. Corrected fluorescence $F^{\char94}$ was additionally normalized over total cell concentration and live cell concentration.
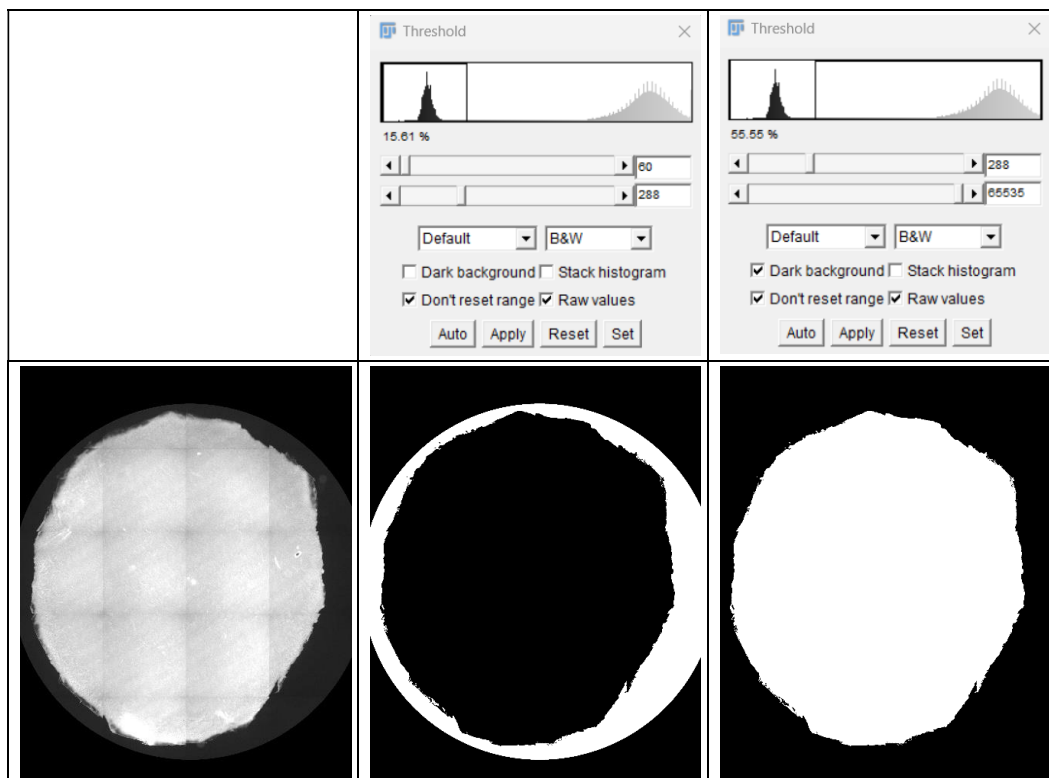
Figure 6 Exemplified by Negative control Suspension, membrane areas were selected based on an ImageJ grey-value threshold. Background area was partly selected with a multi-point free form selection inside the empty well area to get an estimate of the average background fluorescence. Original values were used in calculations.

3.3.5. Protocol 3A: Maturation of THP1 with PMA in T-75 flask (n1, CD13)

Although not resulting in fully satisfactory results, protocol 2 did yield a workable CD14+ cell fraction in the case of PMA (16.2 ng/mL, 72 hrs). Therefore, it was attempted to mature a larger number of cells at a time by stimulating THP1 cells in a T-75 flask rather than a wells plate.

In addition, the lack of success so far warranted a more extensive investigation of cell maturation. On that account, CD13 and HLA-DR expression were decided to be included as respectively a measure for maturity and immaturity.

Originally, HLA-DR had been planned to be included as a marker in n1 of protocol 3, alongside CD13. However, the resulting number of control samples was deemed unworkable due to the combination of limited availability of the flow cytometer and the extensive tuning times associated with experimental controls for fluorescence-overlap compensation. Thus, only CD13 expression was added as a measurand in n1.

In contrast, as fluorescence-overlap compensation controls for CD14 and CD16 ABs had been measured several times this at this point, CD14-only and CD16-only stained conditions offered no further relevant information and were henceforth omitted.

THP1 were seeded in a T-75 flask at the confluency density of $5 * 10^5$ cells/mL[64] and incubated for 72 hrs with PMA (16.2 ng/mL) (13 mL cell suspension in total) or culture medium only (15 mL cell suspension). T-75 flasks were kept in horizontal position to keep differences with the culture conditions of the wells plate of protocol 2 as small as possible. For both the suspended and adhered fractions of Medium-only, as well as the adhered fraction of PMA stimulated, 200 uL cell suspension was added to two sterile FACS tubes. One of each was stained with CD14, CD16 and CD13 AB (3.2.4, p.14) to create [Negative control and Stained sample] for each condition.

For the suspended fraction of PMA stimulated, 200 uL and antibody solution was added to four sterile FACS tubes for the controls [Unstained, CD13-only, CD13&CD14 and CD13&CD16]. 2600 uL was added to another sterile FACS tube and stained with all three antibodies for the stained sample. FC settings were kept consistent with Table 5 (p.21), including the CD13 channel voltage as introduced in n3 of protocol 2 (3.3.3, p.17).

3.3.6. Protocol 3B: Maturation of THP1 with PMA in T-75 flask (n2, CD13 & HLA-DR)

Cells were stimulated in concordance with protocol 3A above. HLA-DR expression was additionally included as a measurand.

For the adhered fractions, 200 uL cell suspension was added to two sterile FACS tubes and one of each stained with CD14, CD16, CD13 and HLA-DR AB (3.2.4, p.14) to produce [Negative control and Stained sample].

For the suspended fraction of the culture medium-only control, 200 uL cell suspension and respective antibody solution was added to 6 sterile FACS tubes for the controls [Unstained, HLA-DR-only, HLA-DR&CD14, HLA-DR&CD16 and HLA-DR&CD13] as well as the fully stained sample.

For the suspended fraction of PMA stimulated, 200 uL cell suspension and respective antibody solution was added to 3 sterile FACS tubes for the controls [Unstained, CD13-only, CD13&HLA-DR]. 1500 uL cell suspension was added to another sterile FACS tube and stained with all four antibodies. Controls were split between PMA and Medium-only suspended cells because of uncertainty regarding expression levels and to safeguard that enough PMA-stimulated suspension cells would be left for sorting.

In addition, appropriate HLA-DR channel voltage was established, as denoted by Table 5 (p.21).

3.3.7. Continued culturing of cells sorted with FACS

Fluorescence-activated cell sorting of PMA-stimulated THP1

After the stimulation of THP1 in T-75 flasks of Protocol 3 (n1) failed to reproduce the CD14+ fractions of the well plate culture of Protocol 2, there were not enough classical monocytes to be sorted for use in extensive subsequent research. Despite the T-75-derived PMA suspended cells totalling to $\sim 1.5 * 10^6$ cells, the mere 10^4 CD14+ cells that could be sorted warranted combined use for a single condition. To not waste the efforts up to that point, cells were instead sorted into two populations based on CD13 expression: one with a considerable shift that was deemed Mature and one without that was deemed Immature. The unsorted cells were kept as a control.

Sterile FACS tubes with 1 mL culture medium were prepared for FACS as detailed in 3.2.6 (p.15). With old compensation values (refer Table 6 on p.23), cells were sorted into CD14+ Classical cells, CD13+ Mature cells and CD13- Immature cells. Gates were set as presented in Figure 24A (p35).

Protocol 4: Extended maturation of CD13++ and CD13+ sorted THP1s with PMA (n1)

The three groups Mature, Immature and Unsorted control were cultured for seven days with a range of PMA concentrations (0;8.1;25;50 ng/mL), illustrated in Figure 7 below, to investigate if relevant information could be discovered about:

1) how more mature cells compare to less mature cells regarding morphology and behaviour, as well as the response to continued stimulation of maturation of PMA
2) how low-concentration PMA pre-stimulated cells compare to the non-pre-stimulated cells of the preceding protocols regarding the response to stimulation with higher PMA levels
3) how FACS-sorted THP1s compare to unsorted cells
4) how extended PMA stimulation affects THP1s that show resistance to maturation in comparison with reported THP1 responses to comparable culture conditions in other labs

Cells were seeded in a 12-wells plate at a density of $\sim 7 * 10^4$ cells/mL, except for CD14+ cells as only $1 * 10^4$ cells were sorted. Attributed to the low cell density, there was no need to refresh the medium throughout the experiment.
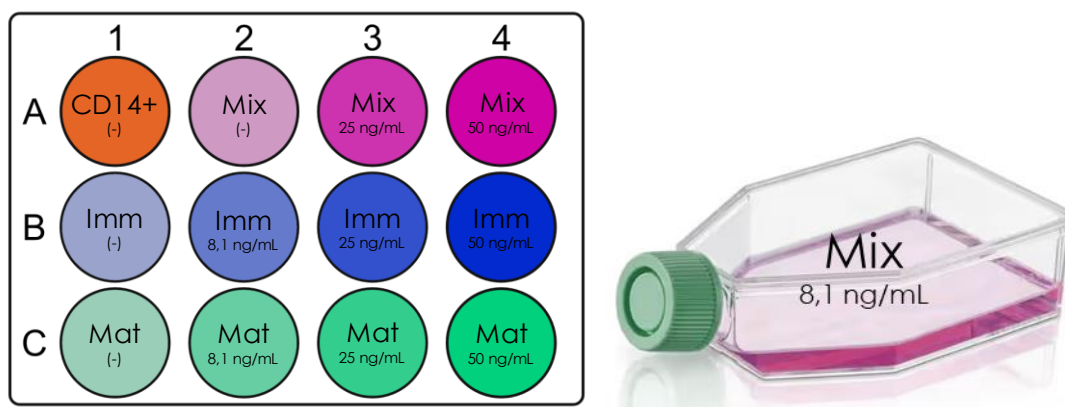
Figure 7 (Left) Plate layout for Extended maturation of sorted cells.
(Right) The leftover condition Unsorted mixture with 8.1 ng/mL PMA was cultured in a T25 flask.

As the absolute number of cells on day 7 was relatively low for all conditions (on average $\sim 3 * 10^4$), and little evidence was discovered to suggest significant differences between fractions, the adhered cells were added to the suspended fraction in case of B4 (Imm 50 ng/mL, $\sim 1 * 10^4$) and C4 (Mat 50 ng/mL, $\sim 1.5 * 10^4$). The adhered fraction was negligible in all other cases and therefore discarded. Cells were resuspended in 400 uL medium. For all conditions, 200 uL [Negative control and Stained sample] were prepared for analysis with flow cytometry (3.4, p.21).

3.4. Flow cytometry

3.4.1. Channel voltages

Flow cytometry is a technology that allows for rapidly successive analysis of several cell characteristics at single-cell level. The FC working principle is illustrated in Figure 9 (p.22). The conversion of scattered light to an electric signal with photodiodes allows for quantification of forward scatter (FSC) as a measure for cell size and side scatter (SSC) as a measure for cell granularity – a quality that represents cell complexity(*Before FlowJoTM | FlowJo, LLC*, n.d.). For consistent and high-intensity scatter behaviour, the interrogating laser is required to be of a smaller wavelength than the cell under investigation. As THP1 and U937 cells are relatively small, the 1.0 filter was used during measurements. By making use of excitation lasers, total cell fluorescence can be quantified to determine the degree of autofluorescence or binding of fluorescent labels.

By setting gates, cells can be grouped based on their characteristics and sorted based on the produced voltages. In fluorescence-activated cell sorting (FACS) cells are sorted based on their fluorescence-produced signal. The FACS working principle is illustrated in Figure 10 (p.22). Voltage settings require to be set such that the resulting signal falls inside the measurable range and are to be kept constant throughout experiments to allow for comparison between them. Figure 8 (below) presents the voltage measurements (in scatterplot) of an unstained sample with appropriate channel voltage settings. Channel voltages were tuned as their respective fluorophore–antibody complex was applied during experimentation. The results are denoted in Table 5 (below).
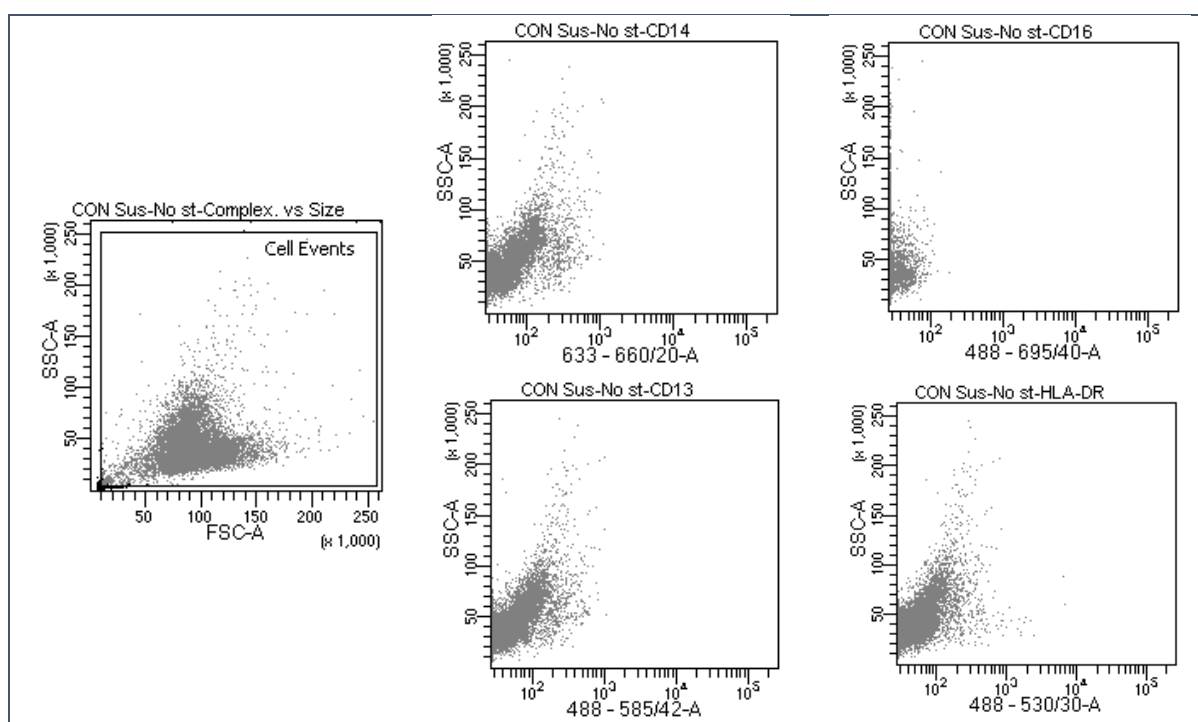
Figure 8 Voltage measurements of an unstained sample. Suitable voltage settings for SSC and FSC result in most cells laying roughly between 50 and 150 (x1000) on both scales. Suitable voltages for fluorescence intensity result in unstained samples (autofluorescence) measuring on average around 10^2, but maximally 10^3, to reserve room within the measurable range for positive samples.

Table 5 Channel voltages for electric conversion of examined qualities to fall within the measurable range

Channel	FSC	SSC	488/530/30	488/585/42	488/695/40	633/660/20
Quality	Size	Complexity	HLA-DR	CD13	CD16	CD14
Voltage (V)	35	300	390	400	450	400
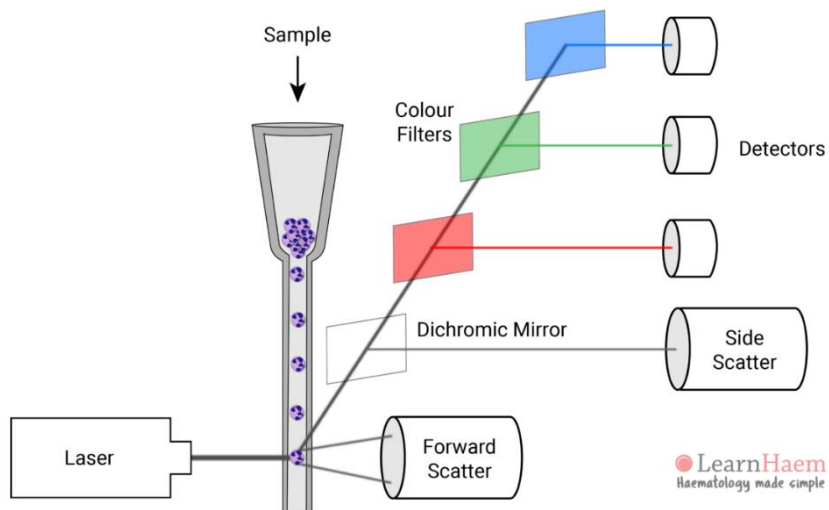
Figure 9 Schematic illustrating the working principle of flow cytometry. Cells are transported at a fast pace past one or more lasers. Cell characteristics determine the intensity and/or wavelength(s) of light that reaches the detectors on the other side. Use of dichroic mirrors and colour filters allows for simultaneous measurement of multiple cell characteristics. The lasers additionally allow for the employment of photosensitive species such as fluorophores. Adapted from LearnHaem[66].
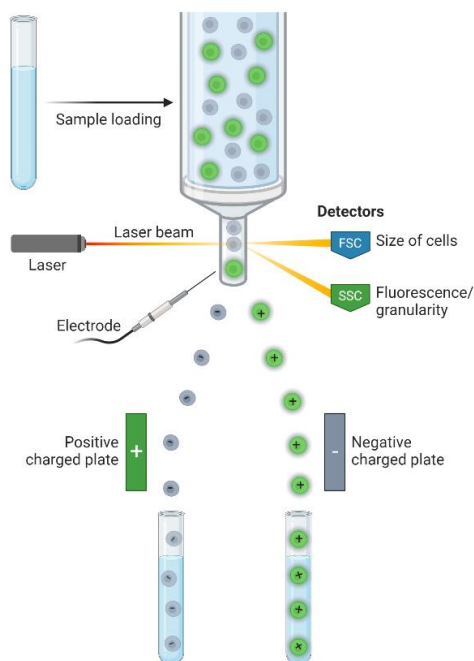
Figure 10 Schematic illustrating the working principle of (fluorescence-activated) cell sorting. Following flow cytometry, an electrode imposes an electrical charge on (fluorescence-based) selected cells that allows electromagnets to steer their trajectory in two directions. By directing the expelled and/or unaffected cells to appropriate containers, cells can be sorted as desired and recovered for further application. Adapted from AAT Bioquest[67].

3.4.2. Fluorescence-overlap compensation

Due to the broad emission spectra of fluorescent labelled antibodies, there tends to be overlap between the target fluorophore and other fluorescent particles in the channel wavelength, resulting in a need for compensation. Fluorescence-overlap compensation values were initially based on the experimental compensation control samples leading to values presented in Table 6 below. However, the subsequent results were heavily suggestive of compensation for fluorescence overlap being too low, leading to re-evaluation based on theoretical spectral overlap.

Multiple ways were investigated: overlap based on full spectrum excitation (FSE), overlap based on laser excitation (LE), overlap based on laser excitation including looped spillover excitation (LEL) and overlap as calculated by SpectraViewer (*ThermoFisher scientific*)[68]. The fluorescence spectra used for calculations, produced with SpectraViewer, have been appended as Figures Figure – 37 (A.1, p.57-p.60). FSE overlap was calculated by dividing FSE emission of overlapping fluorophore by FSE emission of target fluorophore at channel wavelength. The same method was applied to LE emission for LE overlap. LEL additionally considers the target fluorophore emission as a result of the spillover excitation of the target fluorophore by emission of the overlapping fluorophore at channel wavelength. Theoretical values are presented in

Table 7 below, showing FSE being most comparable to the manual estimate. Column *Selected* denotes the new compensation values as used during analysis of all flow cytometry measurements. See also *FACS Fluorescence compensation.xlsx* in the supplementary material.

Table 6 Old compensation values for fluorescence-overlap based on experimental control samples

Channel	Overlapping fluorescence	Compensation (%)
488/695/40	633/660/20	12.00
633/660/20	488/695/40	10.00

Table 7 Comparison between theoretical methods for determining New fluorescence-overlap compensation

Channel	Fluorescence overlap	FACS compensation (%)					
		Full spectrum excitation	Laser excitation	Laser excitation, looped	Spectra-Viewer	Manual Estimate	Selected
488/585/42	488/530	19.35	27	28	33.29	16-20	**21.00**
488/695/40	488/585	2.35	0	0	1.12	9	**11.35**
633/660/20	488/585	5.48	5	6	0.00	5	**5.00**
633/660/20	488/695	12.33	26	33	4.87	20	**12.33**
488/695/40	633/660	50.59	31	40	129.40	51	**50.59**

4 Experimental findings

4.1. Maturity profiles of newly revived THP1 and U937

To investigate the base maturity profile(s) of the cell lines used in this research, CD14 and CD16 expression of newly revived THP1 and U937 cells was measured with flow cytometry (discounting the THP1 10-day resting period). The experimental procedures are detailed in section 3.3.1 (p.16). A selection of results is presented here, for full results refer Table 16 in the Appendix (p.73).

4.1.1. Stock THP1 and U937 comprise two populations that differ in size and complexity

SSCvsFSC scatterplots, presented in Figure 11 (below), reveal (at least) two distinguishable populations, Population 1 (P1, fuchsia) and Population 2 (P2, aqua), in both cell lines: THP1 [87.5% P1; 7% P2] and U937 [96% P1; 2.5% P2]. Compared to P1, P2 has a lower average FSC (THP1 100 vs 50; U937 80 vs 50), meaning P2 cells are smaller in size. In addition, P2 has higher SSC (30 vs 75 in both cell lines), thus higher relative cell complexity than P1 cells. As their natural fluorescence differs, the populations have a different control baseline that require them to be analysed separately for fair positive expression gating.
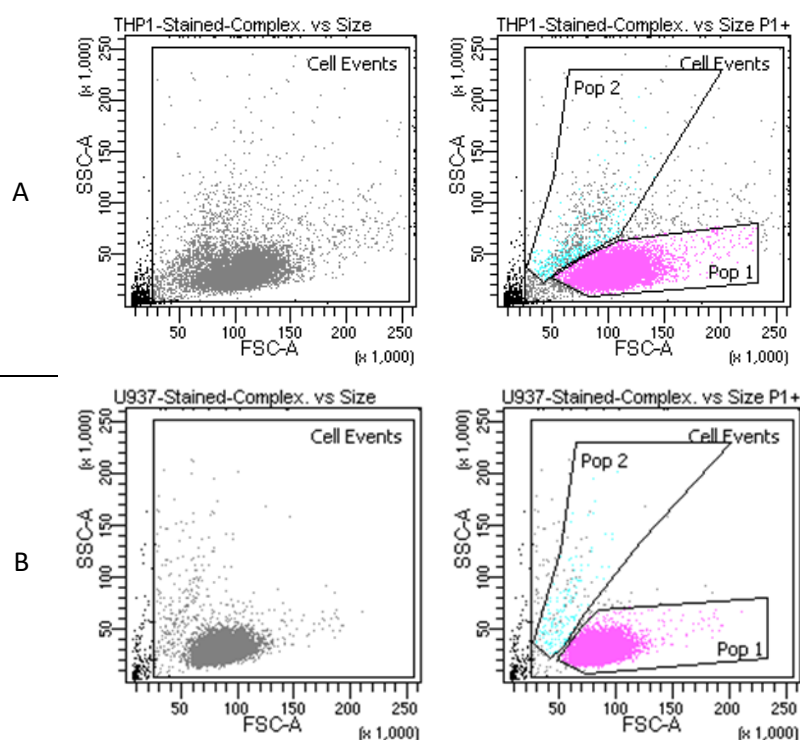
Figure 11 SSCvsFSC scatterplots for newly revived THP1 (A) and U937 (B) cells show 2 distinguishable populations: P1 (fuchsia) and P2 (aqua). P2 has lower FSC and higher SSC compared to P1.
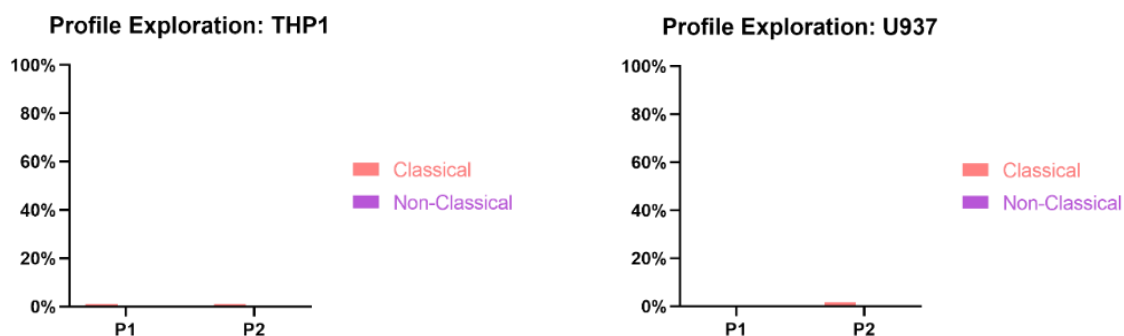
Figure 12 Quantification of maturity profile shares reveals no significant populations with either classical or nonclassical maturity in both newly revived (left) THP1 and (right) U937 cells.

4.1.2. Stock THP1 and U937 have no significant shares of cells with a mature identity

Expression of CD14, CD16 and CD14vsCD16 for P1 and P2 are presented in Figure 13 (below) for newly revived THP1 and Figure 14 (below) for newly revived U937 cells. Separate analysis of CD14vsCD16 for P1 and P2 shows expression of both maturity markers to be negligible for both cell lines. Consequentially, no significant population with either classical or nonclassical maturity can be discovered. It is not surprising that quantification, presented in Figure 12 (p.24), reveals no significant shares of either maturity profile for both cell lines (<2% in all cases).
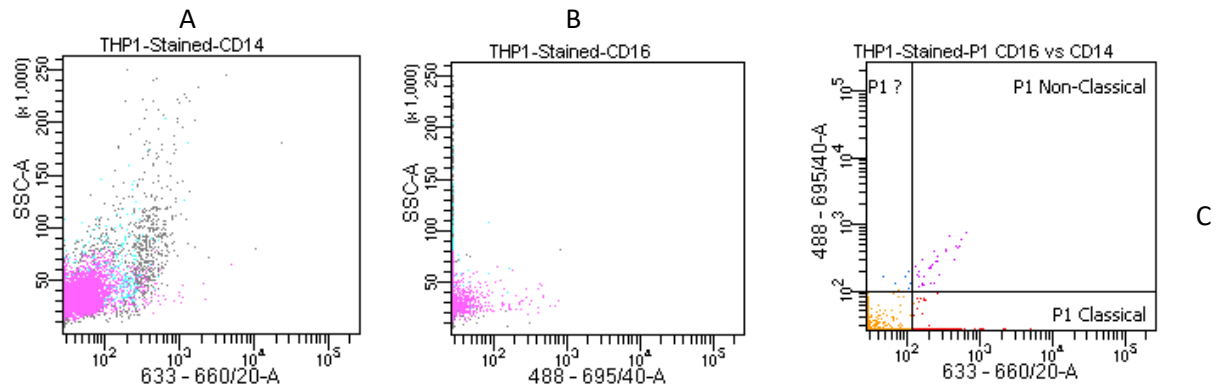
Figure 13 Newly revived THP1 expression of (A) CD14 and (B) CD16. Separate analysis of CD14vsCD16 for (C) P1 and (D) P2 reveals expression levels of both maturity markers to be negligible in both populations.
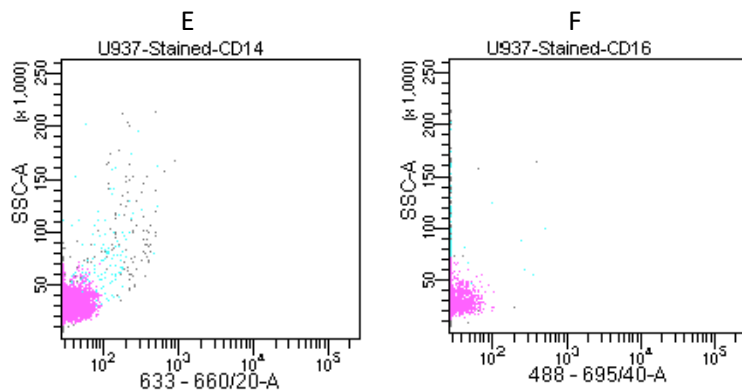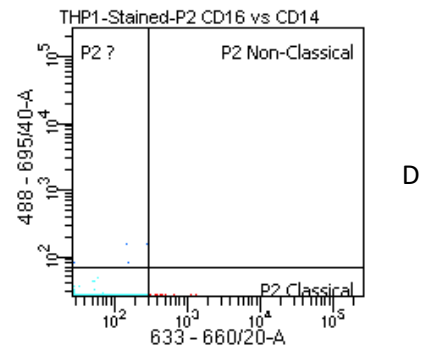
Figure 14 Newly revived U937 expression levels of (E) CD14 and (F) CD16. Separate analysis of CD14vsCD16 for (G) P1 and (H) P2 reveals expression levels of both maturity markers to be negligible in both populations.
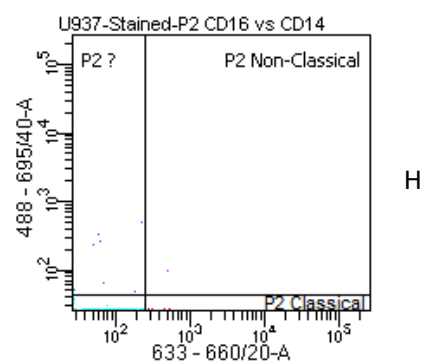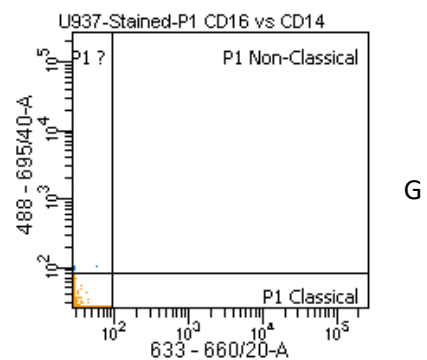
4.2. Protocol 1: Maturation response of THP1 and U937 to PMA and CSF1

To induce a classical maturity profile, THP1 and U937 cells were stimulated for 24 hours with PMA [25;50 ng/mL] and/or CSF1 [10;30 ng/mL] as detailed in section 3.3.2 (p.16).

Brightfield morphology images (400X) are presented in Figure 16 (p.27) for THP1 and Figure 17 (p.28) for U937. Additional 100X magnification images have been appended as Figure 41 (p.63) and Figure 42 (p.64). Morphology indicates both cell lines react to CSF1, with more clumping behaviour compared to the negative control. THP1 shows increased spreading in case of both PMA concentration, while this behaviour is not recognized in U937. Combined stimulation results in the combined behaviour as observed with separate stimulants for all cases.

Quantification of classical and nonclassical shares are presented in Figure 38 (A for THP1, B for U937) below. SSCvsFSC scatterplots have been appended in For full results see the sup. material matrix (Table 16, p.73). The results indicate a possible effect of PMA for both concentrations in both cell lines, seemingly stronger in P2 than P1, although with a maximum population fraction of ~5% none of these conditions reach a fraction large enough for continuing with FACS and use in subsequent research. As the maturity profile fractions remain insignificant, nothing can be said on this matter about differences between P1 and P2 at this time.
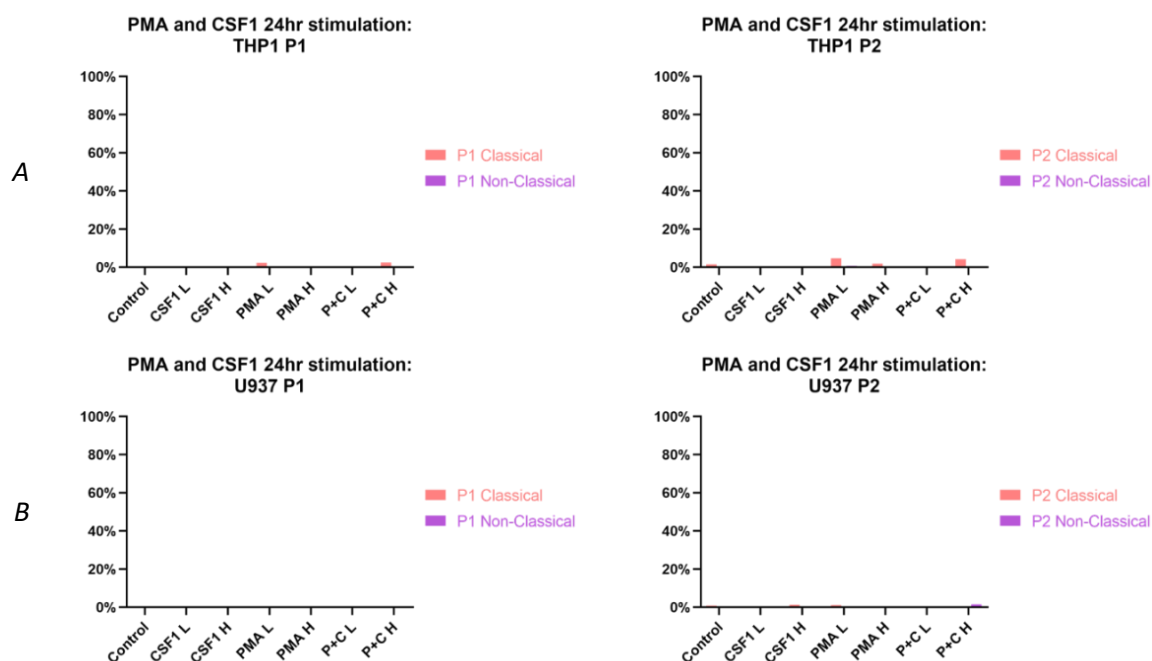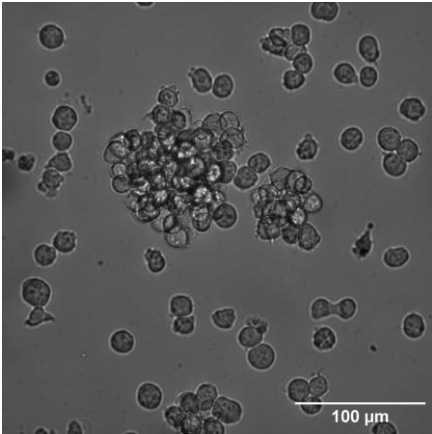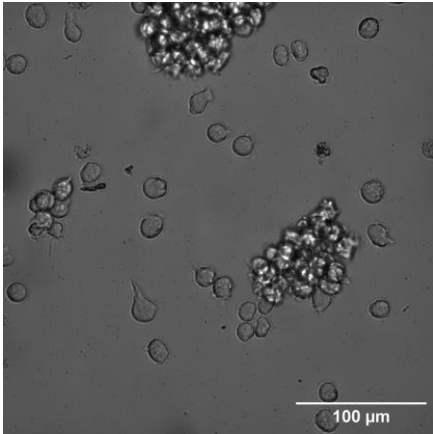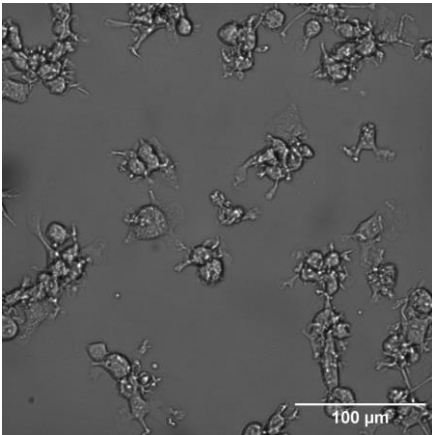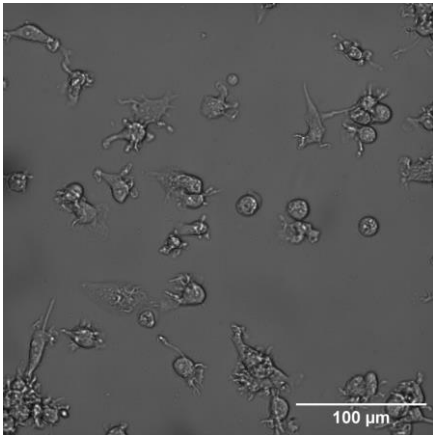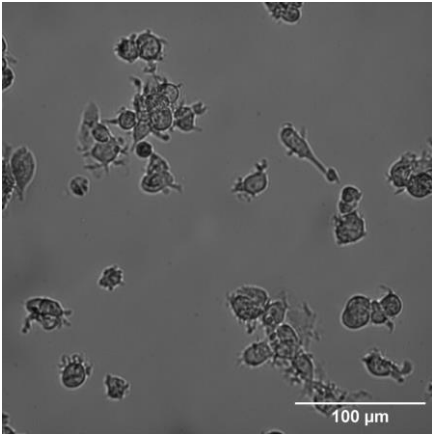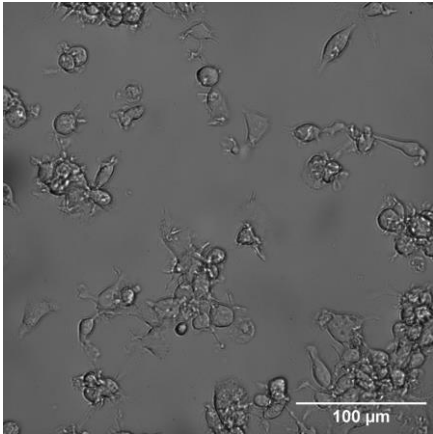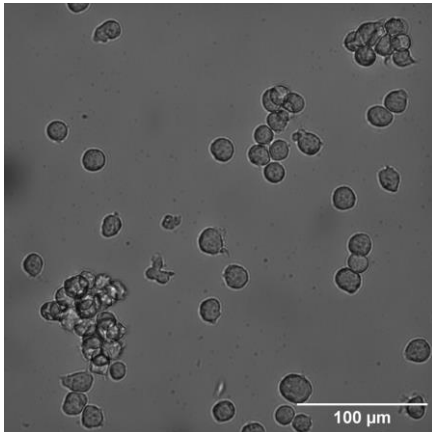
Figure 15 CD14 and CD16 positive fractions of (A) THP1 and (B) U937 cells allow no significant Classical or Non-classical populations to be discovered in either cell line (<5% in all cases).

THP1 (400X)		
	Low	High
CSF1		
PMA		
PMA+CSF1		
NEG		*Figure 16 Brightfield morphology images, magnification 400X. THP1(P18) cells show clumping behaviour when stimulated with CSF1, spreading behaviour when stimulated with PMA, and both behaviours with combined stimulation. Cells were stimulated with CSF1 and/or PMA, at a low concentration for both stimulants (10 ng/mL, 25 ng/mL respectively) as well as a high concentration (30 ng/mL, 50 ng/mL respectively).*
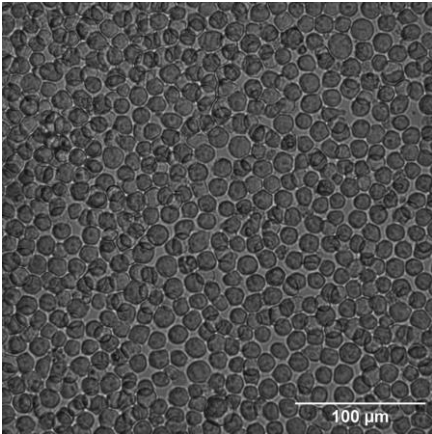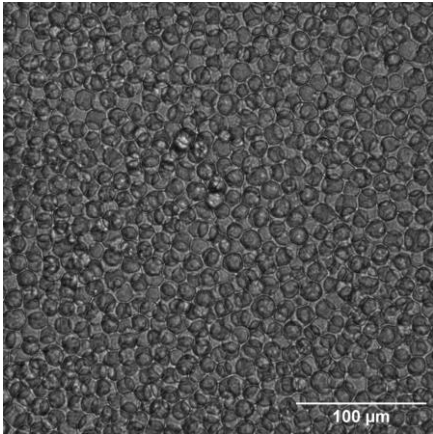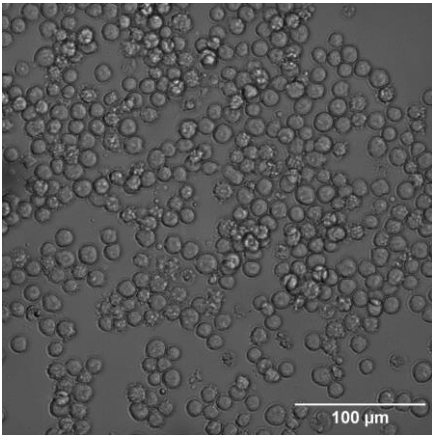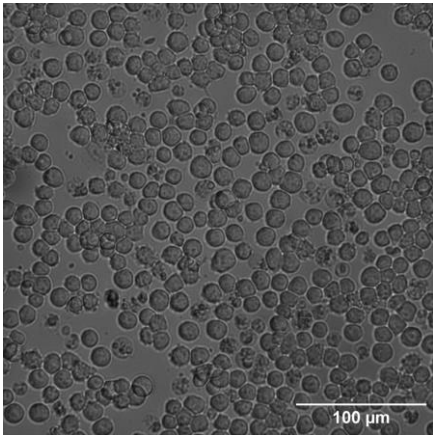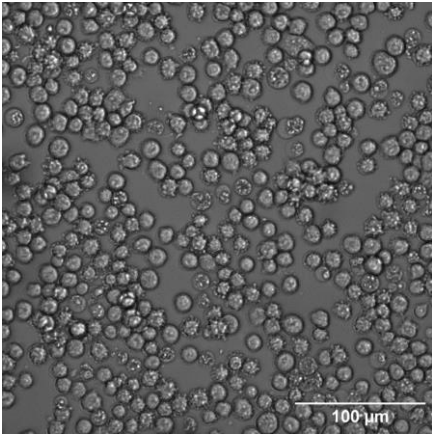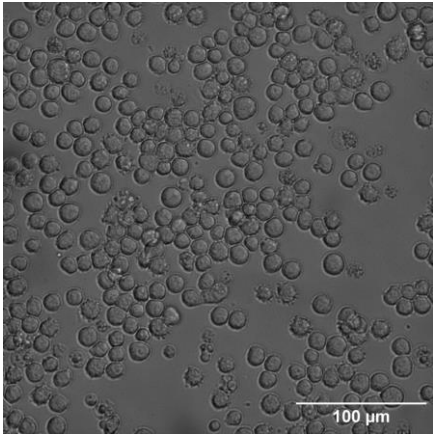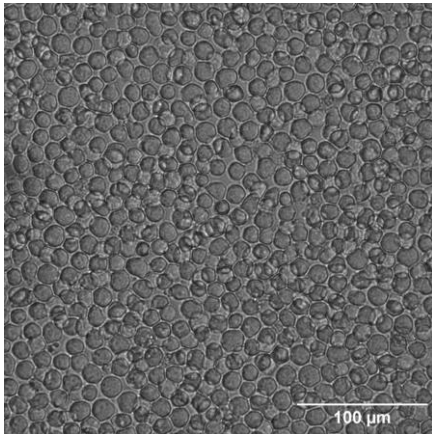
U937 (400X)	
Low	High

Figure 17 Brightfield morphology images, magnification 400X. U937(P18) cells show clumping behaviour when stimulated with CSF1, no spreading behaviour when stimulated with PMA, and clumping behaviour with combined stimulation. Cells were stimulated with CSF1 and/or PMA, at a low concentration for both stimulants (10 ng/mL, 25 ng/mL respectively) as well as a high concentration (30 ng/mL, 50 ng/mL respectively).

4.3. Protocol 2: Maturation response of THP1 to PMA and VD3

Following the unsatisfactory maturation effects of Protocol 1, cells were stimulated according to Protocol 2, detailed in section 4.3 (p.29) Due to the lack of spreading behaviour of U937 and other factors, discussed in detail in section 5.1 (p.45), only THP1 was used going forward. Cells were stimulated with PMA (16.2 ng/mL) and/or Vitamin D3 (260 μg/mL) for 72 hours. Because of a potential effect of adherence vs suspension on results, adhered and suspended fractions were analysed separately. No morphology images could be obtained at this time.

A selection of flow cytometry results and their quantification are presented in Table 14 (p.65). For full results see the sup. material matrix (Table 16, p.73). For the sake of rigor, population 3, also distinguishable in previous results, is henceforth taken into account. P3 has considerably low FSC and SSC in comparison with both P1 and P2, and is likely to be mostly comprised of cell debris. In addition, population 2 can be further split into P2A and P2B based on CD14 autofluorescence; however, as these values change in case of positive CD14 stained cells, we use the 488/585/42 vs 488/530/30 channel values to separate these two groups for analysis. Reasoning behind this is detailed in section 5.1.4 (p.45). It is worth noting at this point that in case of VD3 the average FSC decreases from 100 to 50 and average SSC increases from 75 to ~100 compared to controls, meaning cells are smaller in size and have slightly higher relative complexity. This effect remains in case of combined stimulation with PMA. Furthermore, as n1 PMA results are notably dissimilar from n2 and n3 PMA (lack of P1 and 90% P2 compared to ~45% ± 4%). As the n1 negative controls as well as other stimulation conditions are non-disparate, n1 PMA was considered an outlier and left out of the quantification and further analysis.

Quantification of population fractions (F, p.30) reveals no significant difference between Adhered and Suspended fractions. Results do indicate a significant effect of PMA and Ethanol on P1 and P2 fractions. In case of PMA, P2 share is increased from ~25% to ~45% at the cost of P1 (~65% to ~30%) compared to negative controls (p<0.0001). In case of the Ethanol control, no P1 population is observed, with P2 accounting for roughly 70% of cells (p<0.0001). An increase in P3 from ~3% to ~20% can be observed for both PMA and Ethanol compared to negative controls (~2.5% on average, p<0.05). VD3 seems to further increase the P2 fraction from ~70% to ~90% (p<0.05). Remarkably, VD3 conditions have a P3 fraction that is comparable to that of the negative controls (~3.6% average for all four VD3-stimulated conditions). No notable differences in population fractions can be observed between VD3 stimulation alone and combined stimulation of PMA and VD3.

Quantification of subpopulation fractions 2A and 2B (G, p.30) reveals again no significant differences between Adhered and Suspended fractions.

Quantification of maturity profile fractions (H, p.30) shows clear differences between populations P1, P2A, P2B and P3. P3 can be considered negative for both maturity profiles, with a maximum expression of 4.07% for Non-Classical in P+V Adhered. In the other populations, a clear trend is suggested of PMA stimulation correlating to an increase in Classical maturity expression, although no statistical significance is reached [Adhered: P1 25% (p=0.71), P2A 10% (p=0.98), P3 35% (p=0.25)]. Differences between PMA Adhered and Suspended are statistically negligible (P2B Classical p=0.63). VD3 and P+V do not have a (significant) P1 and P2B population to analyse, but the results for P2A suggest VD3 negates the effect of PMA; the maximum of 0.43% Classical expression in case of P+V Adhered ends up falling below even the negative controls of 2.18% expression.
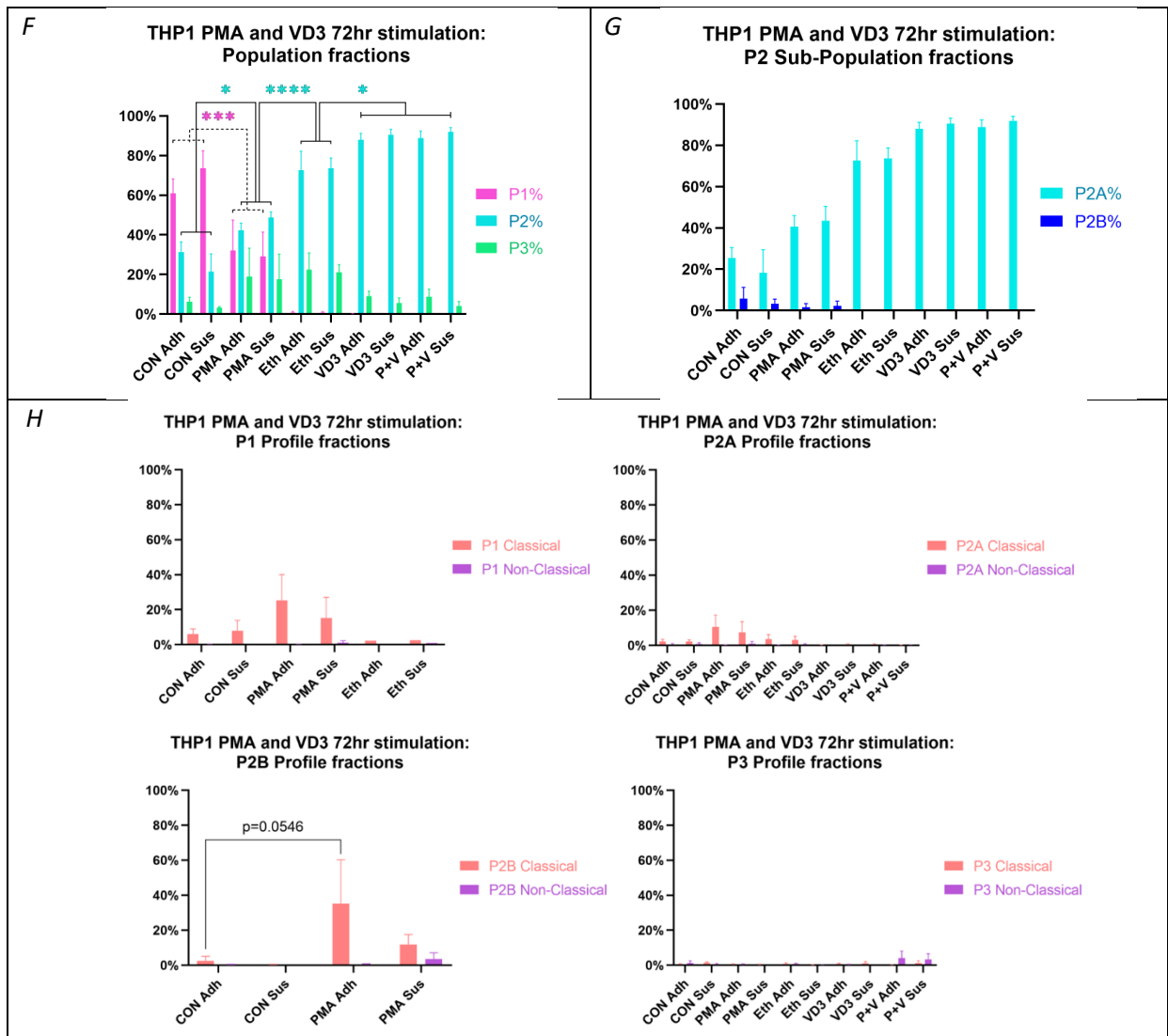
Figure 18 (p.30) presents Viability (A), Size (B) and Adhered fraction (C) for all conditions. No significant effect of PMA on viability could be discovered, while the addition of Ethanol corresponds to a significant decrease in viability from 50% to 30% compared to Control and PMA stimulation. No significant differences could be discovered in size as determined by Luna-I^{TM} cell counter. The adhered fraction was significantly increased in case of PMA and Ethanol stimulation to 35% (p=0.0008) and combined PMA and VD3 stimulation to 36% (p=0.002) compared to 20% adherence in Control.
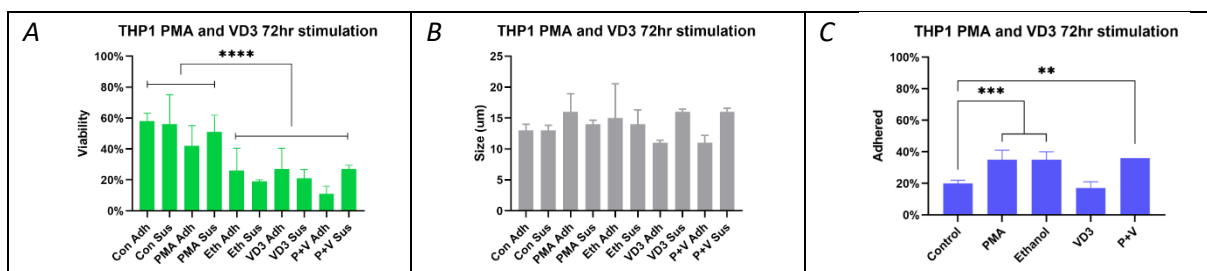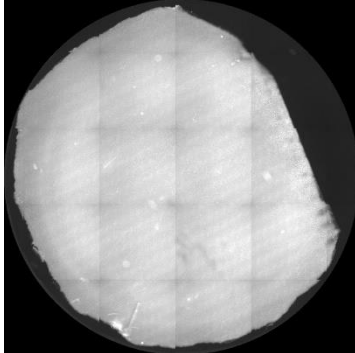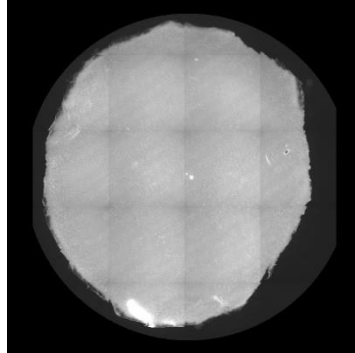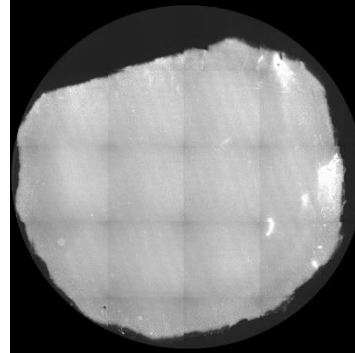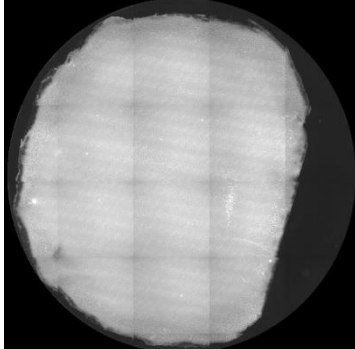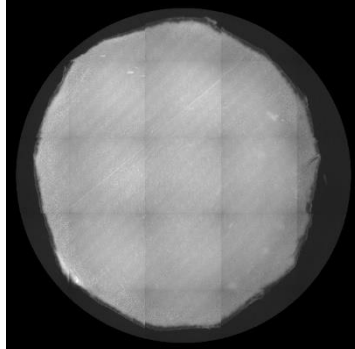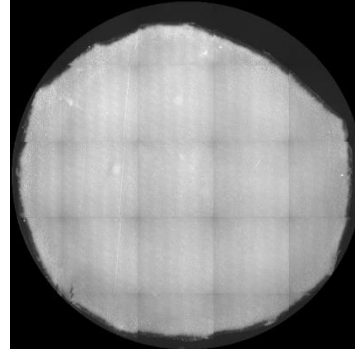
Figure 18 Average A) Viability, B) Size and C) Fraction of Adhered cells for THP1(P20;P18) after 72hr stimulation in a 12 wells plate with PMA (16.2 ng/mL) and/or Vitamin D3 (260 µg/mL). n2(P22) had to be left out due to broken equipment.

4.4. Adhered vs Suspended: TNF-α expression

Post 72hr stimulation, cells were split in adhered and suspended fractions and cultured on top of a TNF-α antibody-coated PVDF membrane, further detailed in section 3.3.4 (p.17). Fluorescence images and quantification are presented in Table 8 (p.31) and Figure 19 (p.31) respectively. Direct quantification of background-subtracted fluorescence (F^) shows no clear differences between adhered and suspended cells. Normalization over total cell concentration reveals a slightly raised expression of TNF-α for PMA adhered, but the trend is in contrast with the negative control where suspended cells have slightly elevated expression levels. Live cell concentration suggests the adhered fraction of PMA stimulated cells produce significantly more TNF-α, although this trend cannot be discovered for either Control Adhered or PMA suspended; one would expect one of these conditions to be elevated comparably such that either PMA stimulation or Adherence results in increased TNF-α expression.

Table 8 THP1(P15) TNFα secretion on coated PVDF membranes
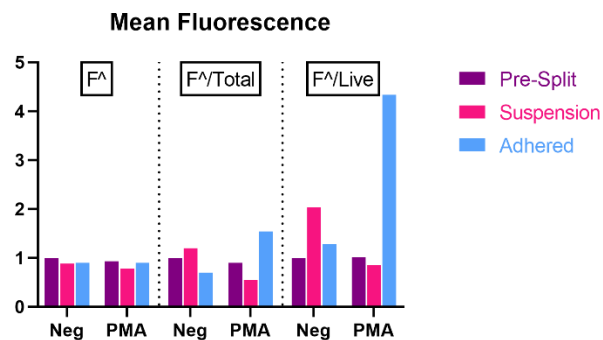
Figure 19 THP1(P15) TNF-α secretion on PVDF membrane quantified

4.5. Protocol 3: Maturation response of THP1 to PMA in T-75

To gain a significant number of Classical mature cells to sort for further research, cells were stimulated 72hrs with PMA in a T75 flask as detailed in sections 3.3.5 (p.19) for n1 and 3.3.6 (p.19) for n2. A selection of flow cytometry results and their quantification are presented here. For full results see the sup. material matrix (Table 16, p.73).

Flow cytometry FSC vs SSC graphs (Figure 20 below) show no immediately obvious differences between culture in a flask versus culture in a wells plate.
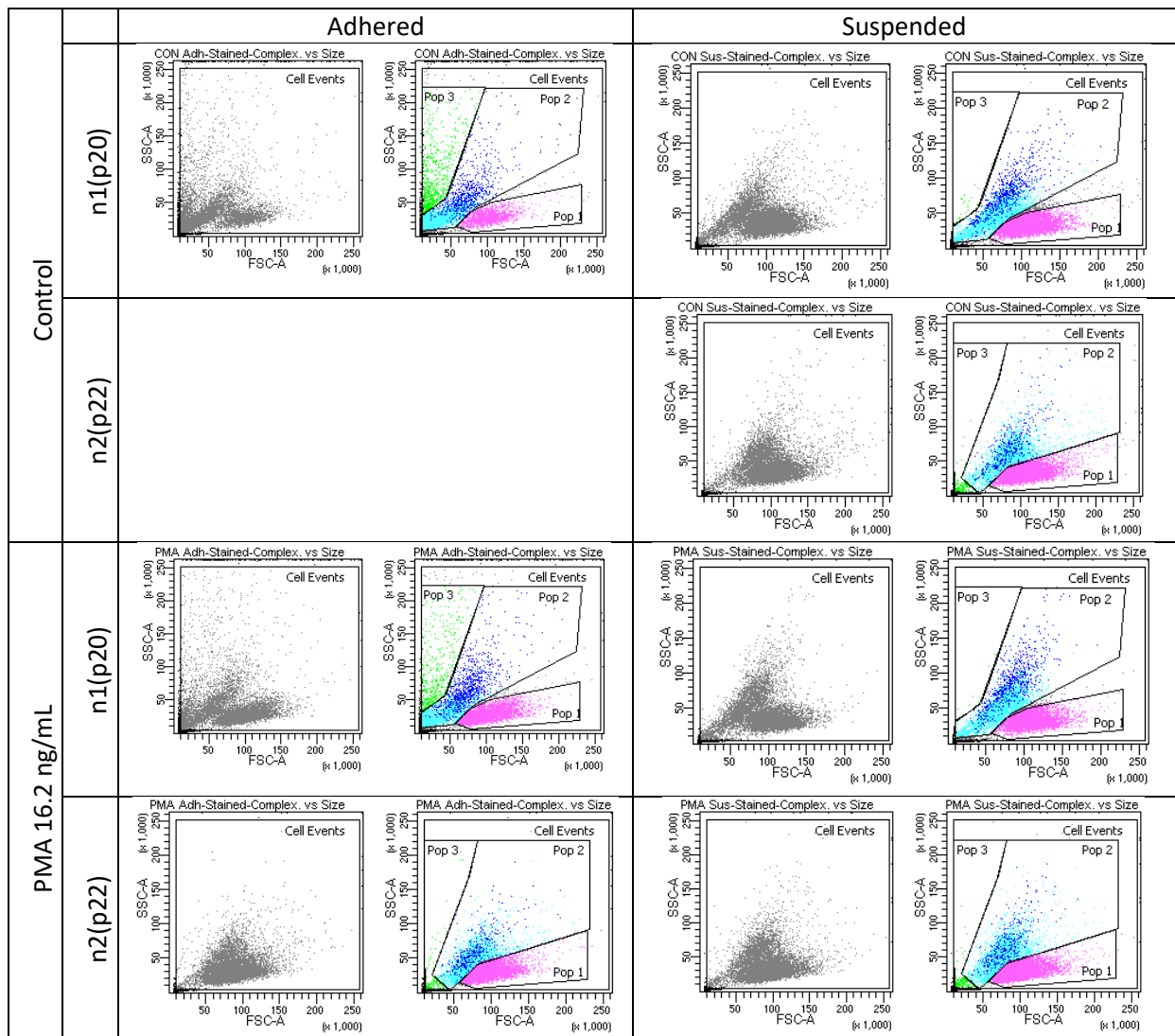
Figure 20 Flow cytometry results for THP1(P20;P22) after 72hr stimulation with PMA (16.2 ng/mL) in a T75 flask. Three populations remain distinguishable.

Population fraction quantification (Figure 21 below) shows a decrease in P1 [60% to 20%] and an increase in P2 [20% to 55%] for Control Adhered compared to stimulation in a wells plate. Furthermore, in both PMA stimulation Adhered and Suspended, P1 is increased [20% to 50%-60%] mostly at the cost of P2 [60% to 40%] compared to wells plate stimulation.

The additional CD13 staining shows cells do express the maturity marker in P1, P2A and P2B. Maturity seems significantly higher in P1 [80%] compared to P2A and P2B [~40% when disregarding CON Adh]. P3 has insignificant CD13 expression in all conditions.
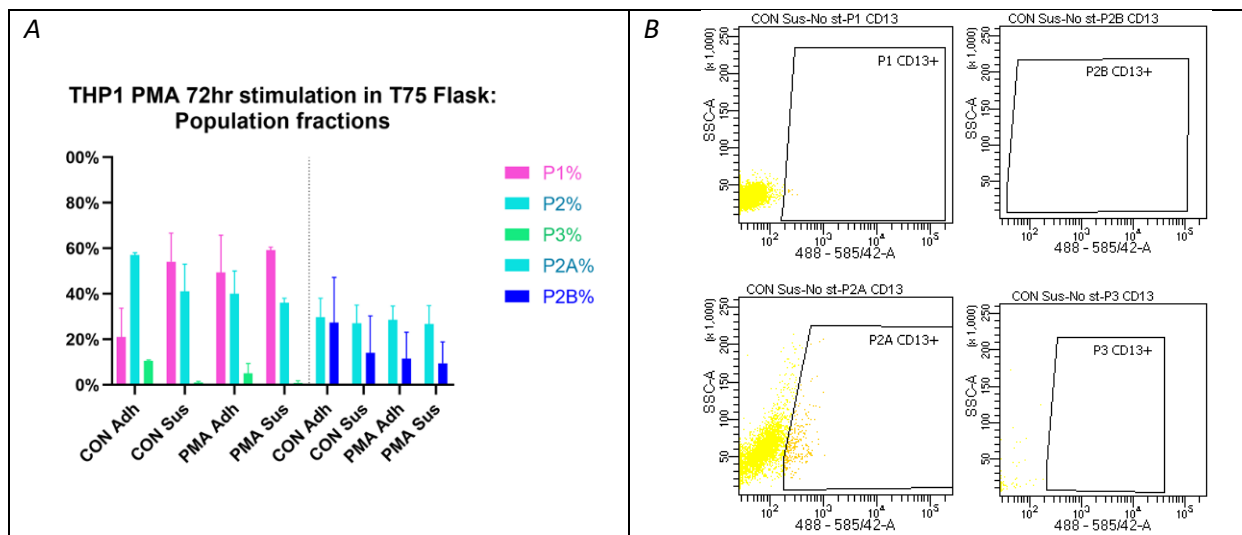
Figure 21 Flow cytometry results for THP1(P20;P22) after 72hr stimulation with PMA (16.2 ng/mL) in a T75 flask. A) Population fractions quantified per condition show an increased P1 compared to previous results. B) CD13 positivity varies between populations, as exemplified by n2 Control Suspension No staining.
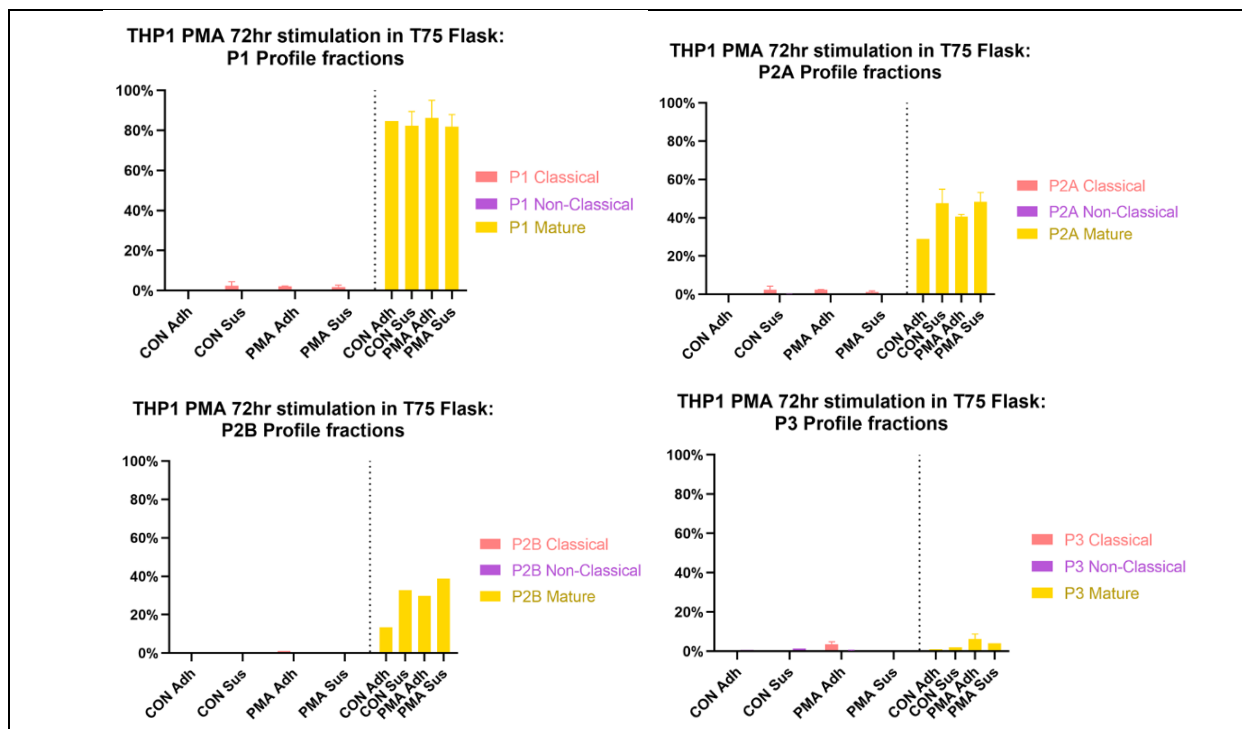
Figure 22 Flow cytometry results for THP1(P20;P22) after 72hr stimulation with PMA (16.2 ng/mL) in a T75 flask. CD13 fluorescence shows P1 has the largest fraction of mature cells (>80% in all conditions), with P2A and P2B having similarly lower fractions (~40%) P3 remains likely to be debris.

Figure 23 below presents Viability (A), Size (B) and Adhered fraction (C) for all conditions. No (statistically) significant differences could be discovered between conditions regarding viability or size. In addition, values are comparable to wells plate stimulation (**Error! Reference source not found.** p.30). On the contrary, adherence fractions are no longer statistically significantly higher in PMA stimulation compared to control in flask culturing like they were in the wells plate (**Error! Reference source not found.** p.30). With about 10% adherence for both conditions, adherence is a little lower in the T75 flask compared to the 12 wells plate of Protocol 2.
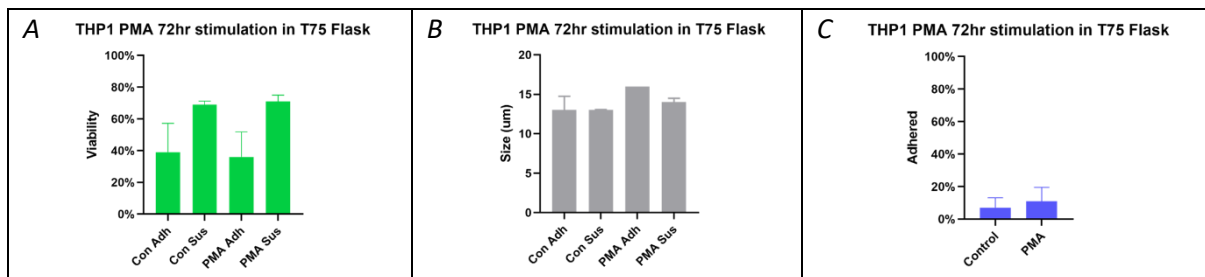
Figure 23 Average A) Viability, B) Size and C) Fraction Adhered cells for THP1(P20;P22) after 72hr stimulation with PMA (16.2 ng/mL) in a T75 flask.

4.6. Continued culturing of Mature, Immature and Classical monocytes

4.6.1. Sorting of Classical mature, Unspecialized mature and Immature THP1 monocytes

Following the stimulation with 16.2 ng/mL PMA for 72 hrs of the previous section (4.5, p.32), the suspended cell fraction was sorted with FACS into Classical mature (OLD.CD14+, CD14+CD13+), Unspecialized mature (OLD.P2, CD14-CD13+) and Immature (OLD.P3, CD14-CD13-) THP1 cells for continued culturing. For further details see method section 3.3.7 (p.20). The flow cytometry results for old compensation values at the time of sorting are presented in Figure 24A (p.35). The FC results were re-analysed after adjusting the compensation values as detailed in section 0 (p.23) and a selection of FC results and their quantification is presented in Figure 24B-D (p.35).

Comparison between old and new compensation results shows that the population sorted as Unspecialized mature (CD14-CD13+) OLD.P2 corresponds to population NEW.P1 (CD14-CD13++), most easily observable in the SSC vs FSC scatterplots that are unaffected by fluorescence overlap compensation. The population sorted as Immature (CD14-CD13-) OLD.P3 corresponds to NEW.P2B (CD14-CD13+). This suggests cells were correctly sorted into a more mature and less mature population.

The population sorted as Classical mature (CD14+CD13+) is a more challenging case: assuming cells remain CD14+ under the new compensation, OLD.CD14+ cells fall in both NEW.P1 and NEW.P2 with a 1:3 ratio as presented in Figure 24 (p.35). Although the localization of the CD14+CD13+ cells under both compensations matches, going forward it must be borne in mind that it is at this point not certain that the cells presenting as CD14+ under both compensations are one and the same.

Average viability and size are presented in Figure 25 (p.36). Viability for sorted cells seems lower compared to unsorted cells, but no statistical significance is reached (p=0.692). No differences in size could be discovered.

Figure 24 Flow cytometry results of 72hr 16.2 ng/mL PMA pre-stimulated THP1(P20) sorting with old compensation used during sorting and new compensation used during analysis. A) Old compensation results showed OLD.P2 (corresponding to NEW.P1) to be CD13+ and were sorted as Mature cells. OLD.P3 (corresponding to NEW.P2B) were based on higher autofluorescence in CD14 and deemed Immature cells. B) NEW.P1 has a significantly higher percentage of CD13+ cells compared to NEW.P2A/B (88% vs 59%;42%). Consequently, OLD.P2/NEW.P1 and OLD.P3/NEW.P2B were correctly sorted as "Mature" and "Immature" cells respectively. C) Assuming OLD.CD14+ cells were indeed CD14 positive, OLD.CD14+ consists of approximately 3:9 = 1:3 Classical NEW.P1 and NEW.P2 cells. D) Analysis with new compensation shows that the sorted population OLD.P3/NEW.P2B contains a negligible number of NEW.P1 cells.
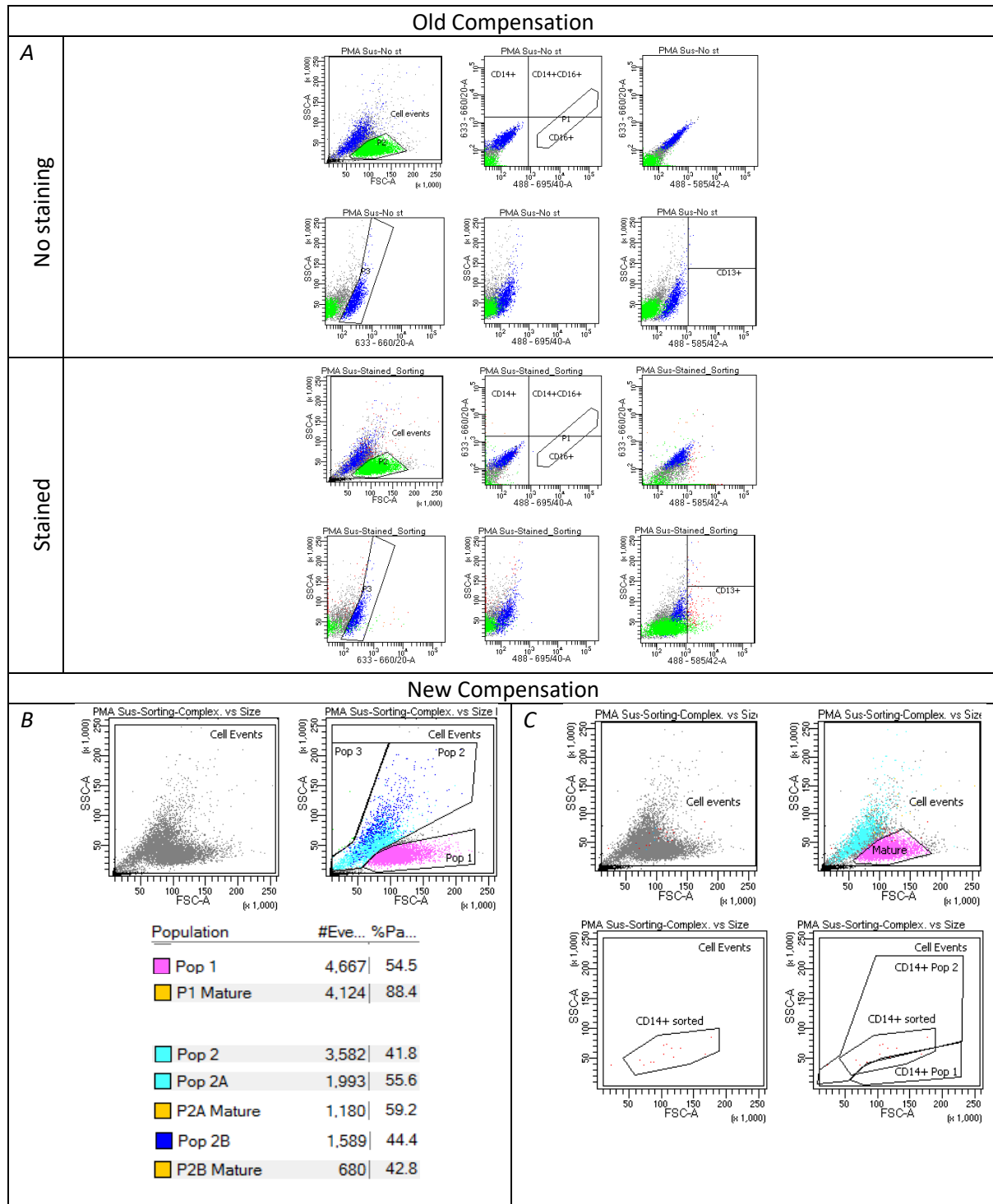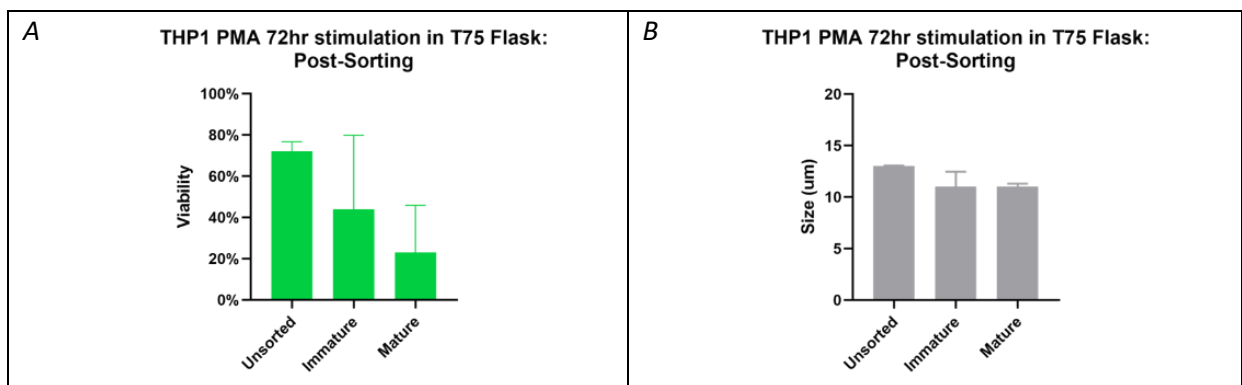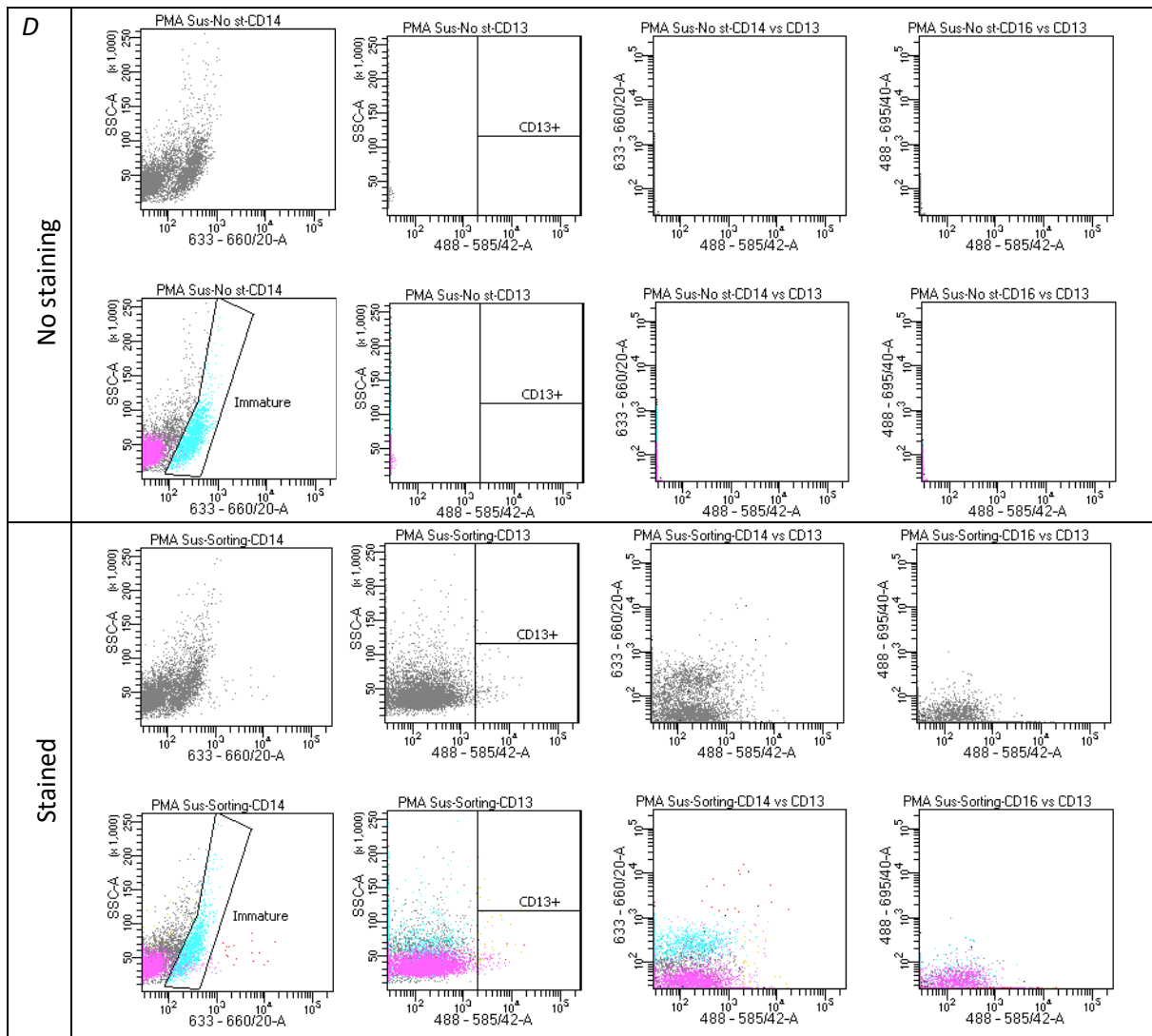
Figure 25 Average A) Viability and B) Size for THP1(P20;P22) Unsorted, Immature and Mature populations after 72hr stimulation with PMA (16.2 ng/mL) in a T75 flask.

4.6.2. Continued culturing of PMA pre-stimulated THP1 cells: Morphology and Behaviour

Following the sorting with FACS, Unspecialized mature (P1, CD14-CD13+) and Immature (P2, CD14-CD13-) cells as well as an unsorted control Mixed were stimulated further for 7 days with a range of PMA concentrations [0;8.1;25;50 ng/mL], further detailed in section 3.3.7 (p.20). Recapitulating results from the previous section, the unsorted mix consisted of roughly 55% P1 and 42% P2 (Figure 24B on p.35). Classical mature cells (CD14+CD13+) were cultured in medium only as there were too few cells for other conditions.

Brightfield morphology images on Day 3 and Day 7 post-sorting are presented in Table 9 (p38) for Classical mature cells and Table 15 (100X magnification for behaviour analysis, appended, p69-72) and Table 10 (200X magnification for morphology analysis, p39-40) for the other sort conditions. Morphology indicated for Classical mature cells some clumping behaviour and little to none spreading behaviour on both days; the low number of cells makes it difficult to determine a change over time as well as to compare with other conditions, however.
Morphology analysis for the other sort conditions indicates increased clumping behaviour in Unspecialized mature compared to Immature and Unsorted samples. Notably, when comparing these results to non-pre-stimulated cells (Figure 16, p.27), all pre-stimulated groups show decreased spreading behaviour for continued 25 and 50 ng/mL PMA stimulation. In addition, the pre-stimulated cells show clumping behaviour comparable to the negative control and high PMA+CSF1 condition for non-prestimulated cells. Behaviour and morphology wise, this makes 72hr 16.2ng/mL PMA pre-stimulated cells after continued stimulation with 25 and 50 ng/mL PMA more comparable to non-stimulated cells (and PMA + high CSF1 stimulated cells) than to directly 24hr 25 and 50 ng/mL PMA stimulated cells.

Table 9. Morphology of CD14+ THP1(P20) cells 3 and 7 days post-sorting. Cells were cultured without stimulation in RPMI medium. Brightfield images taken at 100X magnification for both days, and 200X for Day 7.

A) PMA-prestimulated CD14+ THP1 cells 3 days post-sorting - Negative control (medium only)	

B) PMA-prestimulated CD14+ THP1 cells 7 days post-sorting - Negative control (medium only)	
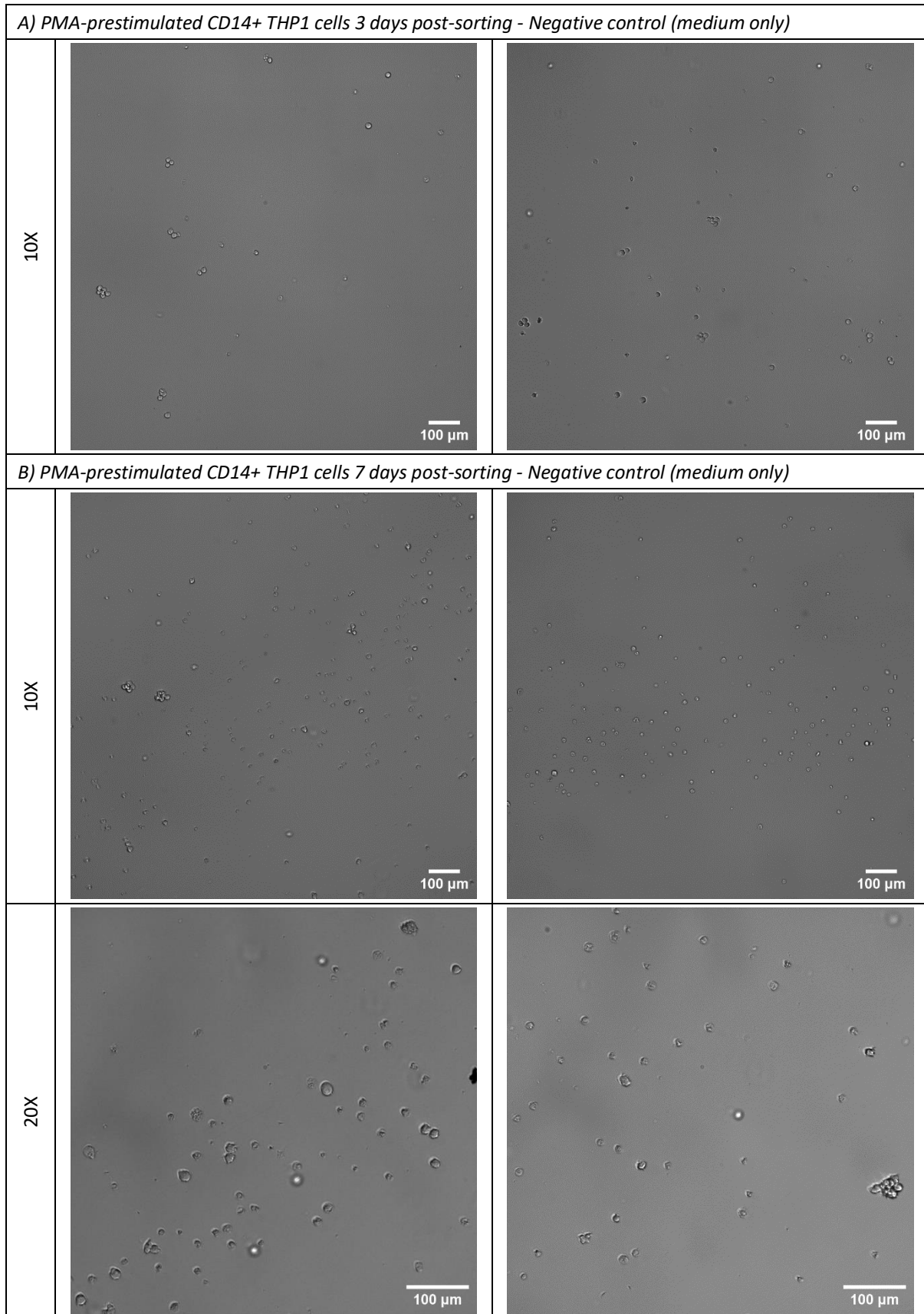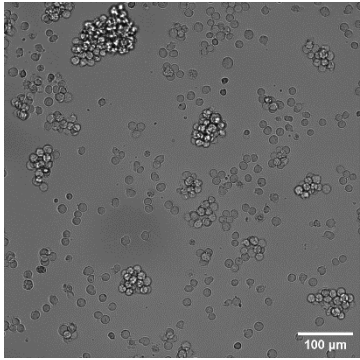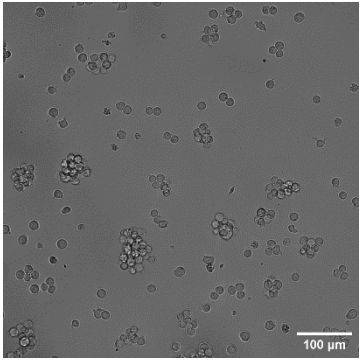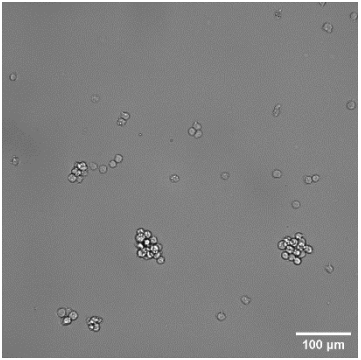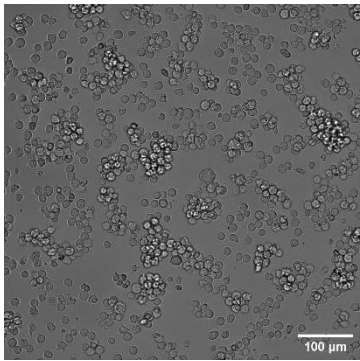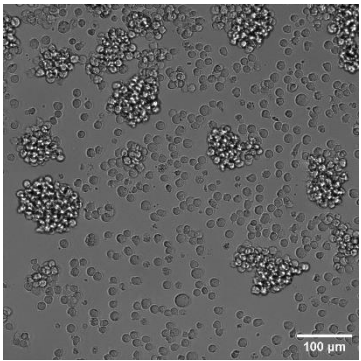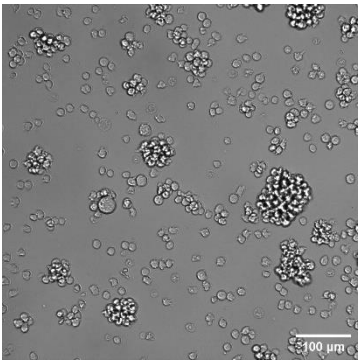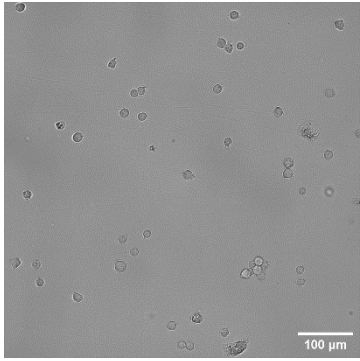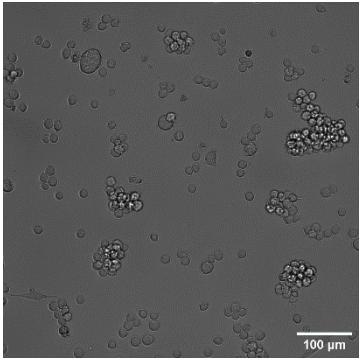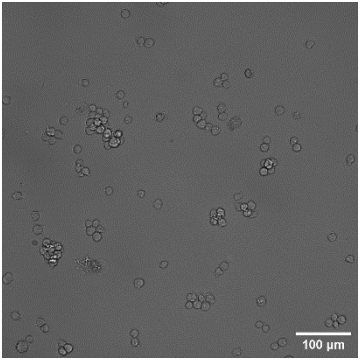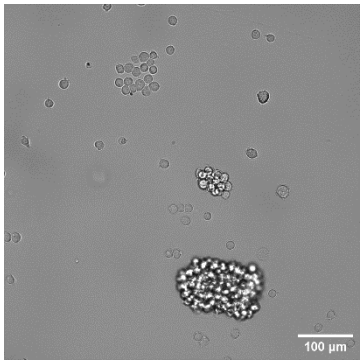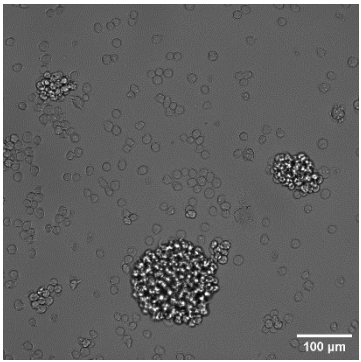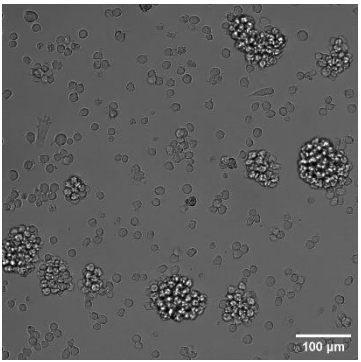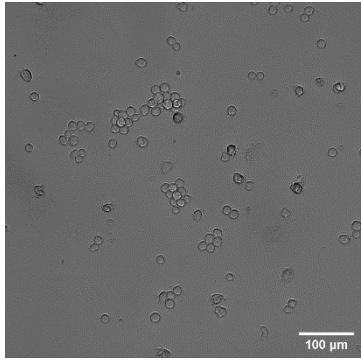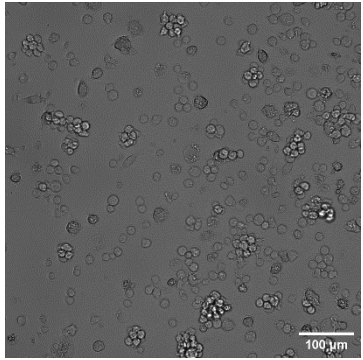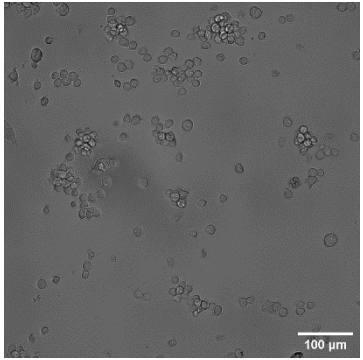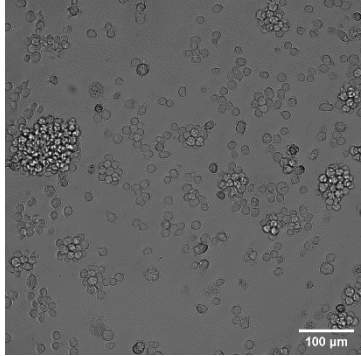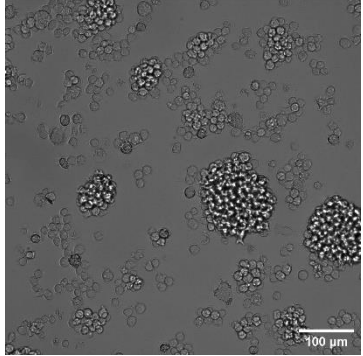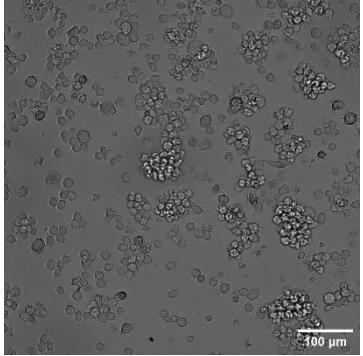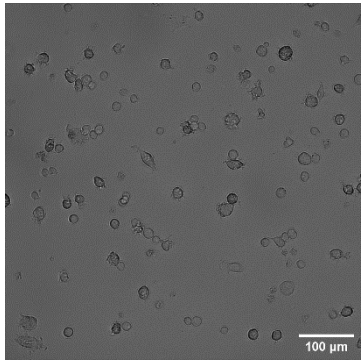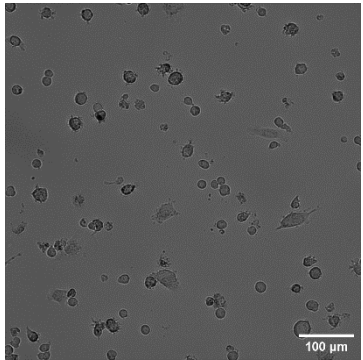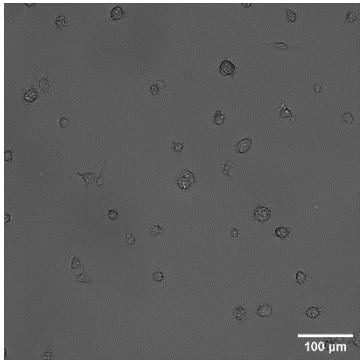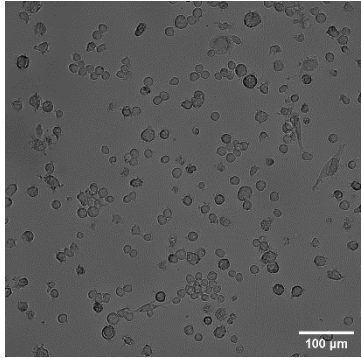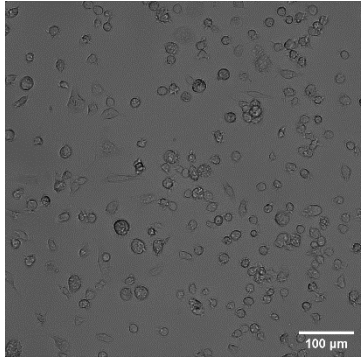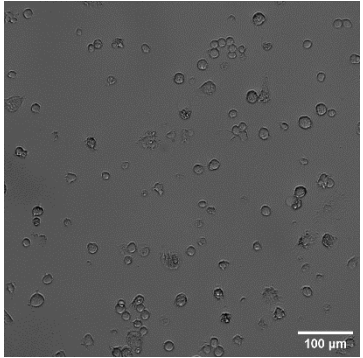
*Table 10. Brightfield images (**200X** for morphology analysis) of 16.2 ng/mL PMA-prestimulated CD14-THP1(P20) cells 7 days post-sorting showing cell morphology. Sorting was based on CD13 expression. Unsorted mix (55% P1, 40%P2) was included as a control. After sorting, cells were cultured with a range of PMA concentrations (0, 8.1, 25, 50 ng/mL presented in A-D respectively). Images were taken of lower and higher cell density areas.*

A) PMA-prestimulated CD14- THP1 cells 7 days post-sorting - Negative control (medium only)		
	Mixed/Unsorted	Immature / P2	Mature / P1

B) PMA-prestimulated CD14- THP1 cells 7 days post-sorting - 8.1 ng/mL PMA stimulation		
	Mixed/Unsorted (T25 flask)	Immature / P2	Mature / P1

C) PMA-prestimulated CD14- THP1 cells 7 days post-sorting - 25 ng/mL PMA stimulation		
Mixed/Unsorted	Immature / P2	Mature / P1

D) PMA-prestimulated CD14- THP1 cells 7 days post-sorting - 50 ng/mL PMA stimulation		
Mixed/Unsorted	Immature / P2	Mature / P1

4.6.3. Continued culturing of PMA pre-stimulated THP1 cells: Maturity profile

A selection of flow cytometry results and their quantification are presented in Table 11 (p.42). For full results see the sup. material matrix (Table 16 F4, p.73). At a quick first glance, SSC vs FSC graphs (A in the table) clearly show an increase in P2 fraction in the case of 50 ng/mL PMA stimulation compared to lower concentrations, but no abnormalities can be discovered. The former finding is supported by quantification of the population fractions (B in the table) which shows a decrease of P1 from ~80% to [35;11;21]% (at the gain of ~15% to [47;69;57]% P2) respectively for Unsorted/Mixed, Immature and Mature under 50 ng/mL PMA stimulation. The 80% P1 fraction for lower PMA concentrations is particularly notable for Immature, as this group was sorted as predominantly P2 cells; a characteristic we do not recognize in these data. Furthermore, the population sorted as CD14+ without further stimulation seems to match the 50 ng/mL PMA stimulation conditions more than the other negative controls with a 13% P1 and 79% P2 share. Within P2 we see a common P2A/P2B ratio of about 1:1 for all conditions, except for CD14+ (-) where the ratio shifts to 20/60≈1:3.

When looking at the maturity profile fractions (E in the table), with an n=1 experiment we do not reach statistical significance for differences in CD13 expression between conditions within the populations P1, P2A and P2B (p>0.228 for all cases). This would mean we have an average maturity of ~97% for P1, ~84% for P2A and ~71% for P2B. In turn, there is no significant difference between P1 and P2A, but P2B has significantly lower maturity compared to P1 (p=0.0005). Statistical significance between conditions is also not reached with CD14 expression (p>0.331 for all cases), but the ~45% CD14+ in P1 for 50 ng/mL PMA in all sort groups (45%;37%;51% for X,I,M respectively) compared to 0% Classical maturity for the controls certainly warrants attention, as does the slight increase to 5~10% CD14+ for 25 ng/mL PMA. The same can be said for P2B, where CD14+ values for the higher PMA concentrations fall in the range of [16-43]%. To a lower degree, we see a similar trend for Classical maturity in P2A with values in the range of [5-18]%.

Table 12 (p.44) presents Viability (A), Size (B) and Adhered fraction (C) for all conditions. Table 13 (p.44) presents Cell counts before staining for flow cytometry as well as the Proliferation rate relative to the Unsorted negative control, assuming exponential cell growth[69] in the form of: $N_t = N_0(1 + r)^t$. Proliferation results show a comparable trend between sort conditions: Proliferation rate decreases with increasing PMA concentration. Proliferation for the Immature negative control is decreased compared to the other negative controls; this is not reflected by the other stimulation conditions of the sorting group. Comparison of these results to literature and their interpretation is detailed in section 5.2.3 (p.49) of the discussion.

When considering Adherence in conjunction with profile fractions, we find for the first time the possibility of a relationship between Adhered fraction and P2 fraction. We also find a possible relationship between Adhered fraction and Classical maturity. These findings are further evaluated in section 5.1.7 of the discussion (p.47).

Table 11 FACS results for pre-stimulated THP1(P20) cells sorted into CD14 positive, Mature and Immature cells and stimulated a second time for 7 days with a range of PMA concentrations [0; 8.1; 25; 50 ng/mL]. A) CD14+ cells cultured in medium show a small P1 and large P2 population. Similarly, higher concentration of PMA shows a decrease in P1 and increase in P2. B) Exemplified by Unsorted PMA 25ng/mL, cells are unlikely to be CD14+CD13- suggesting that cells first mature and then specialize to a Classical profile. C) Quantification of population fractions supports the findings of A regarding the loss of P1 at the gain of P2 in 50 ng/mL PMA and CD14+ (-) cells. D) Quantification of profile fractions shows near 100% maturity of P1 under all conditions, with maturity decreased in P2A and further decreased in P2B for lower PMA concentrations.
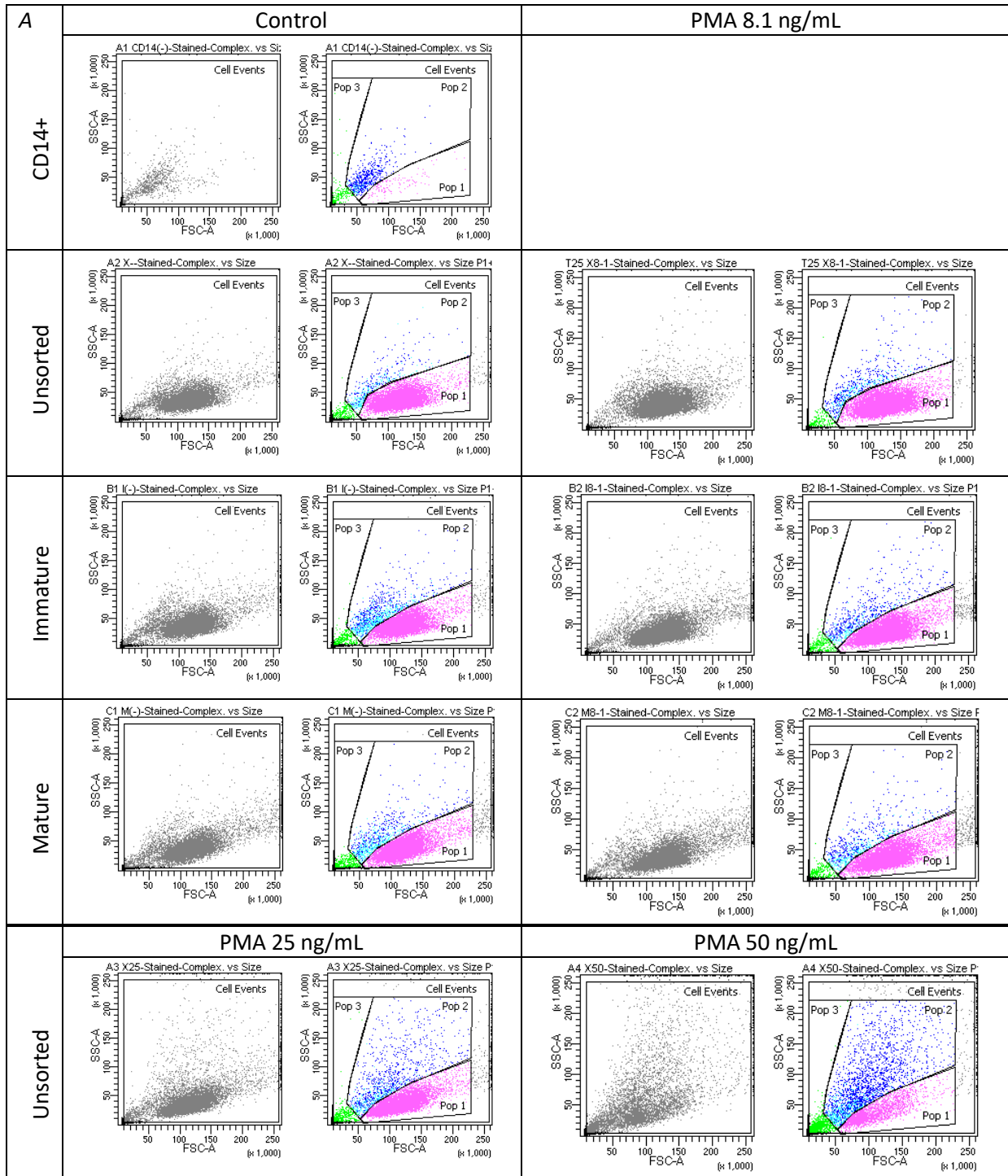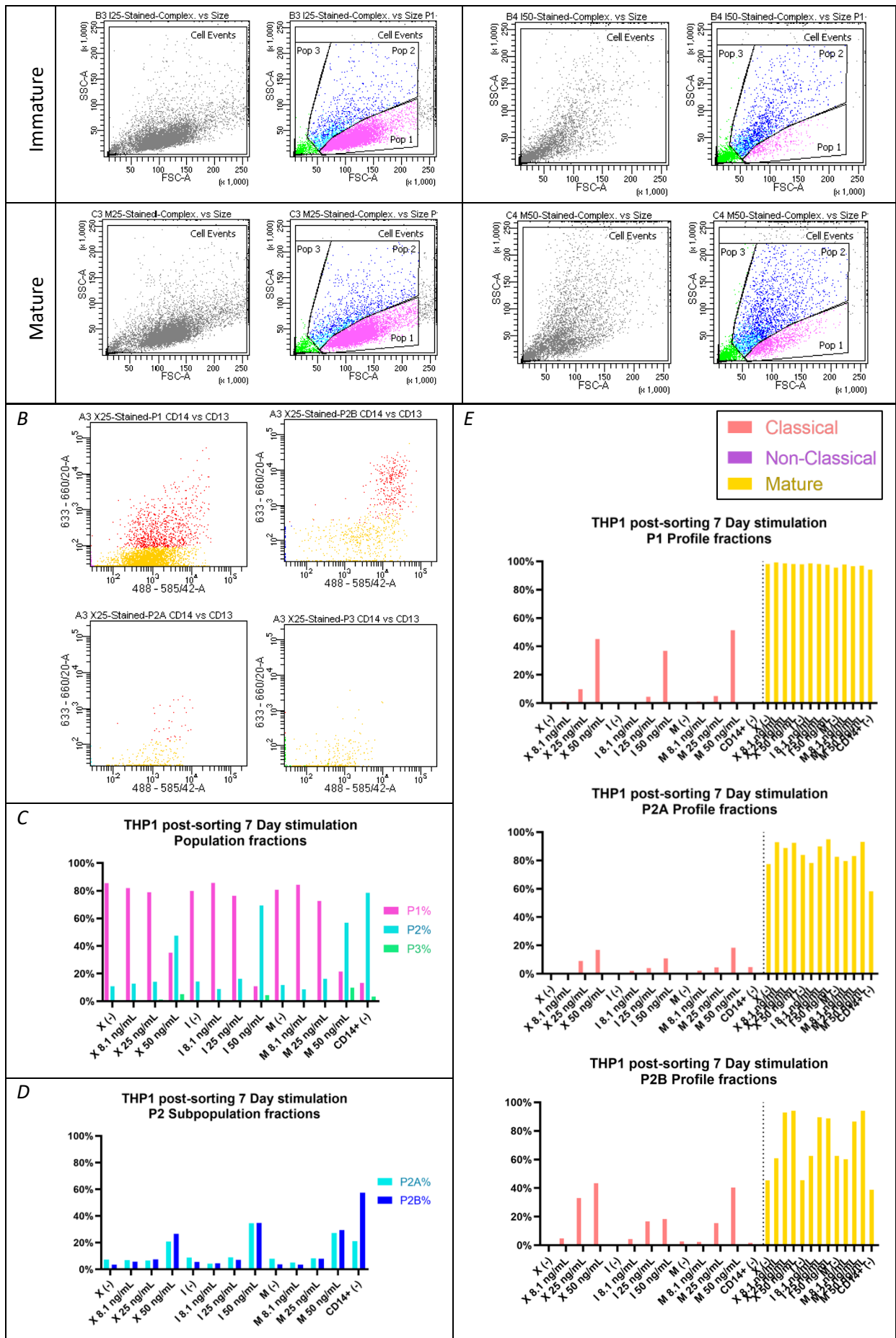
Table 12 A) Fraction Adhered cells, B) Viability and C) Size for THP1(P20) Unsorted, Immature, Mature and CD14+ populations after second time stimulation for 7 days with a range of PMA concentrations [0; 8.1; 25; 50] ng/mL.
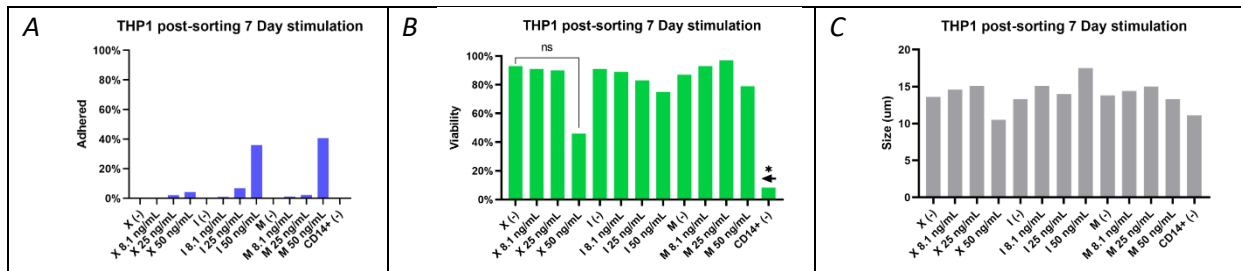
Table 13 A) Total cell count and B) Proliferation rate (relative to Unsorted negative control, assuming exponential growth[69] $N_t = N_0(1+r)^t$) for THP1(P20) Unsorted, Immature, Mature and CD14+ populations after second time stimulation for 7 days with a range of PMA concentrations [0; 8.1; 25; 50] ng/mL.
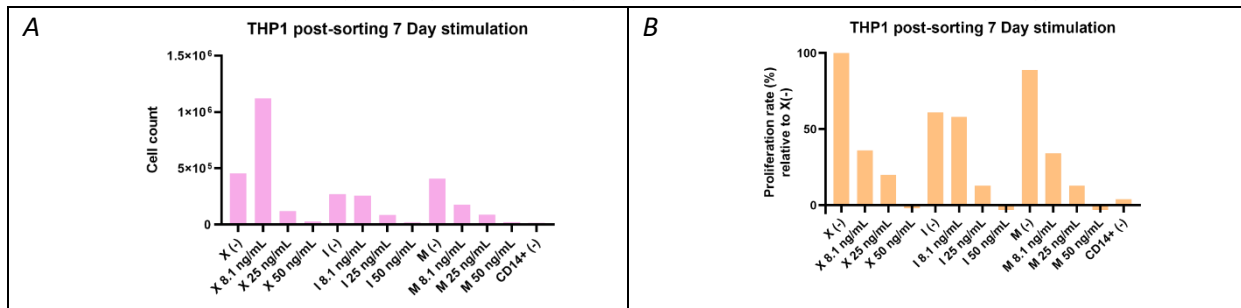
5 Discussion

5.1. Technical considerations

5.1.1. Suitability of U937 for this research

As mentioned in the introduction, multiple reviews have compared suitability of U937 and THP1 as models for monocytic cells and concluded THP1 to be most suitable in most directions of research. The U937 in this research is naturally negative for CD14 expression likewise to THP1, but U937 failed to show the change in spreading behaviour that is typical for macrophagic cells after 24hr 50 ng/mL PMA stimulation. Furthermore, literature on THP1 stimulation was found to be more substantial than for U937, and as this is a Master Thesis, I appreciated having more literature to be available. As there were no arguments fór U937, it was decided to follow the recommendations of the reviews and continue with THP1 only.

5.1.2. Reliability of stainings

All stainings used have shown positive expression compared to unstained controls at one point or another in this research. Single-staining controls were initially used to determine compensation for fluorescence overlap, and all stainings showed clear differences with unstained controls; see the results of Exploration, Protocol 1 and Protocol 2 for CD14 and CD16 stainings, and Protocol 3A and B for CD13 and HLA-DR stainings.
The CD13 staining solution was tested before use by pipetting a droplet on a glass slide and checking with fluorescence microscopy; the staining showed bright fluorescence and was concluded to be in working condition by an independent party.
The HLA-DR staining was newly ordered and been successfully applied in peer-reviewed research. Furthermore, as results were initially negative without stimulation, and selectively positive post-stimulation, it is assumed there was little aspecific binding in case of all stainings. No further experimentation was performed to verify this, however.

To conclude, it is assumed that the stainings have agreeable specificity and sensitivity and are in proper working condition; they are therefore assumed to not significantly affect results.

5.1.3. Reliability of fluorescence overlap compensation and flow-cytometry interpretation

Incorrect fluorescence overlap compensation for flow cytometry, whether too high or too low, directly and crucially impacts results. Initial compensation as presented in Table 6 (p.23) led to all conditions having negligible expression for both CD14 and CD16 in all experiments. Additionally, it should be kept in mind that analysis of (fluorescence-based) flow cytometry data is of a largely subjective nature. Recognition of populations and subpopulations, as well as the determination of cut-offs for gates is dependent on the researcher and therefore subject to human error. However, as the compensation was based on both theoretical values as well as experimental controls, and the current findings are in line with relevant literature, I am fairly confident in the accuracy of both compensation values and expression gating.

5.1.4. Separation of P2A and P2B based on HLA-DR autofluorescence

P2A and P2B had clear differences in autofluorescence for all channels. Up until the addition of HLA-DR in protocol 3B, only the HLA-DR is (reliably) not affected by stainings. As such, HLA-DR autofluorescence was used to distinguish between the two.

5.1.5. Significance of passaging and revival

According to Chanput et al.[70], THP1 cells can be cultured in vitro up to passage 25 (approximately 3 months) without changes in cell sensitivity and activity. Opinions on U937 passaging differ, with the EOCD recommending use up until passage 21 in testing[71] and both professional and personal accounts reporting use of passage 25+, as far as P38[72,73].

U937 cells in this research were used in experimentation until p19, whereafter they were discarded in favor of the THP1 cell line, as detailed previously in section 5.1 (p.45). As such, U937 passaging lies well below any cut-off for reliability. Furthermore, Profile exploration and Protocol 1 were performed with U937 cells of the same revival. It is therefore assumed that neither passaging nor revival origin had a significant effect on the acquired results for the U937 cell line.

THP1 cells were used in experimentation until passage 22. Three different revivals were used over the course of the research. As cells were used at a passaging below the generally reported threshold, the impact of too high passaging is not considered in any of the experiments. In addition, no notable differences could be discovered between passages in any of the experiments; that is, passaging cannot be related to a systemic difference in (sub)population expression, maturity profiles, viability, adherence or cell size.

As previously stated, CD14 expression and thus maturity can differ for unstimulated THP1s and it is prudent to pay special attention to the negative controls. In this research, negative controls of all revivals and passaging were comparable regarding their (negligible) CD14 expression.

It is assumed that for both the U937 and THP1 cell line neither revival nor passaging significantly influenced the acquired results.

5.1.6. Significance of seeding density and cell culture vessel

Cells were kept at equal and recommended seeding density for the respective culture vessel as far as allowed[74]; an exception was made for continued culturing post sorting, as insufficient cells could be sorted. For details refer to the culture protocols (section 3.1, p.12). As cells ended up in lower and higher local cell densities, with no immediately obvious differences in cell morphology or behaviour between densities (see again Table 15 p.69 and Table 10 p.39) the variance in seeding density in this research is not considered to have significantly impact results.

It is important to consider, however, that adherence was notably higher in the case of well plates in Protocol 2 (20% negative control, 40% 16.2 ng/mL PMA and ethanol stimulated, **Error! Reference source not found.**C p.30) than T75 flasks (10% for both negative control and 16.2 ng/mL PMA stimulated, C p.34). Adherence returned to Protocol 2 levels for 50 ng/mL but not for 25 ng/mL PMA stimulated cells in continued culturing in well plates post-sorting (<10% negative control and [8.1; 25] ng/mL PMA stimulation, 40% 50 ng/mL PMA stimulated, Table 12A p.44).

As pre-monocytes, THP1 cells do not generally attach, but can do so in small numbers due to heterogeneity in adherence molecules, charge buildup as a result of excreted products, and (rare) spontaneous differentiation into macrophages[75].

The area to volume ratio of well plates compared to culture flasks offers a partial explanation for the decrease in adherence in the T75 flask compared to the well plate: if relatively fewer cells are within reach of a surface to attach to, the fraction of adhered cells will be lower.

However, area to volume ratio does not explain the discrepancy in adherence for 25 ng/mL PMA stimulation conditions in continued culturing compared to 16.2 ng/mL initial PMA stimulation, as cells were cultured in a 12 wells plate in both experiments. An explanation may be found in the forces exerted on the cells during sorting and continued culturing, further discussed in section 5.1.8 on p.48.

As only the suspended fraction was used in continued culturing following FACS, meaning cells generally will not have come into contact with the culture vessel, it is assumed that the type of cell culture ware had no significant impact on other results than adherence. Comparable (trends in) viability and size between experiments also support this notion. The impact of adherence in and of itself is discussed in the next section.

5.1.7. Significance of adherence

Flow cytometry results
In all conditions, excepting only those stimulated with ethanol, both P1 and P2 are present in both Adhered and Suspended cell fractions; populations P1 and P2 therefore do not correlate to adhered or suspended cells only.

Population fractions, viability and size are comparable between adhered and suspended cells for all conditions of Protocol 2. The same trend can be observed in the case of PMA stimulation in Protocol 3, where no significant differences can be discovered between adhered and suspended cells for population fractions, maturity profile fractions, viability and size. The negative control in Protocol 3 suggests slightly lower levels of maturation for P2A and P2B in the adhered fraction, although with an n1 to go on and values that still fall within the measured range of the other conditions, there is insufficient evidence to assume this difference to be significant.

Degree of adherence is equal between PMA, ethanol and P+V stimulated cells in Protocol 2 (~40%), while P2 shares differ between all three conditions. PMA+vitamin D3 has a P2 share that matches vitamin D3 stimulation, while VD3's adherences matches that of the negative control.

CD13 expression as a measure for degree of maturity is comparable between conditions for P1 and P2A in Protocol 3. Only P2B shows a trend of increased maturity that matches the degree of adherence.

Interestingly, a relationship can be discovered between degree of adherence and CD14 expression in the results of Protocol 3. This raises the question of whether adherence results in CD14 expression, or CD14 expression results in adherence. This result is especially notable considering the increased adherence in Protocol 2 coincides with increased CD14 expression in the case of PMA stimulation, but not ethanol and P+V.

TNF-α expression on PVDF membrane
TNF-α is not expressed differentially relating to adherence, according to both back-ground corrected fluorescence or when normalized over total cell density. When normalizing over cell viability, a significant difference arises for PMA Adhered, but a weaker, yet contradicting trend is found in the negative control. The high expression for PMA Adhered can be explained by an incorrect low measurement for viability caused by cell damage due to prolonged exposure to trypsine or another handling error. Furthermore, stimulation with PMA is known to increase TNF-α expression regardless of adherence[ref]; This raises the question of whether the incubation time of 72 hours might have led to saturation of the membranes, resulting in a faulty reading regardless of actual expression levels. However, as cells were stimulated with a relatively low concentration of PMA (16.2 ng/mL) and other results reflect that this is too low to significantly affect THP1s, the possibility remains that the readings are indeed correct; in this case the too-low PMA stimulation would have indeed resulted in similar expression levels as the negative control. It can only be concluded that this experiment does not provide evidence that adherence affects maturation.

Taking all aforementioned aspects together, the data suggest that in this research adherence does not (predominantly) drive maturation or affect population fractions.

In addition to my own findings, a study by Mograbi et al. demonstrates that the various possible modes of adhesion affect monocytes differently[76].

5.1.8. Significance of sorting, spinning and related stresses

Disregarding for a moment the low viability reading for the unsorted 50 ng/mL PMA condition, comparing unsorted cells to Mature and Immature sorted cells does not reveal a significant effect of FACS on cell viability or size. This matches the findings by Pfister et al.[77], who performed an extensive study on the impact of flow cytometry on the viability of PBMCs and concluded sorting-induced cell stress (SICS) to not have a significant effect.

As introduced in the two preceding sections, however, it is notable that the rate of adherence post-sorting is lower compared to that of the well plate culturing in Protocol 2. Adherence is only markedly increased in the case of 50 ng/ml PMA stimulation of the FACS-sorted groups Mature and Immature, at a level comparable to that of 16.2 ng/ml PMA stimulation for non-pre-stimulated cells. Hence, two factors must be considered: one, adherence for the negative control and low concentration PMA stimulation is comparably lower in all three groups, with Unsorted being differentiated from the Protocol 2 conditions only by the staining step in preparation of FACS and 7 days longer culturing. Two, although the un-upregulated adherence in Unsorted 50 ng/mL PMA stimulation could have been a one-time faulty measurement, it cannot be ruled out based on this information alone that the sorting itself has affected the cells' ability and/or drive for adhesion.

Preparation preceding FACS
A study by Fukuda et al.[78] demonstrated that centrifugation may have affected the cells.

Sorting-induced cell stress (SICS)
Unlike for viability, recent studies have reported significant changes in phenotype for both isolated monocytes and derived macrophages, as well as alterations of up to 10% of the metabolome for peritoneal macrophages following FACS[79,80]. Curiously, a study by Beliakova-Bethell et al.[81] shows no upregulation in 7 common stress genes after FACS.

5.1.9. A note on n2 of Protocol 4

Following protocol 3B, cells of Protocol 4 n2 were successfully sorted, consistent with the FACS that followed protocol 3A. Unfortunately, due to unavailability of the flow cytometer at and around the seven day mark, the experiment had to be cut short on day 4. However, analysis of a midway point might have provided useful insight into the developments taking place during the extended maturation.
Regretfully, however, due to unknown reasons FC results for n2 were highly irregular, with nearly all events resembling the assumed cell debris of population 3 in addition to the absence of any noteworthy expression of any measurands in any condition; on the contrary, population 3 has shown negligible but at the very least identifiable as false-positive expression on a multitude of occasions.

It is worth noting that viability of FACS-sorted cells following protocol 3B could not be quantified with automated cell counting. However, the unsorted control had an agreeable enough viability of 67.4% yet yielded the same irregular results. In addition, the counting prior to flow cytometry showed cells had expanded during the four days of extended maturation with a factor ranging between 2 and 4 for all conditions; comparable with, if not exceeding, cell expansion in n1.

One thing that is striking is the extremely small size measured prior to flow cytometry on day 4: cell size ranged between 5.7 and 8.8 nm for all conditions, with the exception of the Medium-only Unsorted control (12.2 nm) and, highly remarkably, the cells sorted as CD14+ (15.4 nm). Compared

to the sizes of n1, ranging between 10.1 and 17.5 nm and generally consistent with THP1 cell sizes measured throughout this research, n2 cells were alarmingly small.

Considering the flow cytometer is not a sterile environment, as noted previously in 3.2.6 (p.15), chances are the cells suffered an infection or the like. Other than this no factors come to mind that may explain the infelicitous outcome. Regardless, there rests no other option than to consider this a failed experiment and disregard the data acquired postliminary to the FACS sorting.

5.2. Interpretation of results

5.2.1. Identity of (sub)populations
Assuming the acquired results are accurate, we find the following:

P3 has too low FSC and SSC to correspond to intact, living cells. In addition, P3 does not significantly stain positive for any of four stainings over the course of three separate experiments (N=6 replicates in total). P3 is therefore assumed to correspond to dead cells and debris.

Regarding P1 and P2:

-   P1 is larger on average than P2
-   P1 has lower relative complexity than P2
-   P1 has higher maturity and CD14 expression than P2 following stimulation with PMA
-   P1 fraction decreases with increasing PMA concentration at the gain of P2
-   P1 and P2 shares have no causal relationship with adherence
-   In this research, both P1 and P2 THP1 cells express CD13 but not CD14 without stimulation

A possible explanation is P1 being proliferating cells and P2 non-dividing cells.

5.2.2. Effect of vitamin D3 and ethanol on THP1 cell line
In this research no causal relationships could be discovered between maturity profiles or (sub)population fractions and passaging, revival origin, variance in seeding density, cell culture vessel and degree of adherence.

Based on the results of Protocol 2 it can therefore be concluded that Ethanol significantly affects population fractions resulting in a shift from <40% to ~70% for P2 and decrease from 60% to 0% for P1, as well as an increase in P3 from ~3% to ~15%.

VD3 further increases the P2 fraction from ~70% to ~90%, while the P3 fraction remains at the level of the negative control. This suggests a small protective effect of VD3 against the harmful effects of ethanol, although this is not supported by viability results.

Maturation with ethanol and vitamin D3 did not results in significant expression of maturity markers CD14 and CD16. On the contrary, the addition of Vitamin D3, dissolved in ethanol, negated the classical maturation effect of PMA.

5.2.3. Effect of PMA on THP1 cell line
See conclusion.

6 Conclusion

Stock THP1 and U937 were determined to be negative for CD14 and CD16 maturity markers, but do express CD13.

Stimulation with CSF1, ethanol and VD3, either by itself or in addition to PMA, did not lead to expression of maturity markers. On the contrary, vitamin D3 dissolved in ethanol negated maturation.

Stimulation with PMA showed the species of THP1 in this lab to be rather insensitive to stimulation. Stimulation with 50 ng/mL PMA for 24 hrs and <50 ng/mL PMA for 7 days did not result in considerable maturation, but 50 ng/mL continued stimulation of 16.2 ng/mL pre-stimulated cells did. It is therefore concluded that at least 50 ng/mL PMA is required to induce maturation of THP1 promonocytes. In addition, at least at this concentration, cells need to be stimulated for longer dan 24 hours.

No replicable protocol could be established, but the research has provided some interesting insights regarding pre-stimulation with low concentration of PMA.

7 References

1.   Non-alcoholic fatty liver disease (NAFLD) - NHS. Accessed October 22, 2023.
      https://www.nhs.uk/conditions/non-alcoholic-fatty-liver-disease/

2.   Estes C, Razavi H, Loomba R, Younossi Z, Sanyal AJ. Modeling the epidemic of nonalcoholic
      fatty liver disease demonstrates an exponential increase in burden of disease. *Hepatology*.
      2018;67(1):123-133. doi:10.1002/HEP.29466/SUPPINFO

3.   Huh Y, Cho YJ, Nam GE. Recent Epidemiology and Risk Factors of Nonalcoholic Fatty Liver
      Disease. *J Obes Metab Syndr*. 2022;31(1):17. doi:10.7570/JOMES22021

4.   Younossi ZM, Koenig AB, Abdelatif D, Fazel Y, Henry L, Wymer M. Global epidemiology of
      nonalcoholic fatty liver disease—Meta-analytic assessment of prevalence, incidence, and
      outcomes. *Hepatology*. 2016;64(1):73-84. doi:10.1002/HEP.28431

5.   Younes R, Bugianesi E. NASH in Lean Individuals. *Semin Liver Dis*. 2019;39(1):86-95.
      doi:10.1055/S-0038-1677517

6.   Hardy T, Oakley F, Anstee QM, Day CP. Nonalcoholic Fatty Liver Disease: Pathogenesis and
      Disease Spectrum. *https://doi.org/101146/annurev-pathol-012615-044224*. 2016;11:451-
      496. doi:10.1146/ANNUREV-PATHOL-012615-044224

7.   Dyson JK, Anstee QM, McPherson S. Non-alcoholic fatty liver disease: a practical approach to
      diagnosis and staging. *Frontline Gastroenterol*. 2014;5(3):211-218. doi:10.1136/FLGASTRO-
      2013-100403

8.   Ekstedt M, Franzén LE, Mathiesen UL, et al. Long-term follow-up of patients with NAFLD and
      elevated liver enzymes. *Hepatology*. 2006;44(4):865-873. doi:10.1002/HEP.21327

9.   Singh S, Allen AM, Wang Z, Prokop LJ, Murad MH, Loomba R. Fibrosis Progression in
      Nonalcoholic Fatty Liver vs Nonalcoholic Steatohepatitis: A Systematic Review and Meta-
      analysis of Paired-Biopsy Studies. *Clinical Gastroenterology and Hepatology*. 2015;13(4):643-
      654.e9. doi:10.1016/J.CGH.2014.04.014

10.   Wynn TA. Cellular and molecular mechanisms of fibrosis. *J Pathol*. 2008;214(2):199-210.
      doi:10.1002/PATH.2277

11.   Aydin MM, Akcali KC. Liver fibrosis. *The Turkish Journal of Gastroenterology*. 2018;29(1):14.
      doi:10.5152/TJG.2018.17330

12.   Anstee QM, Reeves HL, Kotsiliti E, Govaere O, Heikenwalder M. From NASH to HCC: current
      concepts and future challenges. *Nature Reviews Gastroenterology & Hepatology 2019 16:7*.
      2019;16(7):411-428. doi:10.1038/s41575-019-0145-7

13.   Smith A, Baumgartner K, Bositis C. Cirrhosis: Diagnosis and Management. *Am Fam Physician*.
      2019;100(12):759-770. Accessed October 22, 2023.
      https://www.aafp.org/pubs/afp/issues/2019/1215/p759.html

14.   Albillos A, Lario M, Álvarez-Mon M. Cirrhosis-associated immune dysfunction: Distinctive
      features and clinical relevance. *J Hepatol*. 2014;61(6):1385-1396.
      doi:10.1016/J.JHEP.2014.08.010

15.   Kanwal F, Kramer JR, Mapakshi S, et al. Risk of Hepatocellular Cancer in Patients With Non-Alcoholic Fatty Liver Disease. *Gastroenterology*. 2018;155(6):1828-1837.e2. doi:10.1053/J.GASTRO.2018.08.024

16.   Ginès P, Krag A, Abraldes JG, Solà E, Fabrellas N, Kamath PS. Liver cirrhosis. *The Lancet*. 2021;398(10308):1359-1376. doi:10.1016/S0140-6736(21)01374-X

17.   Younossi ZM, Blissett D, Blissett R, et al. The economic and clinical burden of nonalcoholic fatty liver disease in the United States and Europe. *Hepatology*. 2016;64(5):1577-1586. doi:10.1002/HEP.28785

18.   Paik JM, Golabi P, Younossi Y, Srishord M, Mishra A, Younossi ZM. The Growing Burden of Disability Related to Nonalcoholic Fatty Liver Disease: Data From the Global Burden of Disease 2007-2017. *Hepatol Commun*. 2020;4(12):1769. doi:10.1002/HEP4.1599

19.   Younossi ZM, Stepanova M, Noureddin M, et al. Improvements of Fibrosis and Disease Activity Are Associated With Improvement of Patient-Reported Outcomes in Patients With Advanced Fibrosis Due to Nonalcoholic Steatohepatitis. *Hepatol Commun*. 2021;5(7):1201. doi:10.1002/HEP4.1710

20.   Nguyen MH, Le MH, Yeo YH, et al. Forecasted 2040 global prevalence of nonalcoholic fatty liver disease using hierarchical bayesian approach. *Clin Mol Hepatol*. 2022;28(4):841. doi:10.3350/CMH.2022.0239

21.   Paternostro R, Trauner M. Current treatment of non-alcoholic fatty liver disease. *J Intern Med*. 2022;292(2):190. doi:10.1111/JOIM.13531

22.   Engelmann C, Tacke F. The Potential Role of Cellular Senescence in Non-Alcoholic Fatty Liver Disease. *International Journal of Molecular Sciences 2022, Vol 23, Page 652*. 2022;23(2):652. doi:10.3390/IJMS23020652

23.   Friedman SL, Neuschwander-Tetri BA, Rinella M, Sanyal AJ. Mechanisms of NAFLD development and therapeutic strategies. *Nature Medicine 2018 24:7*. 2018;24(7):908-922. doi:10.1038/s41591-018-0104-9

24.   Trauner M, Fuchs CD. Novel therapeutic targets for cholestatic and fatty liver disease. *Gut*. 2022;71(1):194-209. doi:10.1136/GUTJNL-2021-324305

25.   Lipke K, Kubis-Kubiak A, Piwowar A. Molecular Mechanism of Lipotoxicity as an Interesting Aspect in the Development of Pathological States—Current View of Knowledge. *Cells*. 2022;11(5). doi:10.3390/CELLS11050844

26.   Yao Q, Liu J, Cui Q, et al. CCN1/Integrin $\alpha5\beta1$ Instigates Free Fatty Acid-Induced Hepatocyte Lipid Accumulation and Pyroptosis through NLRP3 Inflammasome Activation. *Nutrients*. 2022;14(18):3871. doi:10.3390/NU14183871/S1

27.   Swanson K V., Deng M, Ting JPY. The NLRP3 inflammasome: molecular activation and regulation to therapeutics. *Nature Reviews Immunology 2019 19:8*. 2019;19(8):477-489. doi:10.1038/s41577-019-0165-0

28.   Wree A, McGeough MD, Inzaugarat ME, et al. NLRP3 inflammasome driven liver injury and fibrosis: Roles of IL-17 and TNF in mice. *Hepatology*. 2018;67(2):736-749. doi:10.1002/HEP.29523

29.   Wree A, Eguchi A, Mcgeough MD, et al. NLRP3 inflammasome activation results in hepatocyte pyroptosis, liver inflammation and fibrosis. *Hepatology*. 2014;59(3):898. doi:10.1002/HEP.26592

30.   Gaul S, Leszczynska A, Alegre F, et al. Hepatocyte pyroptosis and release of inflammasome particles induce stellate cell activation and liver fibrosis. *J Hepatol*. 2021;74(1):156-167. doi:10.1016/J.JHEP.2020.07.041

31.   Cannito S, Morello E, Bocca C, et al. Microvesicles released from fat-laden cells promote activation of hepatocellular NLRP3 inflammasome: A pro-inflammatory link between lipotoxicity and non-alcoholic steatohepatitis. *PLoS One*. 2017;12(3):e0172575. doi:10.1371/JOURNAL.PONE.0172575

32.   Inzaugarat ME, Johnson CD, Holtmann TM, et al. NLRP3 inflammasome activation in hepatic stellate cells induces murine liver fibrosis. *Hepatology*. 2019;69(2):845. doi:10.1002/HEP.30252

33.   Karlmark KR, Weiskirchen R, Zimmermann HW, et al. Hepatic recruitment of the inflammatory Gr1+ monocyte subset upon liver injury promotes hepatic fibrosis. *Hepatology*. 2009;50(1):261-274. doi:10.1002/HEP.22950

34.   Zimmermann HW, Seidler S, Nattermann J, et al. Functional Contribution of Elevated Circulating and Hepatic Non-Classical CD14+CD16+ Monocytes to Inflammation and Human Liver Fibrosis. *PLoS One*. 2010;5(6):e11049. doi:10.1371/JOURNAL.PONE.0011049

35.   Verhoeckx K, Cotter P, López-Expósito I, et al. The impact of food bioactives on health: In vitro and Ex Vivo models. *The Impact of Food Bioactives on Health: In Vitro and Ex Vivo Models*. Published online January 1, 2015:1-327. doi:10.1007/978-3-319-16104-4/COVER

36.   Krenkel O, Puengel T, Govaere O, et al. Therapeutic inhibition of inflammatory monocyte recruitment reduces steatohepatitis and liver fibrosis. *Hepatology*. 2018;67(4):1270-1283. doi:10.1002/HEP.29544/SUPPINFO

37.   Weston CJ, Zimmermann HW, Adams DH. The Role of Myeloid-Derived Cells in the Progression of Liver Disease. *Front Immunol*. 2019;10(APR):893. doi:10.3389/FIMMU.2019.00893

38.   Baffy G. Kupffer cells in non-alcoholic fatty liver disease: The emerging view. *J Hepatol*. 2009;51(1):212-223. doi:10.1016/J.JHEP.2009.03.008

39.   Lee KJ, Kim MY, Han YH. Roles of heterogenous hepatic macrophages in the progression of liver diseases. *BMB Rep*. 2022;55(4):166-174. doi:10.5483/BMBREP.2022.55.4.022

40.   Park JW, Jeong G, Kim SJ, Kim MK, Park SM. Predictors reflecting the pathological severity of non-alcoholic fatty liver disease: comprehensive study of clinical and immunohistochemical findings in younger Asian patients. *J Gastroenterol Hepatol*. 2007;22(4):491-497. doi:10.1111/J.1440-1746.2006.04758.X

41.   Wiering L, Tacke F. Treating inflammation to combat non-alcoholic fatty liver disease. *Journal of Endocrinology*. 2023;256(1). doi:10.1530/JOE-22-0194

42.   Riva A, Mehta G. Regulation of monocyte-macrophage responses in cirrhosis—role of innate immune programming and checkpoint receptors. *Front Immunol*. 2019;10(FEB):430905. doi:10.3389/FIMMU.2019.00167/BIBTEX

43. Cardoso CC, Matiollo C, Pereira CHJ, et al. Patterns of dendritic cell and monocyte subsets are associated with disease severity and mortality in liver cirrhosis patients. *Sci Rep*. 2021;11(1):5923. doi:10.1038/S41598-021-85148-Y

44. Thomas G, Tacke R, Hedrick CC, Hanna RN. Nonclassical Patrolling Monocyte Function in the Vasculature. *Arterioscler Thromb Vasc Biol*. 2015;35(6):1306-1316. doi:10.1161/ATVBAHA.114.304650

45. Kapellos TS, Bonaguro L, Gemünd I, et al. Human Monocyte Subsets and Phenotypes in Major Chronic Inflammatory Diseases. *Front Immunol*. 2019;10(AUG):2035. doi:10.3389/FIMMU.2019.02035

46. Liaskou E, Zimmermann HW, Li KK, et al. Monocyte subsets in human liver disease show distinct phenotypic and functional characteristics. *Hepatology*. 2013;57(1):385-398. doi:10.1002/HEP.26016

47. International Clinical Cytometry Society. Accessed October 25, 2023. https://www.cytometry.org/web/q_view.php?id=201&filter=Interpretation%20and%20Clinical%20Application

48. Liu T, Huang T, Li J, et al. Optimization of differentiation and transcriptomic profile of THP-1 cells into macrophage by PMA. *PLoS One*. 2023;18(7):e0286056. doi:10.1371/JOURNAL.PONE.0286056

49. Riddy DM, Goy E, Delerive P, Summers RJ, Sexton PM, Langmead CJ. Comparative genotypic and phenotypic analysis of human peripheral blood monocytes and surrogate monocyte-like cell lines commonly used in metabolic disease research. *PLoS One*. 2018;13(5):e0197177. doi:10.1371/JOURNAL.PONE.0197177

50. Duweb A, Gaiser AK, Stiltz I, El Gaafary M, Simmet T, Syrovets T. The SC cell line as an in vitro model of human monocytes. *J Leukoc Biol*. 2022;112(4):659-668. doi:10.1002/JLB.1A1221-680R

51. Gately,' CL, Wahl SM, Oppenheim JJ. Characterization of hydrogen peroxide-potentiating factor, a lymphokine that increases the capacity of human monocytes and monocyte-like cell lines to produce hydrogen peroxide. *The Journal of Immunology*. 1983;131(6):2853-2858. doi:10.4049/JIMMUNOL.131.6.2853

52. Aldo PB, Craveiro V, Guller S, Mor G. Effect of Culture Conditions on the Phenotype of THP-1 Monocyte Cell Line. *American Journal of Reproductive Immunology*. 2013;70(1):80-86. doi:10.1111/AJI.12129

53. Osman M, Akkus Z, Jevremovic D, et al. Classification of Monocytes, Promonocytes and Monoblasts Using Deep Neural Network Models: An Area of Unmet Need in Diagnostic Hematopathology. *J Clin Med*. 2021;10(11). doi:10.3390/JCM10112264

54. Takashiba S, Van Dyke TE, Amar S, Murayama Y, Soskolne AW, Shapira L. Differentiation of Monocytes to Macrophages Primes Cells for Lipopolysaccharide Stimulation via Accumulation of Cytoplasmic Nuclear Factor κB. *Infect Immun*. 1999;67(11):5573. doi:10.1128/IAI.67.11.5573-5578.1999

55. García A, Serrano A, Abril E, et al. Differential effect on U937 cell differentiation by targeting transcriptional factors implicated in tissue- or stage-specific induced integrin expression. *Exp Hematol*. 1999;27(2):353-364. doi:10.1016/S0301-472X(98)00038-1

56. Liu HZ, Gong JP, Wu CX, Peng Y, Li XH, You HB. The U937 cell line induced to express CD14 protein by 1,25-dihydroxyvitamin D3 and be sensitive to endotoxin stimulation. *Hepatobiliary Pancreat Dis Int*. 2005;4(1):84-89. Accessed December 19, 2022. https://europepmc.org/article/med/15730927

57. Baek YS, Haas S, Hackstein H, et al. Identification of novel transcriptional regulators involved in macrophage differentiation and activation in U937 cells. *BMC Immunol*. 2009;10:18. doi:10.1186/1471-2172-10-18

58. Biosciences BD. BD FACSAria II User's Guide. Published online 2009.

59. Curtis ASG, Forrester J V., McInnes C, Lawrie F. Adhesion of cells to polystyrene surfaces. *Journal of Cell Biology*. 1983;97(5):1500-1506. doi:10.1083/JCB.97.5.1500

60. Cossarizza A, Chang HD, Radbruch A, et al. Guidelines for the use of flow cytometry and cell sorting in immunological studies*. *Eur J Immunol*. 2017;47(10):1584-1797. doi:10.1002/EJI.201646632

61. Box A, Holmes L, Delay M, et al. Cell Sorter Cleaning Practices and Their Impact on Instrument Sterility. *Journal of Biomolecular Techniques*. 2022;33(1). doi:10.7171/3FC1F5FE.E2675D74

62. McIntyre CA, McCord R, Vrane D. *Decontamination of the BD FACSAria II or BD FACSAria III System Using the Prepare for Aseptic Sort Procedure* .; 2010. Accessed October 25, 2023. https://www.bdbiosciences.com/content/dam/bdb/marketing-documents/FacsariaII_Decontamination.pdf

63. Motoyoshi K. Macrophage colony-stimulating factor (M-CSF). *Nippon rinsho Japanese journal of clinical medicine*. 2016;53 Su Pt 2:726-727. doi:10.1016/B978-0-444-53717-1.01010-6

64. ThermoFisher. Useful Numbers for Cell Culture - NL. Accessed August 21, 2023. https://www.thermofisher.com/uk/en/home/references/gibco-cell-culture-basics/cell-culture-protocols/cell-culture-useful-numbers.html

65. Before FlowJo™ | FlowJo, LLC. Accessed August 28, 2023. https://www.flowjo.com/learn/flowjo-university/flowjo/before-flowjo/58

66. Flow Cytometers - LearnHaem | Haematology Made Simple. Accessed October 24, 2023. https://www.learnhaem.com/courses/flow-cytometry/lessons/flow-cytometers/

67. Fluorescence Activated Cell Sorting (FACS) | AAT Bioquest. Accessed October 24, 2023. https://www.aatbio.com/catalog/fluorescence-activated-cell-sorting-facs

68. Fluorescence SpectraViewer. Accessed August 28, 2023. https://www.thermofisher.com/order/fluorescence-spectraviewer?#!/

69. Cell Doubling Time Calculator. Accessed October 15, 2023. https://www.omnicalculator.com/biology/cell-doubling-time

70. Chanput W, Mes JJ, Wichers HJ. THP-1 cell line: An in vitro cell model for immune modulation approach. *Int Immunopharmacol*. 2014;23(1):37-45. doi:10.1016/J.INTIMP.2014.08.002

71. *Test No. 405: Acute Eye Irritation/Corrosion*. OECD; 2023. doi:10.1787/9789264185333-en

72. 71 questions with answers in U937 CELLS | Science topic. Accessed October 7, 2023. https://www.researchgate.net/topic/U937-Cells

73. Strefford JC, Foot NJ, Chaplin T, et al. The characterisation of the lymphoma cell line U937, using comparative genomic hybridisation and multi-plex FISH. *Cytogenet Cell Genet*. 2001;94(1-2):9-14. doi:10.1159/000048774

74. ThermoFisher. Useful Numbers for Cell Culture - NL. Accessed August 21, 2023. https://www.thermofisher.com/uk/en/home/references/gibco-cell-culture-basics/cell-culture-protocols/cell-culture-useful-numbers.html

75. Why do THP-1 cells adhere? | ResearchGate. Accessed October 13, 2023. https://www.researchgate.net/post/Why_do_THP-1_cells_adhere

76. Mograbi B, Rochet N, Rossi CE and B. Adhesion of human monocytic THP-1 cells to endothelial cell adhesion molecules or extracellular matrix proteins via beta1 integrins regulates heparin binding epidermal growth factor-like growth factor (HB-EGF) expression. *Eur Cytokine Netw*. 1999;10(1):79-86. Accessed October 13, 2023. https://www.jle.com/fr/revues/ecn/e-docs/adhesion_of_human_monocytic_thp_1_cells_to_endothelial_cell_adhesion_molecules_or_extracellular_matrix_proteins_via_beta1_integrins_regulates_heparin_binding_epidermal_growth_factor_like_growth_factor_hb_egf_expression._90110/article.phtml?tab=texte

77. Pfister G, Toor SM, Sasidharan Nair V, Elkord E. An evaluation of sorter induced cell stress (SICS) on peripheral blood mononuclear cells (PBMCs) after different sort conditions - Are your sorted cells getting SICS? *J Immunol Methods*. 2020;487. doi:10.1016/J.JIM.2020.112902

78. Fukuda S, Schmid-Schönbein GW. Centrifugation attenuates the fluid shear response of circulating leukocytes. *J Leukoc Biol*. 2002;72(1):133-139. doi:10.1189/JLB.72.1.133

79. Nielsen MC, Andersen MN, Møller HJ. Monocyte isolation techniques significantly impact the phenotype of both isolated monocytes and derived macrophages in vitro. *Immunology*. 2020;159(1):63. doi:10.1111/IMM.13125

80. Binek A, Rojo D, Godzien J, et al. Flow Cytometry Has a Significant Impact on the Cellular Metabolome. *J Proteome Res*. 2019;18(1):169-181. doi:10.1021/ACS.JPROTEOME.8B00472/ASSET/IMAGES/LARGE/PR-2018-00472T_0005.JPEG

81. Beliakova-Bethell N, Massanella M, White C, et al. The effect of cell subset isolation method on gene expression in leukocytes. *Cytometry Part A*. 2014;85(1):94-104. doi:10.1002/CYTO.A.22352

Appendix

A.1. Spectra used in determining fluorescence-overlap compensation

A.1.1. Full spectrum excitation Fluorescence spectra
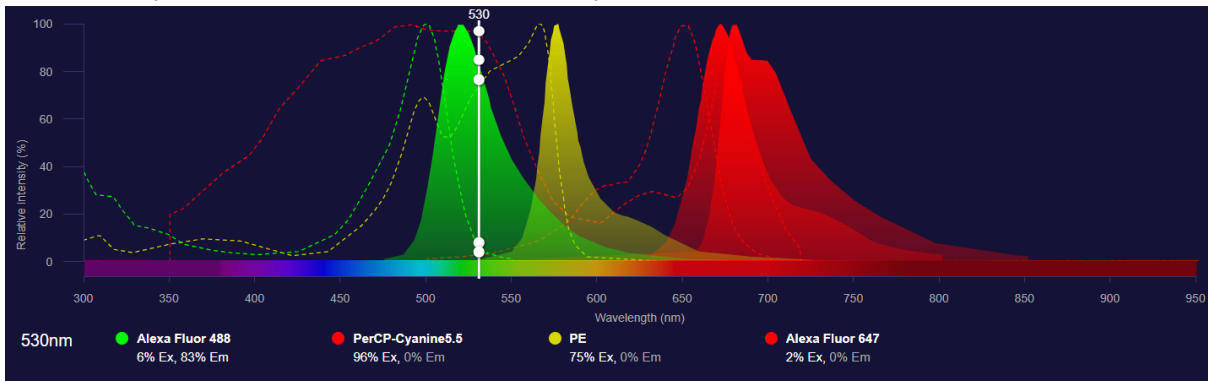
Figure 26 Fluorescence overlap at 530nm. Image produced with SpectraViewer[68].
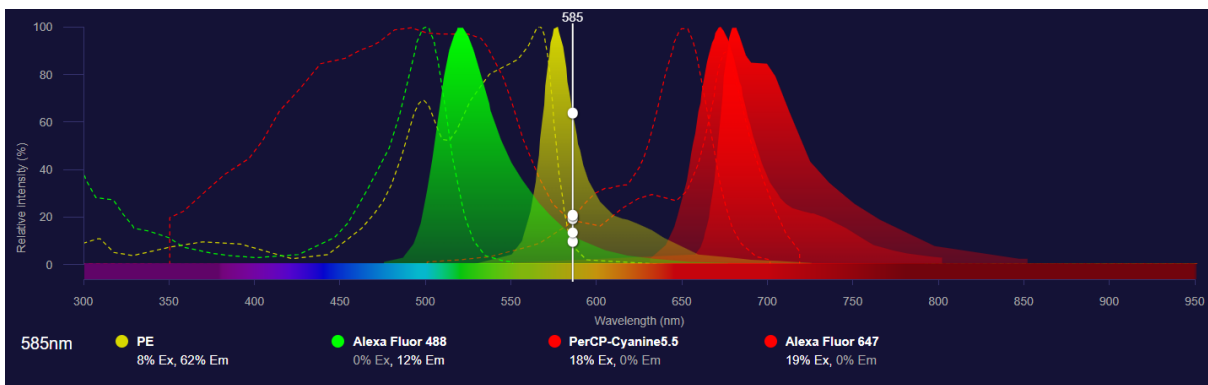
Figure 27 Fluorescence overlap at 585nm. Image produced with SpectraViewer[68].
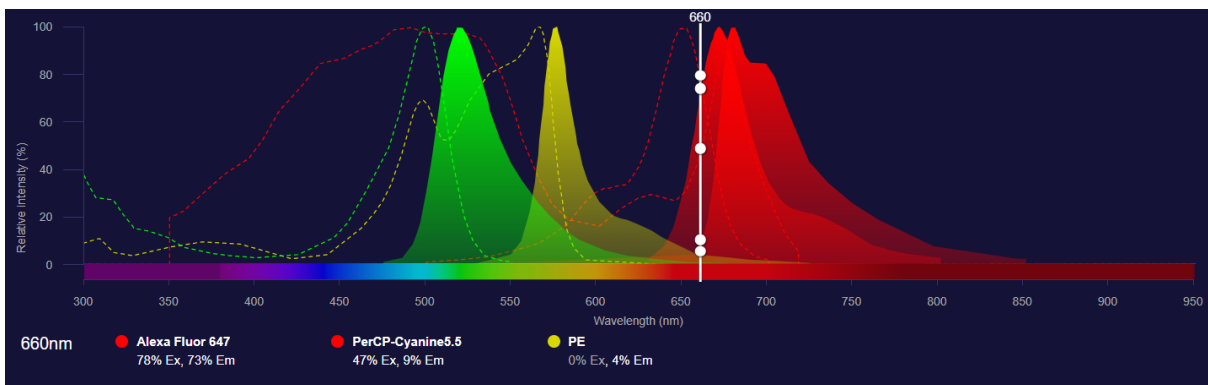
Figure 28 Fluorescence overlap at 660nm. Image produced with SpectraViewer[68].
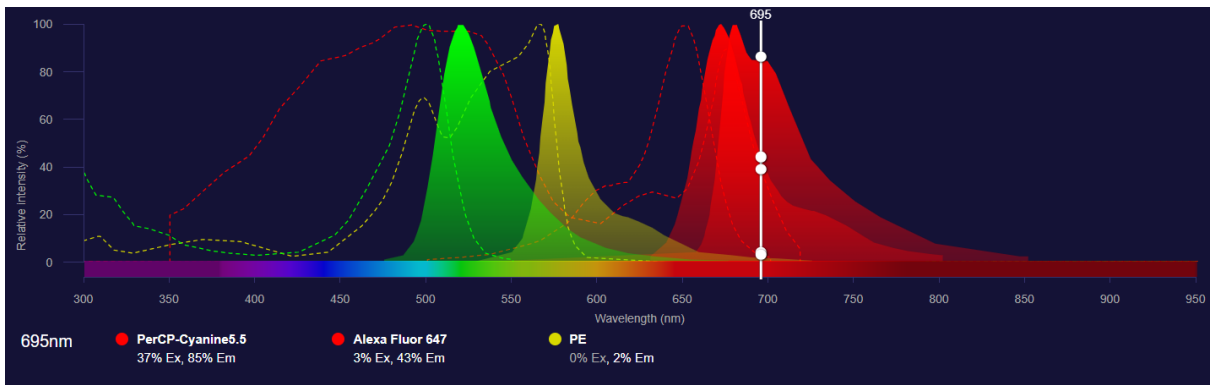
Figure 29 Fluorescence overlap at 695nm. Image produced with SpectraViewer[68].

A.1.2. Excitation with 488nm and 630nm lasers
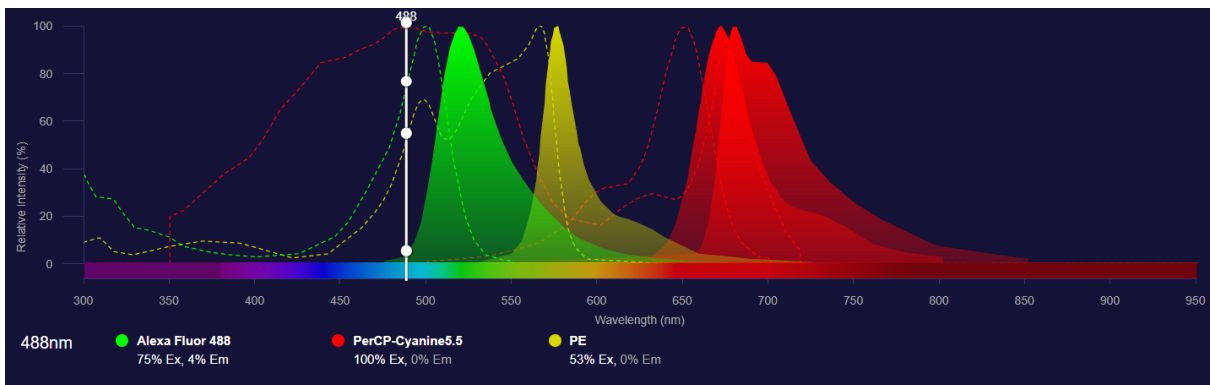
Figure 30 Excitation with 488 nm laser. Image produced with SpectraViewer[68].
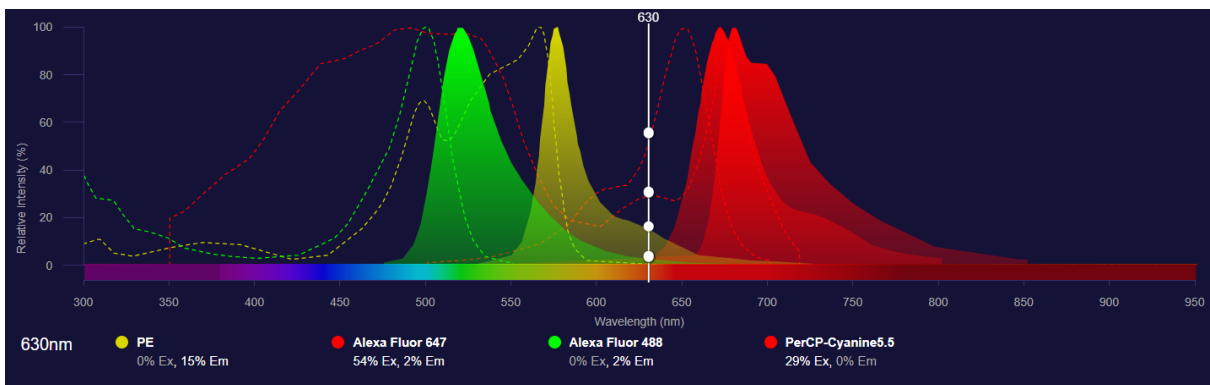
Figure 31 Excitation with 630 nm laser. Image produced with SpectraViewer[68].

A.1.3. Emission with 488nm laser
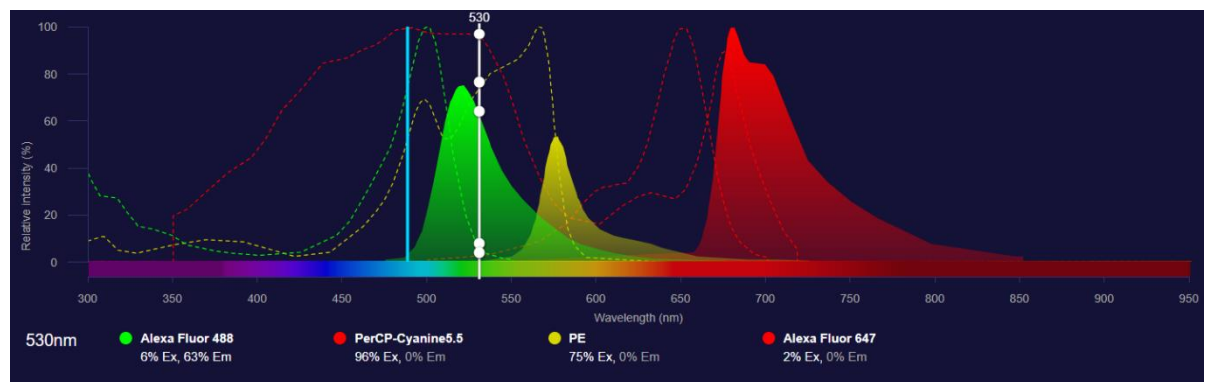
Figure 32 Emission at 530nm with 488nm laser. Image produced with SpectraViewer[68].
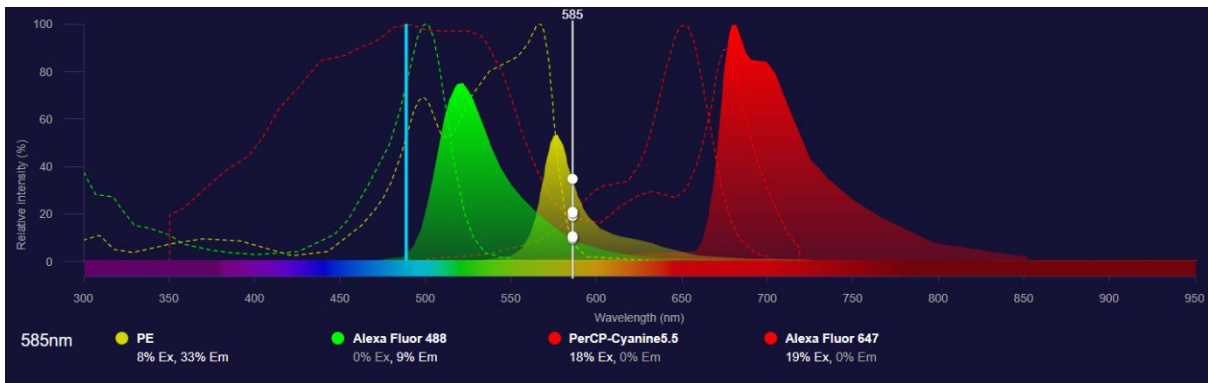
Figure 33 Emission at 585nm with 488nm laser. Image produced with SpectraViewer[68].
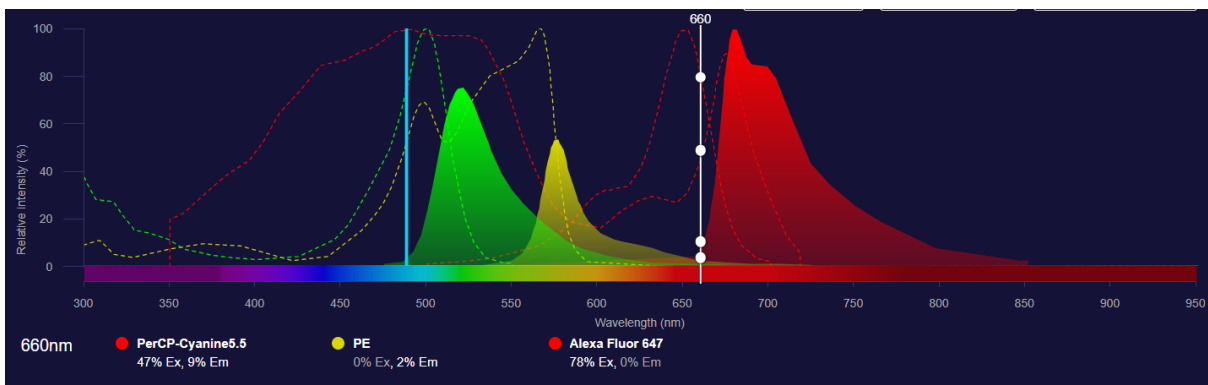
Figure 34 Emission at 660nm with 488nm laser. Image produced with SpectraViewer[68].
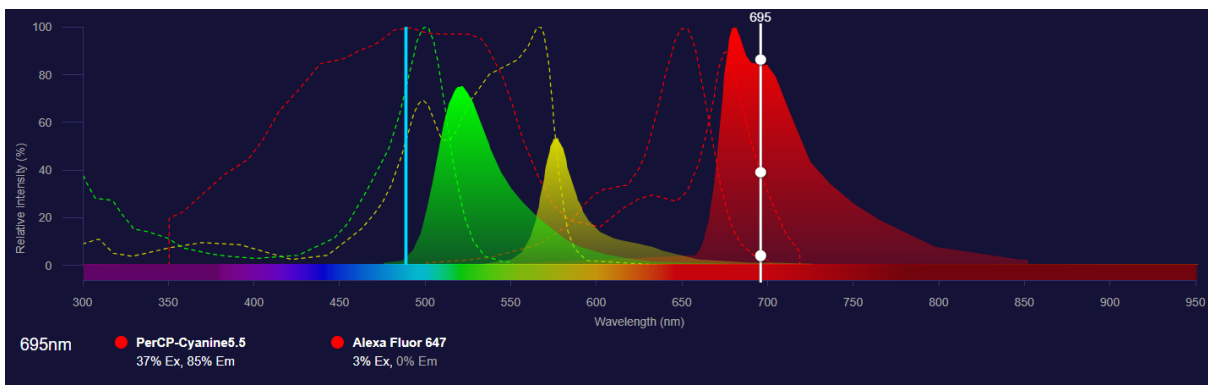
Figure 35 Emission at 695nm with 488nm laser. Image produced with SpectraViewer[68].

A.1.4. Emission with 630nm laser
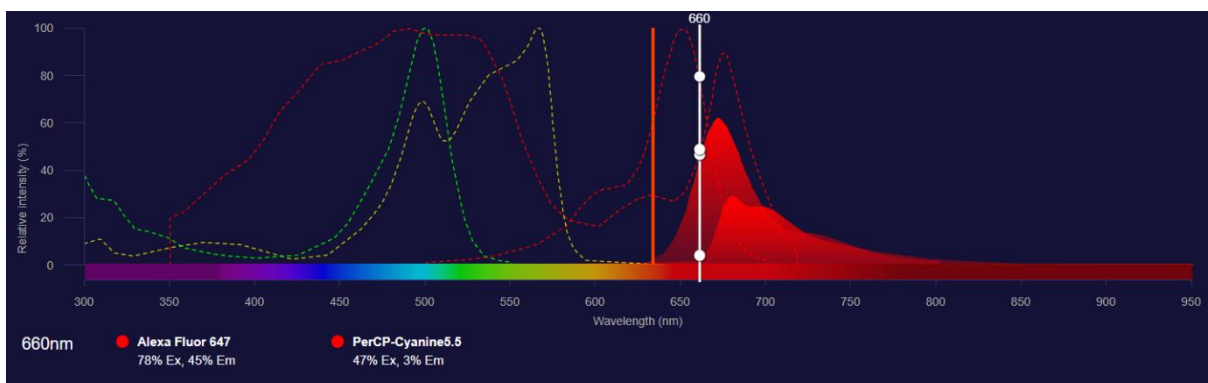
Figure 36 Emission at 660nm with 633nm laser. Image produced with SpectraViewer[68].
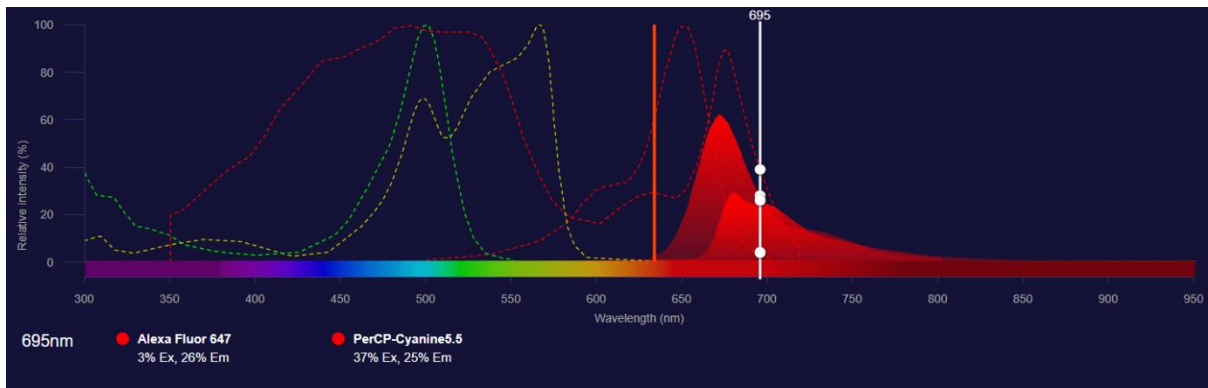
Figure 37 Emission at 695nm with 633nm laser. Image produced with SpectraViewer[68].

A.2. Protocol 1: SSCvsFSC results – THP1
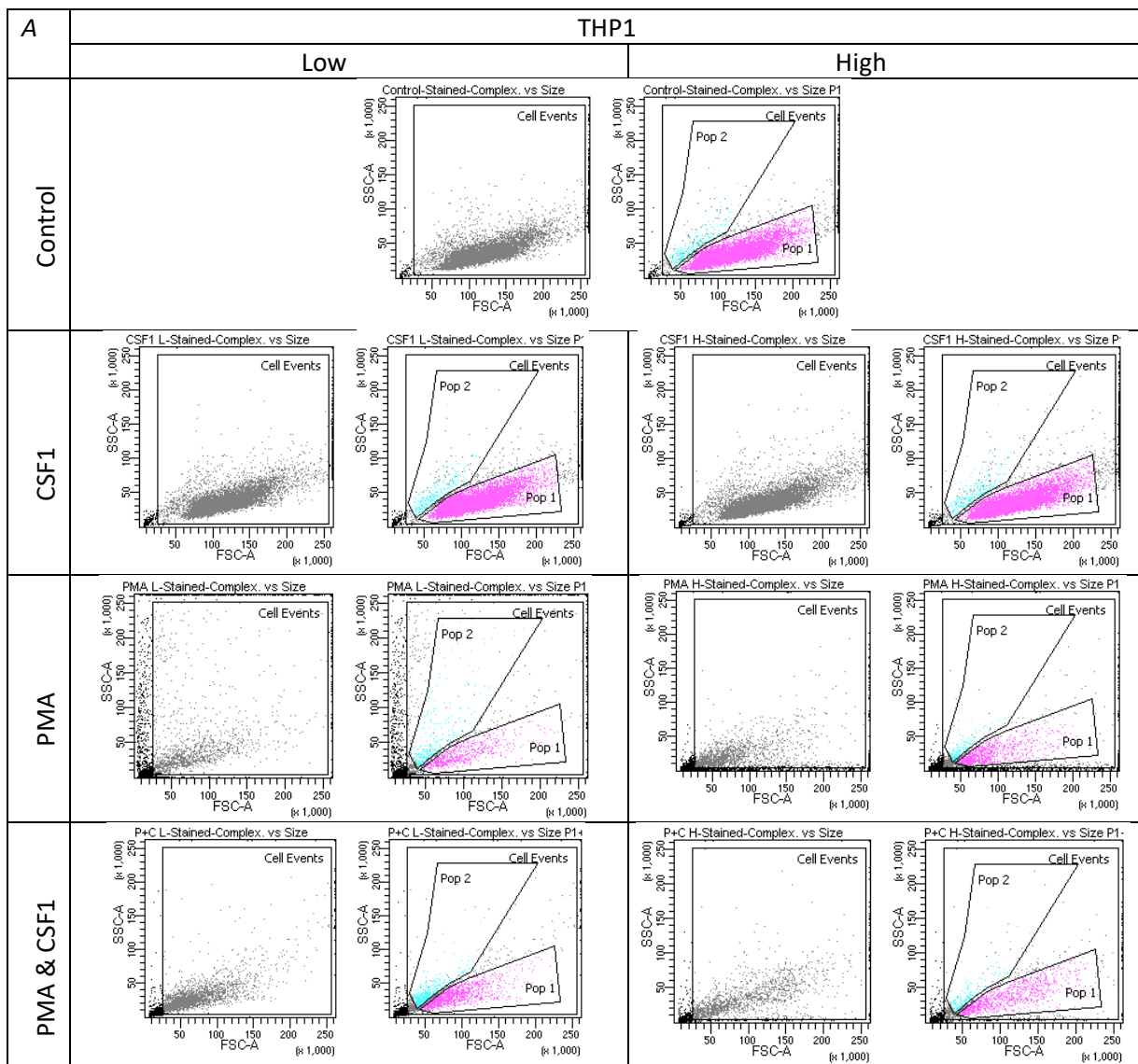
Figure 38 Flow cytometry results show THP1(P18) cells remain CD14 and CD16 negative after 24hr stimulation with PMA [25;50 ng/mL] and/or CSF1 [10;30 ng/mL]. SSC vs FSC scatterplot for THP1 cells respectively show 2 distinguishable populations (3 in THP1 PMA Low).

A.3. Protocol 1: SSCvsFSC results - U937
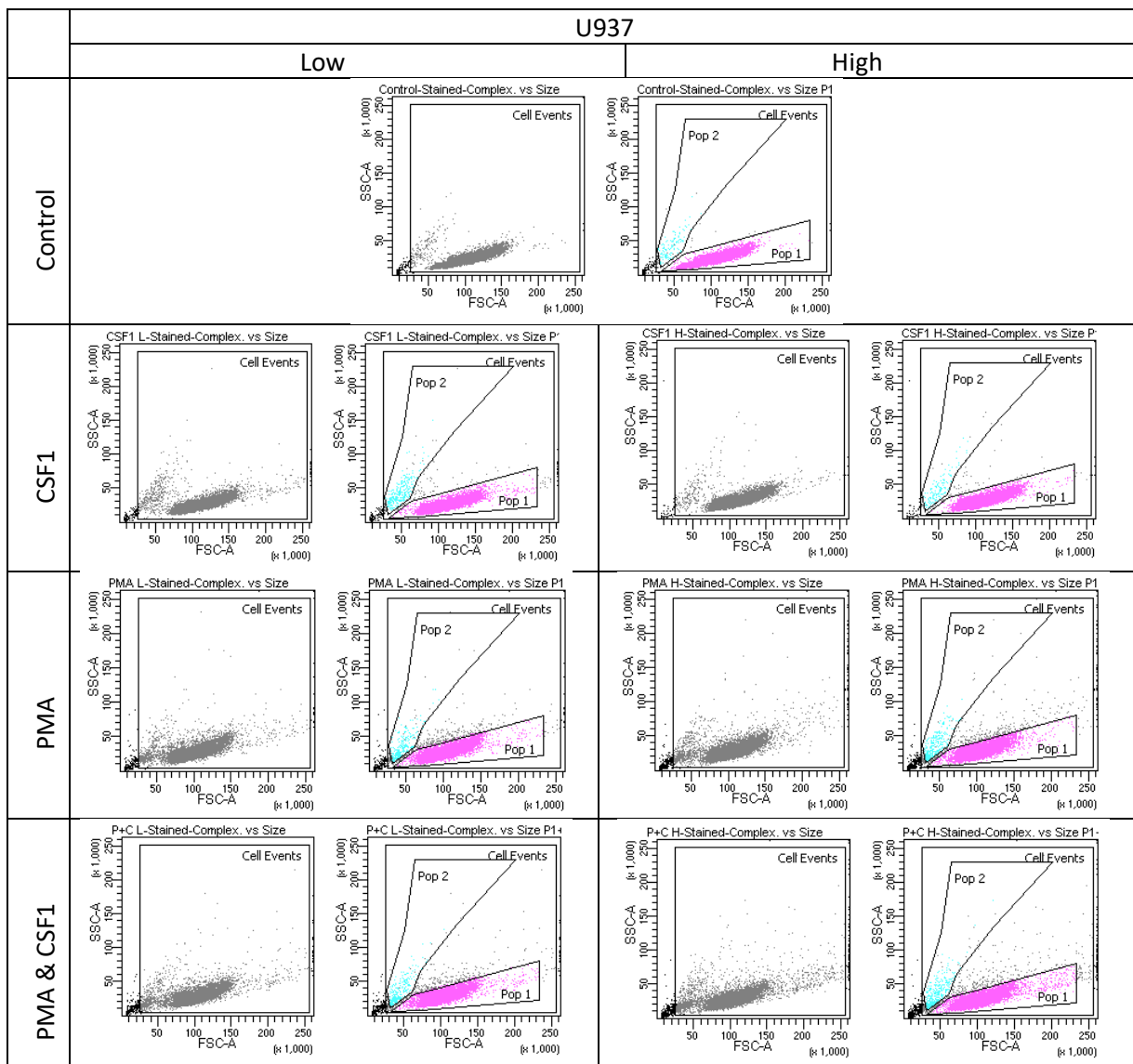
Figure 39 Flow cytometry results show U937(P19) cells remain CD14 and CD16 negative after 24hr stimulation with PMA [25;50 ng/mL] and/or CSF1 [10;30 ng/mL]. A&C) SSC vs FSC scatterplot for U937 cells respectively show 2 distinguishable populations.
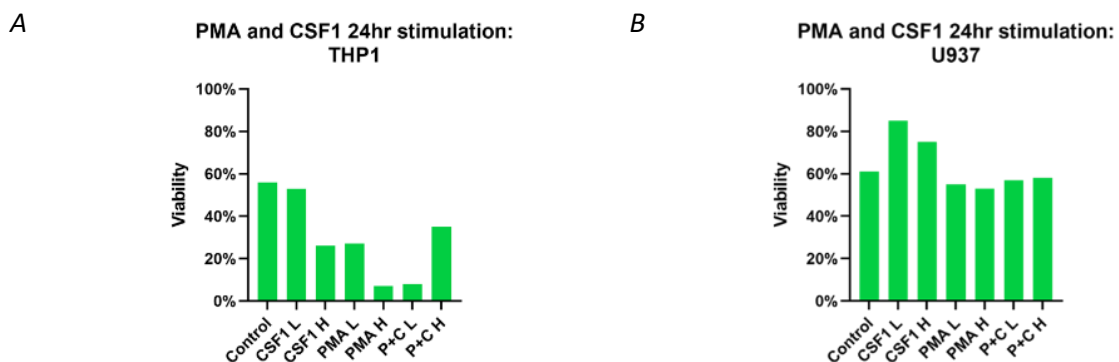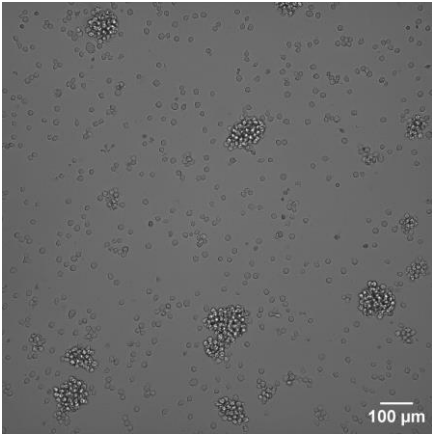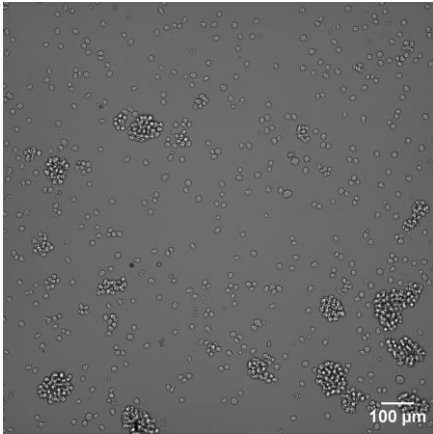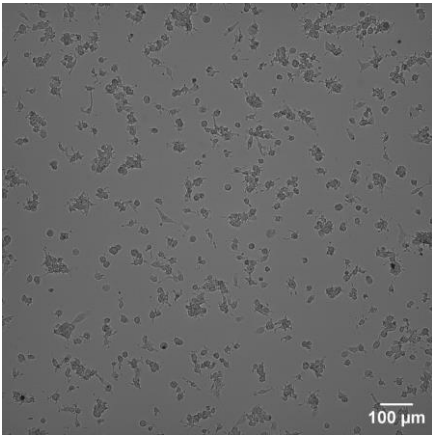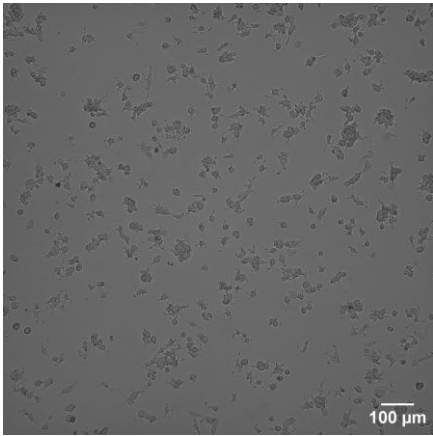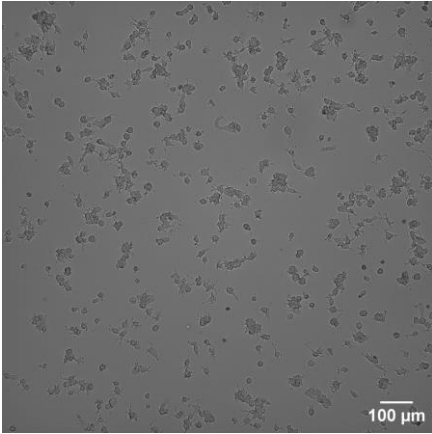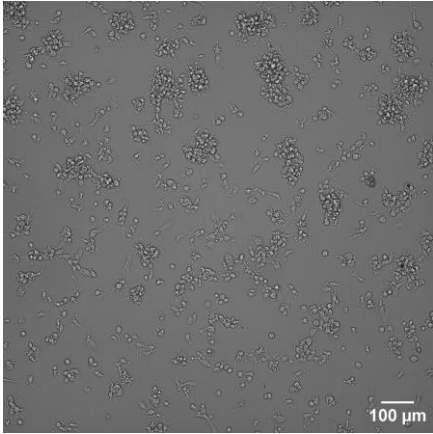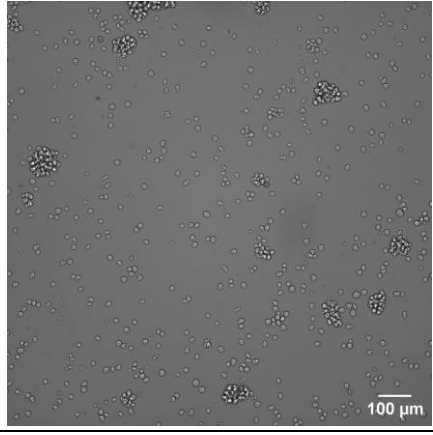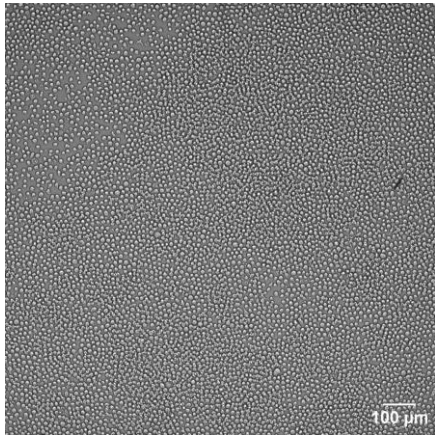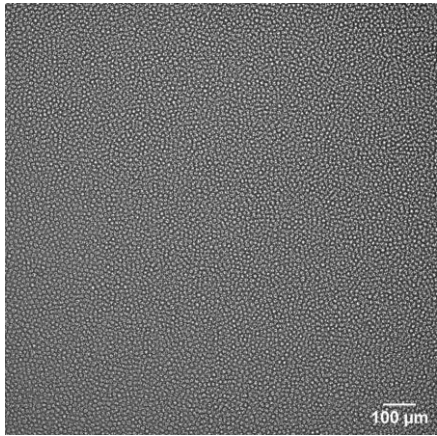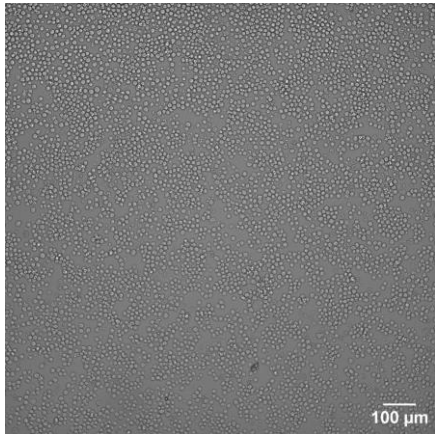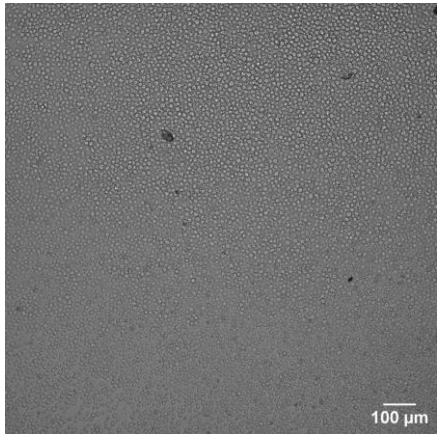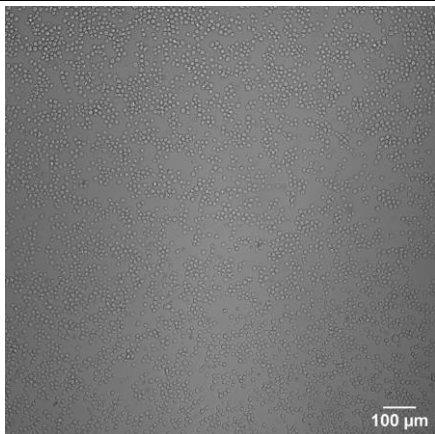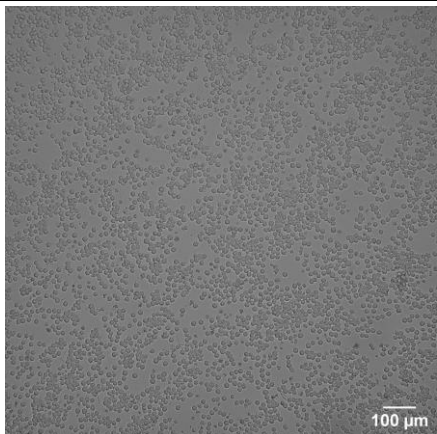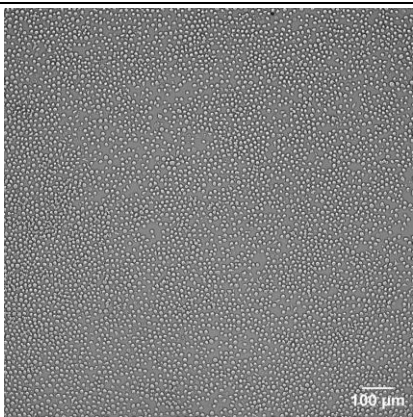
Figure 40 Viability for (A) THP1(P18) and (B) U937(P19) after 24hr stimulation with PMA [25;50 ng/mL] and/or CSF1 [10;30 ng/mL].

	Low	High
CSF1		
PMA		
PMA+CSF1		
NEG		*Figure 41 THP1(P18) cells show clumping behaviour when stimulated with CSF1, spreading behaviour when stimulated with PMA, and both behaviours with combined stimulation. Cells were stimulated with Low (10 ng/ml) and High (30 ng/mL) concentrations CSF1 or/and Low (25 ng/ml) and High (50 ng/mL) concentrations PMA. Brightfield morphology images, magnification 100X.*

	Low	High
CSF1		
PMA		
PMA+CSF1		
NEG		*Figure 42 U937(P18) cells show clumping behaviour when stimulated with CSF1, no spreading behaviour when stimulated with PMA, and clumping behaviour with combined stimulation. Cells were stimulated with Low (10 ng/ml) and High (30 ng/mL) concentrations CSF1 or/and Low (25 ng/ml) and High (50 ng/mL) concentrations PMA. Brightfield morphology images, magnification 100X.*

A.6. Protocol 2 –Flow cytometry results

Table 14 Flow cytometry results for THP1(P20;P22;P18) after 72hr stimulation with PMA (16.2 ng/mL) and/or Vitamin D3 (260 µg/mL). A) SSC vs FSC scatterplots show 3 distinguishable populations in the Control group, with differing relations between complexity and size. Results suggest stimulation with PMA and Ethanol cause cells to shift from P1 to P2, while VD3 further increases complexity relative to size and decreases average cell size. Combined stimulation with PMA and VD3 shows no further changes in complexity vs size and average cell size compared to VD3 alone. B) Autofluorescence in the CD14 channel relative to complexity differs between the three populations, as exemplified by Control Suspension Unstained. In addition, based on CD14 channel autofluorescence P2 can be further split into P2A (cyan) and P2B (dark blue) that require separation for proper gating. Note: due to a mistake in the visual settings, P2B is not shown as a separate dark blue subset in n3; this does not affect the quantified results. C-E) CD14 and CD16 positivity varies between populations, as exemplified by Control Suspension Stained. F) Population fractions quantified per condition support observations made in A. G) P2 sub-populations P2A and P2B quantified per condition; P2B is increased in case of PMA and Ethanol stimulation and disappears with VD3 stimulation. H) Classical and Non-Classical Profile fractions quantified per population show a significant increase in Classical monocytes in case of PMA stimulation, but no other conditions.
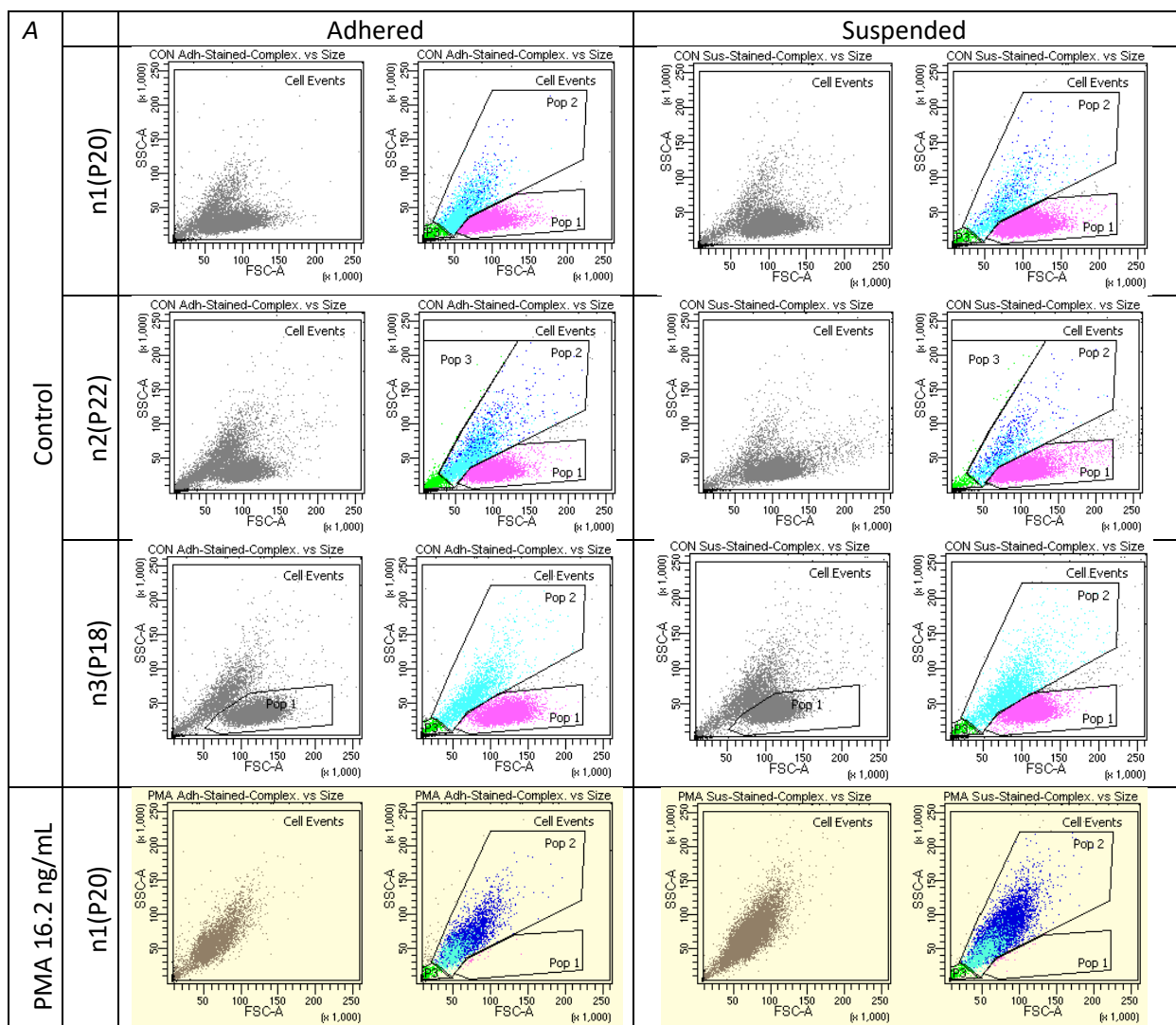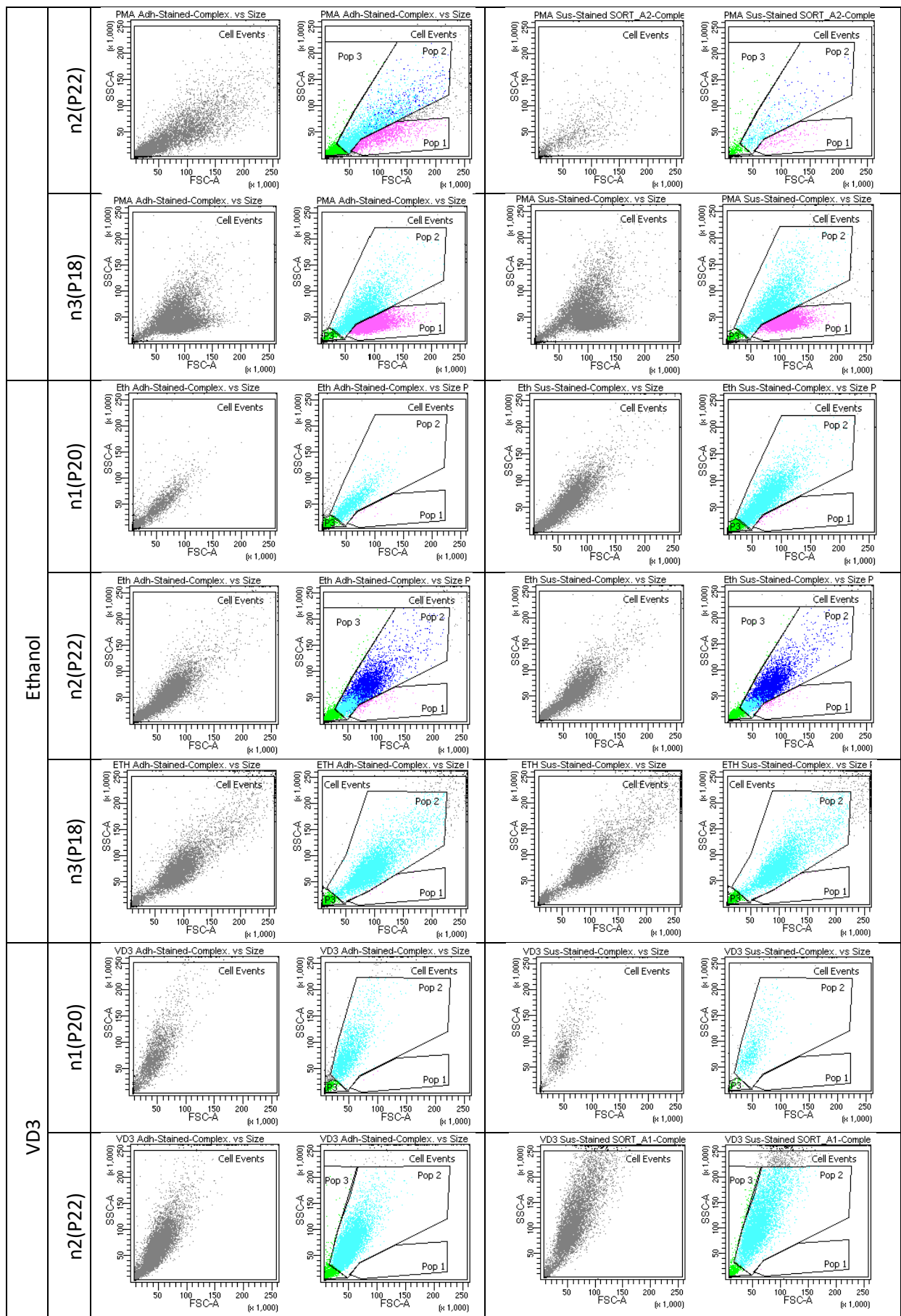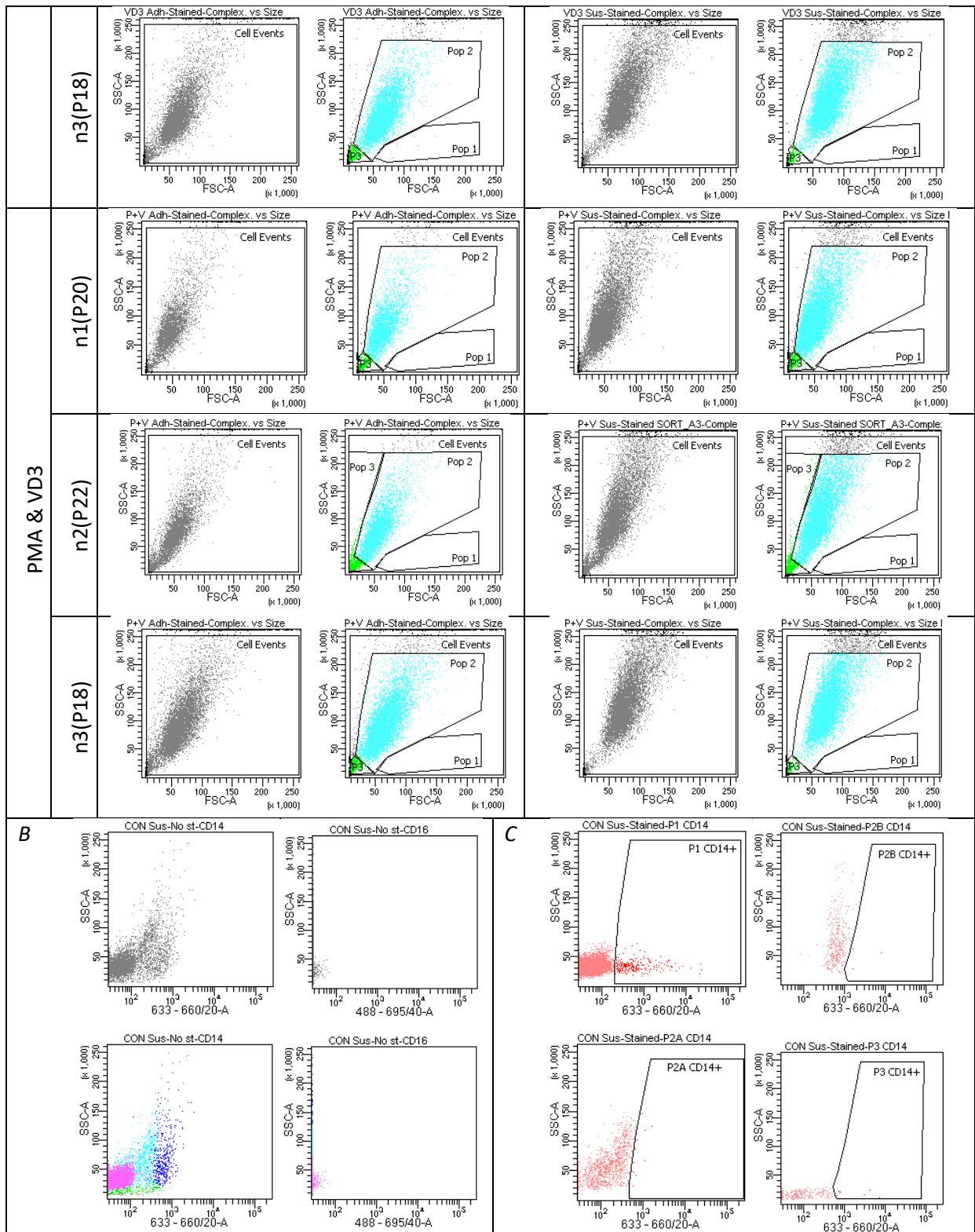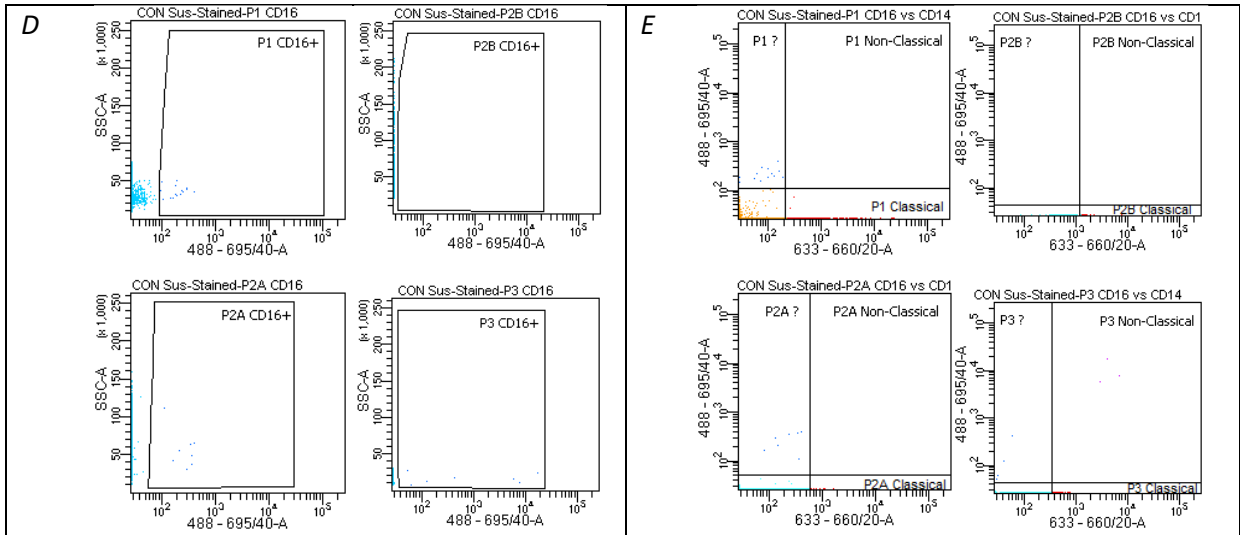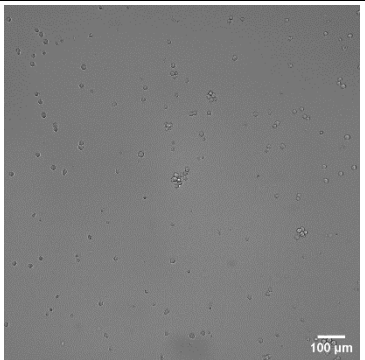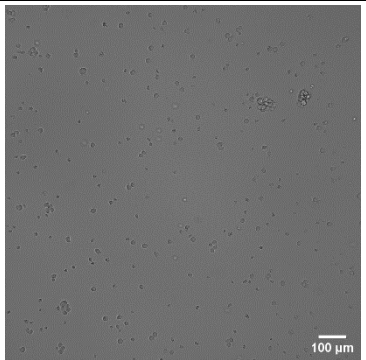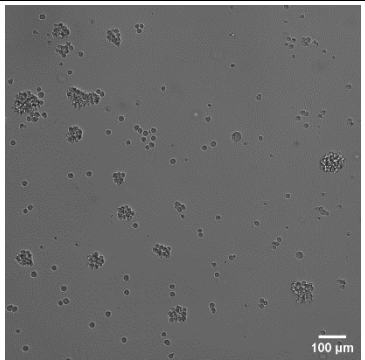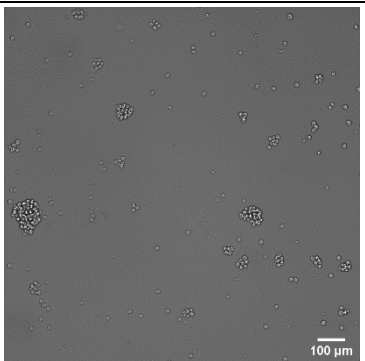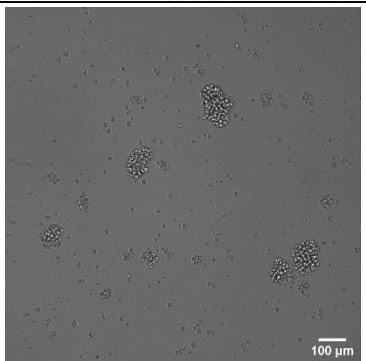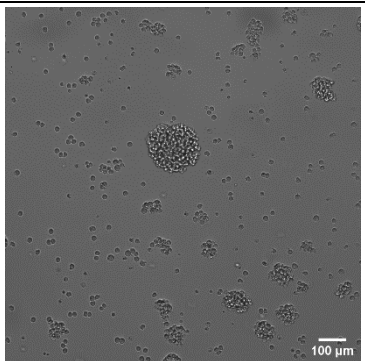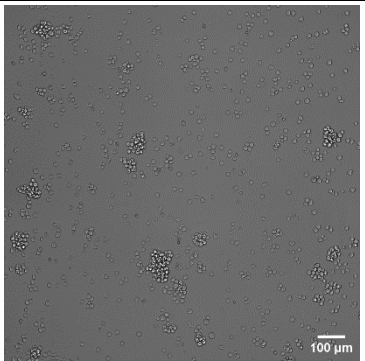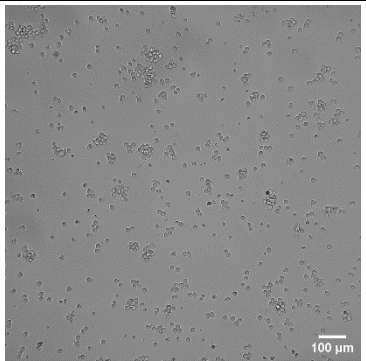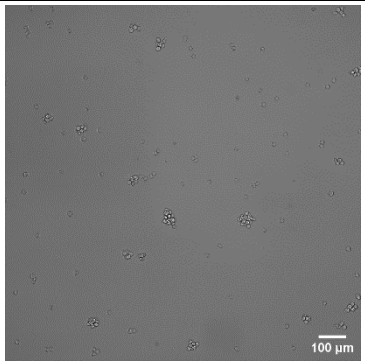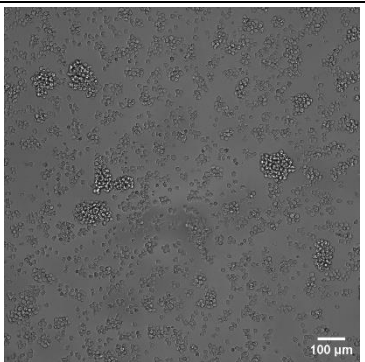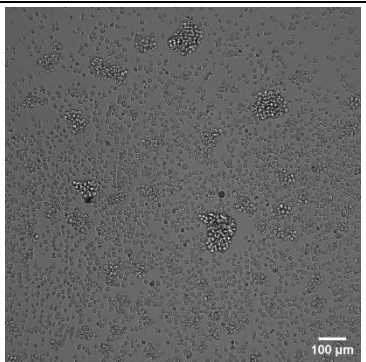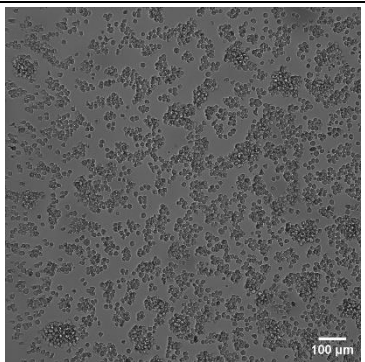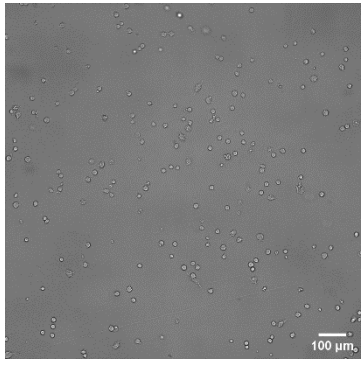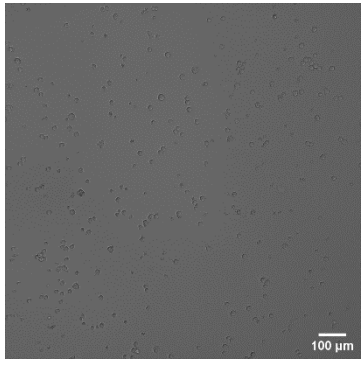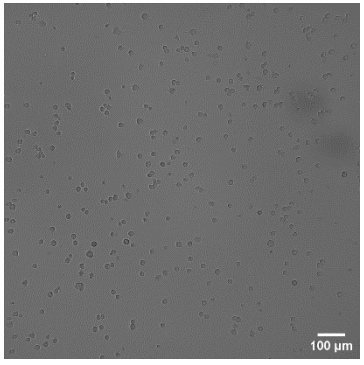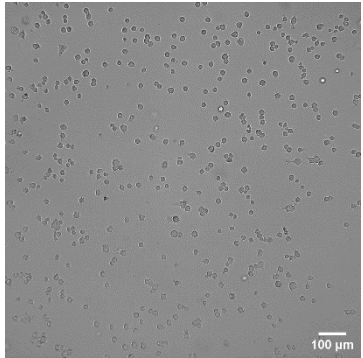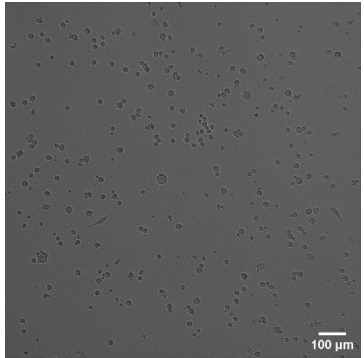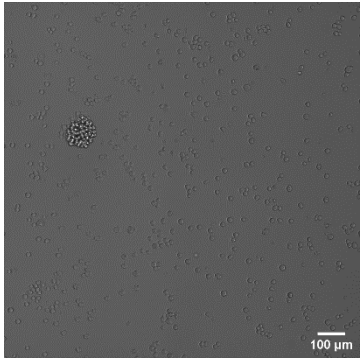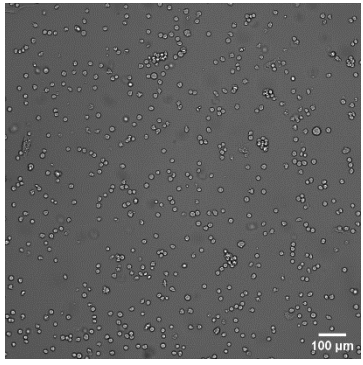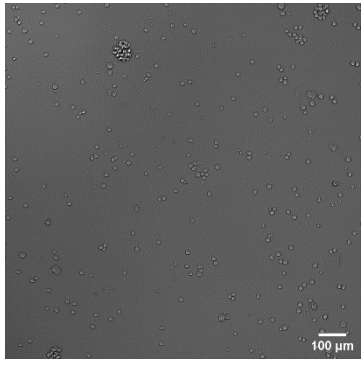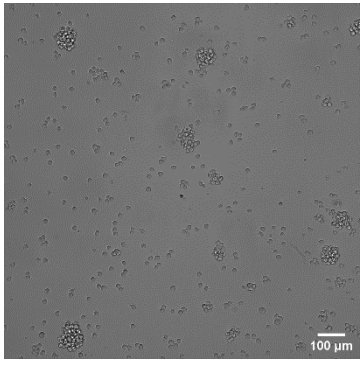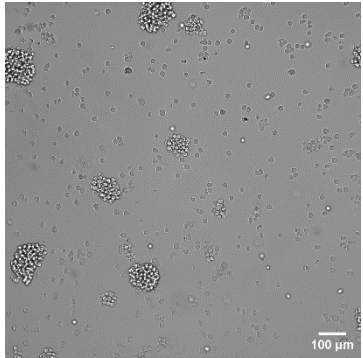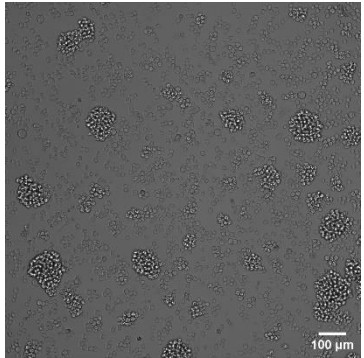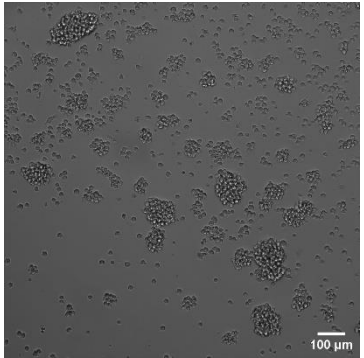
*Table 15. Brightfield images (**100X** for behaviour analysis) of 16.2 ng/mL PMA-prestimulated CD14- THP1(P20) cells 3 and 7 days post-sorting show that Mature cells exhibit more clumping behaviour. Sorting was based on CD13 expression. Unsorted mix (55% P1, 40%P2) was included as a control. After sorting, cells were cultured with a range of PMA concentrations [0, 8.1, 25, 50] ng/mL presented in A-D respectively. Images were taken of lower and higher cell density areas.*

A1 PMA-prestimulated CD14- THP1 cells 3 days post-sorting - Negative control (medium only)

	Mixed/Unsorted	Immature / P2	Mature / P1
Lower local cell density			
Higher local cell density			

A2 PMA-prestimulated CD14- THP1 cells 7 days post-sorting - Negative control (medium only)

	Mixed/Unsorted	Immature / P2	Mature / P1
Lower local cell density			
Higher local cell density			
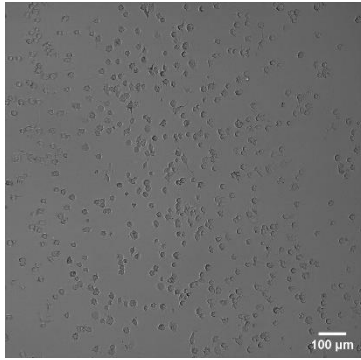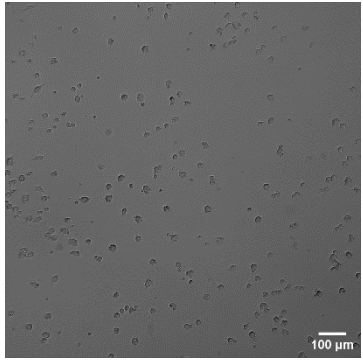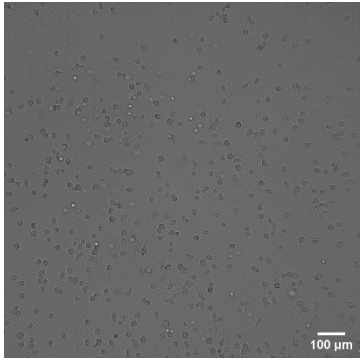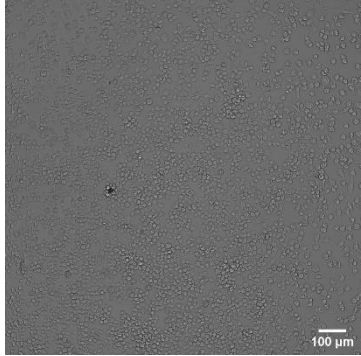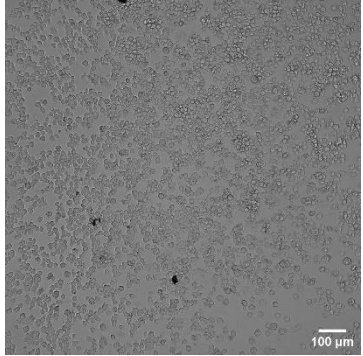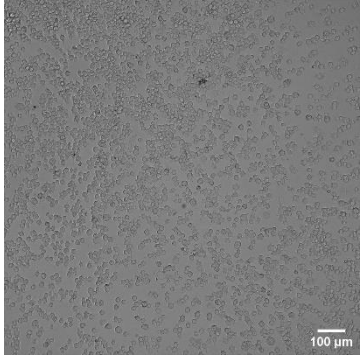
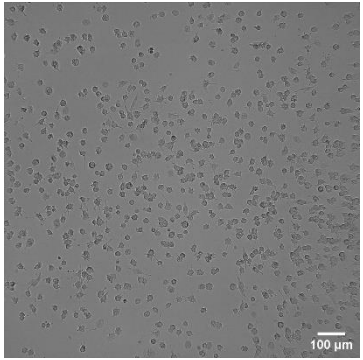| B1 PMA-prestimulated CD14- THP1 cells 3 days post-sorting - 8.1 ng/mL PMA stimulation		
Mixed/Unsorted (T25 flask)	Immature / P2	Mature / P1

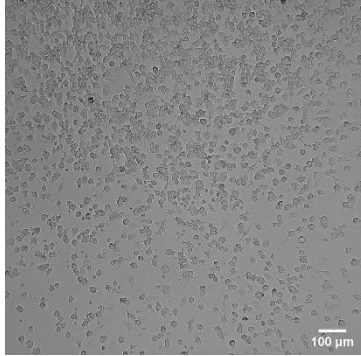Lower local cell density

Higher local cell density
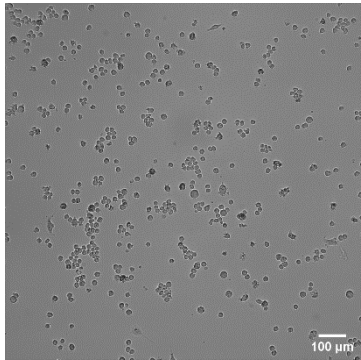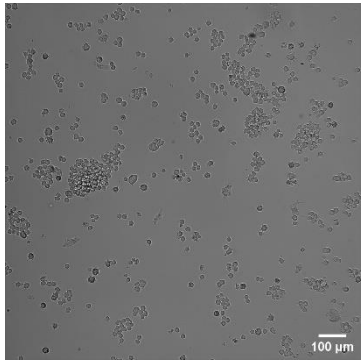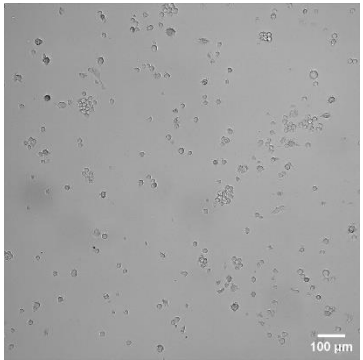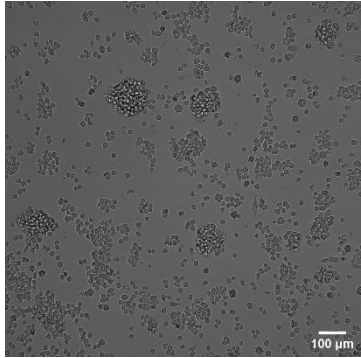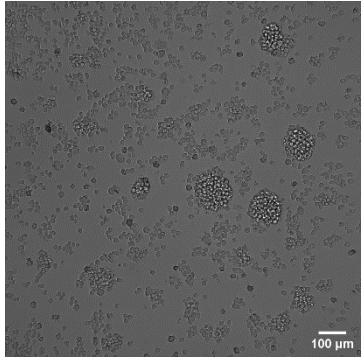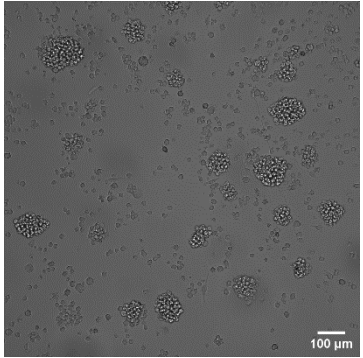
B2 PMA-prestimulated CD14- THP1 cells 7 days post-sorting - 8.1 ng/mL PMA stimulation		
Mixed/Unsorted (T25 flask)	Immature / P2	Mature / P1

Lower local cell density

Higher local cell density
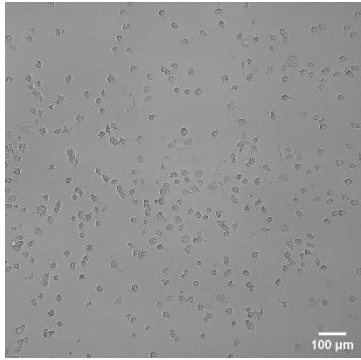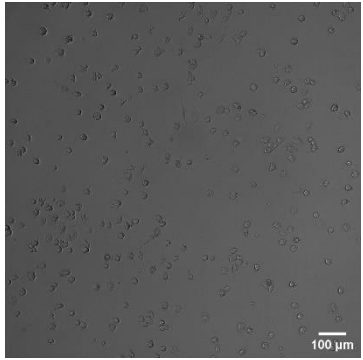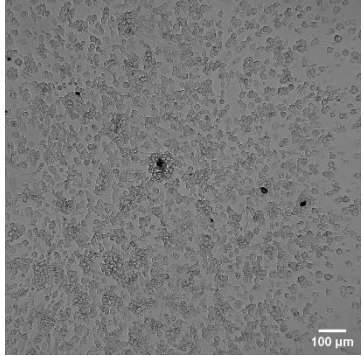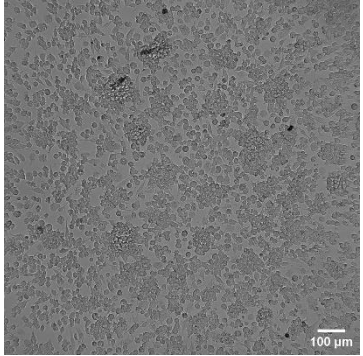
C1 PMA-prestimulated CD14- THP1 cells 3 days post-sorting - 25 ng/mL PMA stimulation		
Mixed/Unsorted	Immature / P2	Mature / P1

Lower local cell density

Higher local cell density
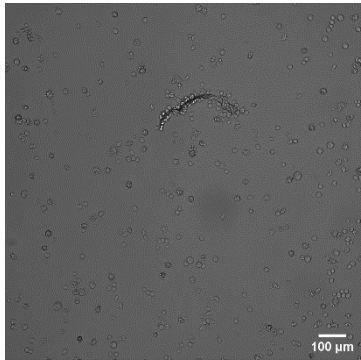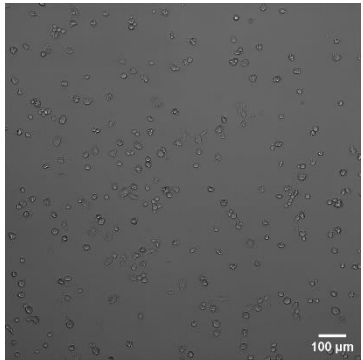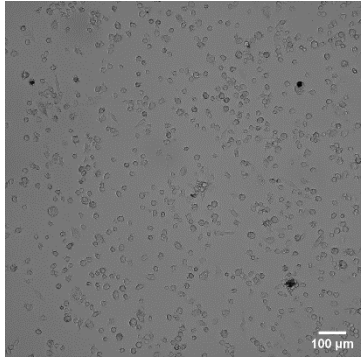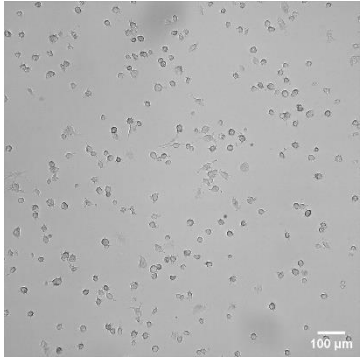
C2 PMA-prestimulated CD14- THP1 cells 7 days post-sorting - 25 ng/mL PMA stimulation		
Mixed/Unsorted	Immature / P2	Mature / P1

Lower local cell density

Higher local cell density

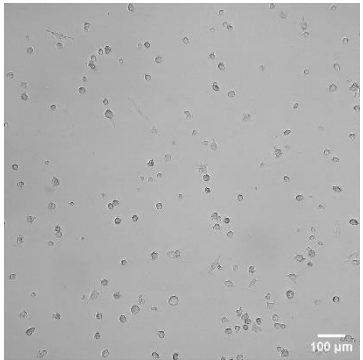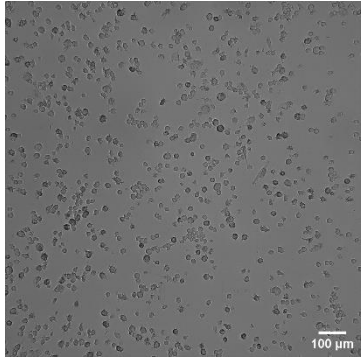| D1) PMA-prestimulated CD14- THP1 cells 3 days post-sorting - 50 ng/mL PMA stimulation		
Mixed/Unsorted	Immature / P2	Mature / P1

D2) PMA-prestimulated CD14- THP1 cells 7 days post-sorting - 50 ng/mL PMA stimulation		
Mixed/Unsorted	Immature / P2	Mature / P1

A.7. Flow cytometry data matrix

Table 16 Supplementary flow cytometry data matrix with filenames and paths

Experiment	File name	Path
THP1 and U937 profile exploration (THP1)	2022-12-02 Exploration cALL-Batch_Analysis_THP1 stitched	"...\Experiments\FINAL RESULTS\FACS data CompAll stitched PDFs\2022-12-02 Exploration cALL-Batch_Analysis_THP1 stitched.pdf"
THP1 and U937 profile exploration (U937)	2022-12-02 Exploration cALL-Batch_Analysis_U937 stitched	"...\Experiments\FINAL RESULTS\FACS data CompAll stitched PDFs\2022-12-02 Exploration cALL-Batch_Analysis_U937 stitched.pdf"
Protocol 1: PMA and CSF1 24hr stimulation (THP1)	2022-12-09 P+C THP1 cALL-Batch_Analysis stitched	"...\Experiments\FINAL RESULTS\FACS data CompAll stitched PDFs\2022-12-09 P+C THP1 cALL-Batch_Analysis stitched.pdf"
Protocol 1: PMA and CSF1 24hr stimulation (U937)	2022-12-16 P+C U937 cALL-Batch_Analysis stitched	"...\Experiments\FINAL RESULTS\FACS data CompAll stitched PDFs\2022-12-16 P+C U937 cALL-Batch_Analysis stitched.pdf"
Protocol 2: PMA and VD3 stimulation 72hr (n1)	2023-01-27 P+V THP1 n1 cALL-Batch_Analysis_COMPLETE stitched	"...\Experiments\FINAL RESULTS\FACS data CompAll stitched PDFs\2023-01-27 P+V THP1 n1 cALL-Batch_Analysis_COMPLETE stitched.pdf"
Protocol 2: PMA and VD3 stimulation 72hr (n2)	2023-02-10 P+V THP1 n2 cALL-Batch_Analysis_COMPLETE stitched	"...\Experiments\FINAL RESULTS\FACS data CompAll stitched PDFs\2023-02-10 P+V THP1 n2 cALL-Batch_Analysis_COMPLETE stitched.pdf"
Protocol 2: PMA and VD3 stimulation 72hr (n3)	2023-03-31 P+V THP1 n3 cALL-Batch_Analysis_COMPLETE stitched	"...\Experiments\FINAL RESULTS\FACS data CompAll stitched PDFs\2023-03-31 P+V THP1 n3 cALL-Batch_Analysis_COMPLETE stitched.pdf"
Protocol 3: PMA stimulation 72hr in flask (n1)	2023-04-14 PMA Flask n1 CD13 cALL-Batch_Analysis_Sus and Adh stitched	"...\Experiments\FINAL RESULTS\FACS data CompAll stitched PDFs\2023-04-14 PMA Flask n1 CD13 cALL-Batch_Analysis_Sus and Adh stitched.pdf"
(Old compensation for sorting)	2023-04-14 PMA Flask n1 CD13 cALL-Batch_Analysis_SORT stitched	"...\Experiments\FINAL RESULTS\FACS data CompAll stitched PDFs\2023-04-14 PMA Flask n1 CD13 cALL-Batch_Analysis_SORT stitched.pdf"
Protocol 3: PMA stimulation 72hr in flask (n2)	2023-04-28 PMA Flask n2 HLA-DR cALL-Batch_Analysis_generous stitched	"...\Experiments\FINAL RESULTS\FACS data CompAll stitched PDFs\2023-04-28 PMA Flask n2 HLA-DR cALL-Batch_Analysis_generous stitched.pdf"
Continued culturing (Day 7 post Protocol 3)	2023-04-21 PMA Flask n1 PMA SUS Day7 cALL-Batch_Analysis stitched	"...\Experiments\FINAL RESULTS\FACS data CompAll stitched PDFs\2023-04-21 PMA Flask n1 PMA SUS Day7 cALL-Batch_Analysis stitched.pdf"